

Unfalsified control : data-driven control design for performance improvement

Citation for published version (APA):

Helvoort, van, J. J. M. (2007). *Unfalsified control : data-driven control design for performance improvement*. [Phd Thesis 1 (Research TU/e / Graduation TU/e), Mechanical Engineering]. Technische Universiteit Eindhoven. <https://doi.org/10.6100/IR631347>

DOI:

[10.6100/IR631347](https://doi.org/10.6100/IR631347)

Document status and date:

Published: 01/01/2007

Document Version:

Publisher's PDF, also known as Version of Record (includes final page, issue and volume numbers)

Please check the document version of this publication:

- A submitted manuscript is the version of the article upon submission and before peer-review. There can be important differences between the submitted version and the official published version of record. People interested in the research are advised to contact the author for the final version of the publication, or visit the DOI to the publisher's website.
- The final author version and the galley proof are versions of the publication after peer review.
- The final published version features the final layout of the paper including the volume, issue and page numbers.

[Link to publication](#)

General rights

Copyright and moral rights for the publications made accessible in the public portal are retained by the authors and/or other copyright owners and it is a condition of accessing publications that users recognise and abide by the legal requirements associated with these rights.

- Users may download and print one copy of any publication from the public portal for the purpose of private study or research.
- You may not further distribute the material or use it for any profit-making activity or commercial gain
- You may freely distribute the URL identifying the publication in the public portal.

If the publication is distributed under the terms of Article 25fa of the Dutch Copyright Act, indicated by the "Taverne" license above, please follow below link for the End User Agreement:

www.tue.nl/taverne

Take down policy

If you believe that this document breaches copyright please contact us at:

openaccess@tue.nl

providing details and we will investigate your claim.

Unfalsified Control: Data-Driven Control Design for Performance Improvement

PROEFSCHRIFT

ter verkrijging van de graad van doctor aan de
Technische Universiteit Eindhoven, op gezag van de
Rector Magnificus, prof.dr.ir. C.J. van Duijn, voor een
commissie aangewezen door het College voor
Promoties in het openbaar te verdedigen
op maandag 17 december 2007 om 16.00 uur

door

Jeroen Johannes Michiel van Helvoort

geboren te Vlijmen

Dit proefschrift is goedgekeurd door de promotor:

prof.dr.ir. M. Steinbuch

Copromotor:

dr.ir. A.G. de Jager



This dissertation has been completed in partial fulfillment of the requirements of the Dutch Institute of Systems and Control DISC for graduate study.

Copyright © 2007 by J.J.M. van Helvoort. All rights reserved.

A catalogue record is available from the Eindhoven University of Technology Library.

Unfalsified Control: Data-Driven Control Design for Performance Improvement/
by Jeroen J.M. van Helvoort. – Eindhoven : Technische Universiteit Eindhoven,
2007. Proefschrift. – ISBN: 978-90-386-1167-9

Typeset by the author with the pdfL^AT_EX documentation system.

Cover design: JWL Boekproducties / Jeroen van Helvoort, inspired by the work
of M.C. Escher.

Reproduction: Gildeprint Drukkerijen B.V., Enschede, The Netherlands.

To my parents

To Linda

Samenstelling promotiecommissie:

prof.dr.ir. René de Borst,	(voorzitter)
prof.dr.ir. Maarten Steinbuch,	(promotor)
dr.ir. Bram de Jager,	(copromotor)
prof.dr. Robert Babuška, TU Delft,	(lid kerncommissie)
prof.dr. Henk Nijmeijer,	(lid kerncommissie)
prof. Michael G. Safonov, USC, Los Angeles, USA,	(lid kerncommissie)
prof.ir. Okko Bosgra,	
prof.dr.ir. Stefano Stramigioli, UTwente.	

Contents

1	Introduction	1
1.1	System-in-the-loop approach to improve performance	1
1.2	Flaws of model-based control design	2
1.3	Data-driven control design	4
1.4	Problem statement	5
1.5	Data-driven control design approaches	7
1.6	Contributions	11
1.7	Structure	14
2	Unfalsification	15
2.1	Unfalsification of hypotheses	15
2.2	Unfalsified Control	15
2.3	Elements of Adaptive Unfalsified Control	17
3	Ellipsoidal Unfalsified Control	21
3.1	Preliminaries	21
3.2	Performance requirement	21
3.3	Fictitious reference	22
3.4	Controller structure	24
3.5	Noise analysis	26
3.6	Unfalsified Set	27
3.7	Unfalsification	27
3.8	Update ellipsoidal Unfalsified Set	28
3.9	Controller selection	31
3.10	Summary and remarks	34
4	Stability of Ellipsoidal Unfalsified Control	37
4.1	Preliminaries	37
4.2	BIBO stability	37
4.3	Feasibility	39

4.4	Discarding of demonstrably destabilizing controllers	40
4.5	Limited number of switches	41
4.6	Summary and remarks	46
5	Application of Ellipsoidal Unfalsified Control	47
5.1	Simulation: Plant	47
5.2	Simulation: Design	48
5.3	Simulation: Results	52
5.4	Experiment: Plant	58
5.5	Experiment: Design	61
5.6	Experiment: Results	64
6	Multivariable Ellipsoidal Unfalsified Control	75
6.1	Plant properties	75
6.2	Controller structure	76
6.3	Performance requirement	77
6.4	Unfalsified Set	77
6.5	Controller selection	78
6.6	Stability	79
6.7	Simulation	80
6.8	Summary and remarks	87
7	Batch Adaptive Unfalsified Control	89
7.1	Introduction	89
7.2	Direct unfalsified controller design - Solution via convex optimization	90
7.3	Batch Adaptive Unfalsified Control	92
7.4	Experiment	96
7.5	Summary and remarks	106
8	Conclusions	109
8.1	Ellipsoidal Unfalsified Control	109
8.2	Batch Adaptive Unfalsified Control	110
8.3	Applicability of Ellipsoidal Unfalsified Control	111
9	Recommendations	113
9.1	Open issues	113
9.2	Extensions	116
	Bibliography	119
	Summary	125
	Samenvatting	127

Dankwoord	129
Curriculum Vitae	131

Chapter 1

Introduction

T*HIS* introductory chapter presents the background of the research in this thesis. It is argued that regular model-based control design contains inherent drawbacks that can be overcome with data-driven control design. This chapter defines the problem statement and explains the choice for the framework of Unfalsified Control. The main contributions are formulated and the structure of this thesis is sketched.

1.1 System-in-the-loop approach to improve performance

To achieve better and faster production, machines are pushed to their limits in capacity and capability. Invariably, this induces increased demands on the controllers that manage these systems. In many high-tech systems, motion controllers are at the base of the controller architecture, since they immediately influence the operating speed and precision of the machines. By improving the motion controllers, the effective capacity and capability of the systems are enhanced.

The accuracy of the controlled system defines its achieved performance. To achieve an increase in performance, advanced control design methods are used such as (multivariable) H_∞ - and (mixed-) μ -synthesis and higher order feedforward design. However, these model-based methods encounter limits on the achievable performance, for which in Section 1.2 some insights are provided. To overcome

these limitations and to improve the performance beyond model-based control design, in this thesis an alternative approach is examined, namely the approach of system-in-the-loop data-driven control design.

In contrast to regular model-based (off-line) control design, in data-driven control design no model of the plant is used to derive the controller. The application of system-in-the-loop enables that the controller is designed using data from the actual system it is going to control, under realistic operating conditions. Consequently, the controller can optimize the closed-loop performance on the actual system instead of on a model of that system. This procedure evades the need to accurately model the plant and to be robust to all hypothetical disturbances, parasitic dynamics and operating conditions, but considers only those that actually occur.

In this thesis, we focus on high performance motion systems. Typically, motion systems operate at small sample times ($\mathcal{O}(\text{ms})$) and actuation is relatively cheap, as it only requires electrical power. Therefore, it is relatively easy to gather large amounts of experimental data. This data enables the construction of dedicated models, which can then be used for advanced control design. However, as is shown next, even with good models still the performance of the controlled system is limited.

1.2 Flaws of model-based control design

In model-based controller design, a controller for a motion system is designed using a model of the system. The model is constructed using first principles, prior knowledge and/or experimental data, and it represents the behavior of the system. A controller is designed for the acquired model, using a model-based design technique. A common method for model-based control design is loopshaping, see for instance (Skogestad and Postlethwaite, 2005). Thereupon, the controller designed with the model is then applied to the plant.

Deviations in the dynamics, either over time, over different products, over task or over operating condition, are captured in an uncertainty description. Control design methods as H_∞ - and (mixed-) μ -synthesis employ these uncertainty descriptions to design controllers that are robust for the entire range of the dynamics.

The effectiveness of these model-based control design techniques largely depends on the derivation of accurate and suitable models, including an uncertainty description and a characterization of the noises and disturbances acting on the plant.

However, as shown in the extensive overview by Hjalmarsson (2005), modeling for control is far from trivial and subject to extensive research. Furthermore, the author clearly explains that “the only possible way to reduce the size of the [enormous set of models that is consistent with the observations, including infinite dimensional non-linear models,] is to introduce prior information, both on the system dynamics and the noise.” On the contrary, it is also observed that there is a “necessary leap of faith in system identification,” since “stability and performance guarantees require the true system to be accounted for in the model set delivered by the system identification.” Moreover, the quest for a model of the true physical system is futile, since any model depends on the particular input and may differ drastically for different inputs (Skelton, 1989).

Besides the difficulties of modeling, even a good model might not provide the desired level of performance. The structure arising from model identification generally does not readily fit the structure needed for control design. This is overcome by rewriting the model or by outer-bounding the set of models, introducing conservatism and thereby hampering performance. Robust control design techniques derive a controller for the resulting model set, thereby possibly introducing additional conservatism since they are robust to *at least* the entire model set that includes all uncertainties and disturbances.

Another important observation is that the model-based controllers are robust to all possible deviations in the dynamics, even if these deviations are not present in a single setup. Furthermore, the controllers are designed to suppress the entire ensemble of possible disturbances that affect the performance, even those that do not act on the system at present.

From Bode’s sensitivity integral it is derived that a decrease of the Sensitivity transfer function to suppress uncertainties and disturbances at certain frequency ranges always impedes suppression at other frequencies, at least for linear systems with a relative degree of 2 or higher (Skogestad and Postlethwaite, 2005). Therefore, ideally, suppression is desired only at those frequencies where it is needed most to improve the performance (Steinbuch and Norg, 1998). In frequency ranges that do not hamper the performance, the Sensitivity transfer function can be increased without being penalized.

Summarizing, even though most motion systems have the pleasant characteristic that models are capable of describing the dynamics quite accurately, a model-based control design technique might not result in adequate performance. Therefore, the alternative approach of data-driven control design is considered next.

1.3 Data-driven control design

An alternative approach for control design is the application of the system-in-the-loop principle. With system-in-the-loop, measurements are performed on the actual system, under realistic operating conditions. This naturally leads to data-driven control design, which adapts the controller to measurement data obtained from the actual system.

Definition 1.1 (Data-driven control design) *Data-driven control design is the synthesis of a controller using measurement data acquired on the actual system to be controlled, without explicitly using (non-)parametric models of the system to be controlled during adaptation.*

The definition states that measurement data is to be used in the adaptation of the controller. Nevertheless, if a model or other plant information or assumptions are available, they can be used in the initialization of the algorithm. In fact, its use is encouraged, for instance in the design of the controller structure, in the selection of the initial controller and in the determination of the performance requirements, to ensure that all information about the plant is used in the design of the controller such that the chances that a stabilizing and performing controller results are maximized.

In some literature, the term “data-based control design” is used as a synonym for data-driven control design as defined here, see for instance (Woodley et al., 1999; Kostić, 2004; Kostić et al., 2004; Aangenent et al., 2005). However, since the term “data-based” is also used to refer to control using databases (Pan and Lee, 2003; Ando, 2004) or the control of databases (Hiraoka et al., 2003), it is ambiguous and, accordingly, avoided here.

In (Kostić, 2004), the synthesis of controllers using models that are identified with experimental data is referred to as “model-based data-driven control design,” since in identification of the plant model experimental data is used. However, since these methods rely on explicit models of the plant, they do not satisfy the definition given

here of a data-driven control design.

In the synthesis of the data-driven controller, the measurements on the actual system are used, including its disturbances and noises. This implies that the controller is designed for the actual conditions. Ideally, this results in a controller that has large suppression at the frequency ranges where the performance is influenced most, and has limited suppression where only a little decrease in the performance results. Since from Bode's sensitivity integral it is derived that for suppression at certain frequencies results in less suppression in other frequency ranges, at least for linear systems with a relative degree of 2 or higher, to reach the best performance is to concentrate suppression in the regions where it is needed most. Data-driven control design implicitly addresses this topic, with the additional benefit that the elaborate and conservatism-introducing detour of plant modeling is omitted.

Inevitably, data-driven control design also suffers from drawbacks. Besides the complexity of the algorithms involved, which may require large online computational power, it is generally hard to guarantee stability without (cumbersome) assumptions on the plant and disturbances. Although most data-driven control design methods incorporate some sort of stability proof, they generally rely on system knowledge like the order of the plant or its relative degree (Egardt, 1979; Åström and Wittenmark, 1995), or they require a sufficiently exciting input signal of some order (Rohrs et al., 1985). As a consequence, these methods still require a considerable amount of plant modeling and manual experiment design. Additionally, the closed loop is tuned to specific conditions, and the effects of a change in these conditions on the controller and its adaptation are unclear in general.

1.4 Problem statement

Several demands are formulated for a data-driven control design method for performance improvement of motion systems:

- To overcome the flaws of model-based control design that were identified in Section 1.2, the candidate algorithm should only marginally depend on models of the plant. Ideally, plant information should be considered as *a priori* information to initialize the algorithm, but during adaptation with measurement data the plant model should have no effect, thereby avoiding the implications of inherent assumptions and approximations of the model. Consequently, the achievable result should be independent of the quality and

applicability of a plant model.

- For maximum independence of model-based design techniques, the candidate algorithm should not rely on an implicit model. Many data-driven control design techniques rely on an implicit model, and although this model reflects the instantaneous behavior of the system in the loop, it also introduces some of the assumptions and approximations of modeling.
- For maximum performance, the controller should adapt to the dynamics and disturbances of the actual plant encountered during normal operation, without the addition of any auxiliary signal. This implies that the control design algorithm should not depend on dedicated experiments, but that it should adapt under normal operation instead. Furthermore, signals injected in the loop needed for the adaptation of the controller parameters should be omitted. For immediate adaptation, the algorithm should perform realtime adaptation, i.e., adaptation at the sample rate.
- A guarantee for stability is hard to give for data-driven control design methods, since they can not rely on the established theory of model-based stability. Nevertheless, for data-driven control design techniques it is equally important to provide such a guarantee.
- The computational load of the algorithm is important, especially with real-time adaptation, since the sample time of motion systems typically is short. All computations should be finished within one sample time for online implementation. For batch adaptation, the constraints on the computation time can be relaxed.

As already described in the previous section, current methods only partially meet these demands. In the next section, an overview of common approaches of data-driven control design is presented, and their fulfillment of the demands is discussed.

Based on the preceding, the problem statement that is addressed in this thesis is: “Derive a data-driven control design method that is applicable for the performance improvement of motion systems, hence, that meets the specified demands.”

The approach to solve this problem is presented in Section 1.6. But first, an overview and discussion of current approaches is discussed.

1.5 Data-driven control design approaches

Since many years now, a considerable amount of effort is focussed on data-driven control design methods. A multitude of approaches exists, originating from different design perspectives and priorities. Although this thesis is primarily focussed on performance improvement, other works might emphasize robustness for model uncertainties or avoidance of the modeling step altogether. These different viewpoints result in different (sub-)optimal data-driven design strategies.

Roughly, data-driven control design can be divided in indirect methods, which still uses an implicit model, and direct methods. Furthermore, some approaches can be applied recursively in realtime, i.e., at the sample rate, whereas other methods can only be applied batch-wise.

From the methods that exist for data-driven control design, here, the most common data-driven control design approaches are discussed. This overview is by no means exhaustive or complete, but rather meant as a short introduction to some of the methods.

1.5.1 Self Tuning Regulator

The Self Tuning Regulator is introduced by Åström and Wittenmark (1972, 1973). It is an indirect method, since implicitly it uses an ARX model for which the parameters are estimated using least squares. Then a minimum variance controller is designed analytically with this model without addressing uncertainties (i.e., certainty equivalence principle). This results in an unbiased optimal controller if the parameters are constant and the noise is white. Numerous literature on extension and applications of the Self Tuning Regulator appeared in the 80's and 90's, see for instance (Åström and Wittenmark, 1995) and references therein.

1.5.2 Model Reference Adaptive Systems

The Model Reference Adaptive System dates back to the early 60's. This method uses a reference model that defines the desired output for a given command signal. The controller is adapted using the error between the actual and the desired output. In (Egardt, 1979) it is shown that the Model Reference Adaptive Systems and the Self Tuning Regulator are in fact two special cases in one general framework.

In (Rohrs et al., 1985) it is explicitly shown that under some conditions, e.g., a sinusoidal output disturbance at any frequency, stability of Model Reference

Adaptive Systems is not guaranteed. With a “sufficiently exciting” input signal in the “proper frequency range” this problem might be suppressed (Åström, 1985). However, then it remains to determine these properties.

1.5.3 Iterative Feedback Tuning

Several methods exist for Iterative Feedback Tuning, e.g., in the time domain (Hjalmarsson, 2002) and in the frequency domain (Kammer et al., 2000). In (De Bruyne and Kammer, 1999) a guarantee for stability is provided, using the ν -gap (Vinnicombe, 1993).

In Iterative Feedback Tuning, a cost-function is explicitly defined. This cost-function is minimized by determination of its gradient to the controller parameters, which is achieved using a dedicated experiment. In this dedicated experiment, the error of a preliminary experiment is inserted as the reference signal. For Single-Input/Single-Output systems and under assumption of linearity, the gradient is derived from the measurement data of this experiment. The gradient is unbiased only if the disturbances in the two experiments are uncorrelated. The method is applied batch-wise, due to the dedicated experiment.

1.5.4 Extremum Seeking Control

The data-driven method of Extremum Seeking Control optimizes for a feedback controlled system an objective function that is known to have an extremum. It uses a probing signal and demodulation to recover the gradient of the objective function to the controller parameters (Krstić, 2000). Stability of the adaptive system is proven with the averaging method, which shows that the closed loop system converges to a small neighborhood of the extremum (Krstić and Wang, 2000).

1.5.5 Virtual Reference Feedback Tuning

Virtual Reference Feedback Tuning (Campi et al., 2002) is a single-shot data-driven control design method, that designs a controller from a batch of data. The controller is shaped such that the closed loop matches a desired behavior. For this, a cost-function is minimized using a fictitious reference to predict the performance of the controllers. Some plant knowledge has to be available to be able to specify the desired behavior, for if the desired behavior can not be matched by the actual closed-loop, stability is not ensured (Hjalmarsson, 2005).

In (Kostić, 2004; Kostić et al., 2004) an alternative for Virtual Reference Feedback Tuning is proposed, without inversions and with less filtering operations.

1.5.6 Markov Data-Based LQG Control

Markov Data-Based LQG Control is an indirect method that estimates the Markov parameters (impulse response coefficients) from given measurement data, for which a finite-horizon LQG controller is derived (Shi and Skelton, 2000). A receding horizon algorithm can be constructed to track plant changes over time (Aangenent, 2003; Aangenent et al., 2005).

Although the algorithm results in good tracking even for time-varying plants, no guarantee exists for stability and performance. The receding horizon controller is real-time implementable for a small prediction horizon only.

1.5.7 Fixed Structure Iterative Learning Control

This method recursively adapts the gains in a restricted structure feedforward controller (Van der Meulen et al., 2007). It employs an optimization that is convex in the controller parameters and shows good performance in the experimental design of a feedforward controller. However, since this method requires convex optimization, it is not suited for generic feedback control design but seems limited to specifically structured cases and feedforward design (Van der Meulen, 2005). And even for the specific feedback structures, dedicated experiments are needed to derive the gradients of the error to the controller parameters.

1.5.8 Multiple Model Adaptive Control

In Multiple Model Adaptive Control the uncertainty is divided in smaller regions, assigning a model to each subinterval. Online model-matching is used to detect what model contains the actual plant and, subsequently, the controller for this model is inserted in the loop. Since this controller only has to be robust for a smaller uncertainty region, the performance that can be achieved is higher under the assumption that the correct region is detected by the model-matching. In (Athans et al., 2005) an overview is given of several methods and several switching procedures.

Although models are made for the plant, online data is used to select the specific controller to be implemented, making this method a data-driven control design method.

Paul et al. (2005) use the direct method of Multiple Controller Adaptive Control to evaluate the performance of the controllers, without the risk of model-mismatch that possibly results in instability.

1.5.9 Unfalsified Control

This data-driven, plant-model-free control design approach is introduced in (Safonov and Tsao, 1997) and it recursively falsifies controllers from a candidate set that fail to satisfy a performance requirement, given measured data. The controllers whose ability to meet the performance requirement is not contradicted by the available data are said to be unfalsified, and one controller that is unfalsified is implemented. If the unfalsification procedure is repeated over time, a recursive algorithm is constructed.

Some plant knowledge is required to determine the maximum achievable performance and to select the candidate controllers. Restrictions apply to the controller class, the controllers have to be Stably Causally-Left-Invertible (Paul, 2005), although current works offer a relaxation (Zhang and Ioannou, 2006; Manuelli et al., 2007).

1.5.10 Discussion of existing techniques

The existing data-driven control design techniques meet the demands to a varying degree. However, they also exhibit presumably insurmountable deficiencies.

The Iterative Feedback Tuning, Extremum Seeking Control and Fixed Structure Iterative Learning Control algorithms require dedicated inputs in the experiment, thereby compromising or at least restricting normal operation.

The Model Reference Adaptive System, Self Tuning Regulator, Markov Data-Based LQG Control and Multiple Model Adaptive Control algorithms largely depend on implicit models and model-based control design techniques, although for the latter this is relaxed with the Multi Controller Adaptive Control approach of Paul et al. (2005).

The Virtual Reference Feedback Tuning algorithm is limited to batch-wise adaptation. Besides, as is observed in (Lecchini et al., 2002), Virtual Reference Feedback Tuning results in a sub-optimal solution, thereby sacrificing performance. Nevertheless, it can be used as a data-driven method for initialization of other methods.

Within the framework of Unfalsified Control, the adaptation of the controller parameters is independent of a plant model. Although the controller structure can

be designed with plant model knowledge, the adaptation is entirely based on observed data. Moreover, the falsification of candidate controllers does not rely on an implicit model, since it relies solely on data-driven inferred performance. Furthermore, the concept can be implemented both with realtime adaptation and with batch-wise adaptation. The concept does not require dedicated experiments but performs the adaptation during normal operation.

Undeniably, several issues arise in the application of Unfalsified Control, which have to be addressed for implementation on a motion system. To mention a few: a computationally cheap implementation, guaranteed stability and a generalization to multivariable controllers.

1.6 Contributions

In order to solve the problem statement as defined in Section 1.4, the goal of this thesis is to adapt Unfalsified Control such that it is applicable for performance improvement of motion systems. This implies that the method should be fit for online realtime adaptation, and that multivariable controllers should be handled. Furthermore, the applicability of the method is to be demonstrated in simulations and in experiments.

Unfalsified Control can be implemented with adaptation of the controller at the sample rate (realtime adaptation, (Tsao and Safonov, 2001)) or at a lower rate (e.g., batch adaptation (Woodley et al., 1999)). In batch adaptation, the unfalsification algorithm is applied only after a batch of data is collected. As a benefit, the computational load to compute the Unfalsified Set, which is the set of controllers that are unfalsified, is of minor importance, since no hard constraint is put on the calculation time if the time between two batches is not strict. Conversely, realtime adaptation puts a hard constraint on the computational load during experimental implementation, since the method has to come up with a new Unfalsified Set and unfalsified controller to implement within one sample time. The computational load for batch adaptation seems harder, however, the batch implementation allows for longer calculation times, thereby relaxing the hard constraint. Because of the challenge of the hard constraint on the computational load, the focus of this work is on realtime adaptation. In Chapter 7, a side-step to batch adaptive unfalsified control is provided.

In realtime adaptation, the set of unfalsified controllers is updated every time step to reflect the information contained in new measurement data. In some works,

e.g., (Jun and Safonov, 1999; Collins and Fan, 1999; Brozenec et al., 2001), a discrete set of controllers is selected, such that only a finite set of controllers has to be evaluated. As a consequence, the computational load is directly linked to the number of initial candidate controllers. However, considerable plant knowledge has to be available for a substantiated choice of the selection of the parameters. In other works, (Safonov and Tsao, 1997; Tsao and Safonov, 2001; Tsao et al., 2003), the set of candidate controllers is defined by a continuous region, hence containing infinitely many controllers, thereby discarding the constraint of a limited number of candidate controllers.

In (Tsao and Safonov, 2001), the unfalsification algorithm involves a Linear Programming optimization problem. This property makes them less suitable for implementation with realtime adaptation on a system with a fast sample rate, such as a motion system, since the optimization might be too computationally demanding to finish within every sample time even for relatively simple control laws.

An optimization problem can be avoided, if an approximation of the Unfalsified Set is considered. In (Cabral and Safonov, 2004), the Unfalsified Set is approximated by an outer-bounding ellipsoid, the update of which is computed by the ellipsoid algorithm (Boyd et al., 1994). This algorithm provides an analytical update, which is computationally cheap. However, the update algorithm uses one half-plane through the center of the ellipsoid, the ‘cutting plane,’ as an approximation of the separation between control parameter sets that are falsified by the new measurement data and control parameter sets that are unfalsified by it. As a consequence, this cutting plane can only be applied when the current control parameter set (which in (Cabral and Safonov, 2004) is the center of the current ellipsoidal Unfalsified Set) is falsified. When the current control parameter set is unfalsified, the ellipsoid is not changed and the newly acquired unfalsification information is discarded. Other algorithms can be used to tighter bound the approximation of the intersection of the two ellipsoids to improve convergence. However, as stated by Henrion et al. (1998), “the problem of describing the ellipsoid of smallest volume that contains the intersection of given ellipsoids is NP-hard.” Solutions often rely on iterative optimization procedures (such as LMI optimizations) and, although subject to extensive research for many years, only in a few exceptional cases the exact solution is known. The exact solutions are known, for instance, when the ellipsoid is exactly sliced in half (as in Cabral and Safonov (2004)), when the centers of two intersecting ellipsoids coincide, or when at least one ellipsoid degenerates into two parallel half-spaces (Katsaggelos et al., 1991; Pronzato and Walter, 1994; Maksarov and Norton, 1996; Ros et al., 2002). When these methods are applied to intersections that do not match these cases, an outer-bounding ellipsoid might result, however, it will not be of minimal volume, resulting in slow convergence.

To summarize, if no compromises are made with respect to convergence and accuracy, then the intersection procedure is computationally demanding.

In the work presented here, Ellipsoidal Unfalsified Control is introduced. In Ellipsoidal Unfalsified Control, the problem of a computationally demanding intersection procedure is overcome by a suitable choice for the performance requirement and the controller structure, hence, without compromises with respect to convergence and accuracy. The region of unfalsified control parameters, the Unfalsified Set, is described by an ellipsoid $\mathcal{E}(t_{k-1})$. At each sample step, new measurement data specifies a region of unfalsified controllers, $\mathcal{U}(t_k)$, which is a degenerate ellipsoid and is described by two parallel half-spaces. Consequently, the ellipsoid $\mathcal{E}(t_k)$, which is the minimal-volume outer-bounding ellipsoidal approximation of the intersection $\mathcal{E}(t_{k-1}) \cap \mathcal{U}(t_k)$, can be computed analytically. The current controller parameter set does not need to be falsified for the update of $\mathcal{E}(t_k)$ and, moreover, two cutting planes are defined, neither of which is restricted to pass through the center of the ellipsoid. Since the ellipsoid $\mathcal{E}(t_k)$ can be computed analytically, the update is fast and likely to be suited for Unfalsified Control with realtime adaptation.

Sufficient conditions are provided to guarantee the stability of this plant-model-free control design method, based on the results in (Stefanovic et al., 2005). It only needs the fundamental feasibility assumption, i.e., the assumption that in the initial candidate controller pool there is at least some region with control parameter sets that fulfill the performance requirement at all times. If this assumption is fulfilled, stability can be guaranteed by a suitable selection of the settings of the adaptive control algorithm.

Clearly, the strength of a data-driven control design method is best demonstrated with real-life experiments. While simulations might provide useful insights on isolated phenomena, the method typically is desired to work with the entire ensemble of phenomena as encountered in experiments, such as friction, sensor and actuator noise, saturations, quantization, computational delays, to mention only a few. Besides, contrary to simulations where the computation time at each sampling instant is unrestricted because realtime evaluation is not required, with realtime implementation on a physical system the sample time imposes a limit on the computation time. The results of the application of this data-driven control design method to a motion system are shown and evaluated, together with the realization of the specific design choices.

Furthermore, in this thesis the extension of the Ellipsoidal Unfalsified Control algorithm to multi-input multi-output (MIMO) plants is provided. A diagonal

controller can be constructed by applying the current Ellipsoidal Unfalsified Control algorithm to several inputs and outputs (decentralized control). However, the performance with decentralized control may be poor because no attempt is made to counteract the interactions (Skogestad and Postlethwaite, 2005). To overcome this shortcoming, an extension to the Ellipsoidal Unfalsified Control framework is proposed to cover general, full-block multivariable controllers.

1.7 Structure

The philosophy of Unfalsification is recalled in Chapter 2, and an introduction to Unfalsified Control is provided. In Chapter 3, the theory of Ellipsoidal Unfalsified Control is introduced, and it is shown how the design choices lead to a computationally cheap update of the set of unfalsified controllers. Preliminary results on Ellipsoidal Unfalsified Control can also be found in (Van Helvoort et al., 2005, 2008). Stability of Ellipsoidal Unfalsified Control is proven in Chapter 4, with only the assumption of feasibility, see also (Van Helvoort et al., 2006a,b). The results of the implementation of Ellipsoidal Unfalsified Control in simulation and experiment, as also will appear in (Van Helvoort et al., 2007a), is presented in Chapter 5. These results clearly indicate the applicability of the proposed method on a real life system. In Chapter 6, the extension of the proposed method to full-block multivariable controllers is presented, as also appeared in (Van Helvoort et al., 2007b,c). Chapter 7 presents the application of Unfalsified Control with the same design choices as Ellipsoidal Unfalsified Control, however, with a batch-wise adaptation. The contents are based on (Verkooijen, 2007), and will also appear in (Van Helvoort et al., 2007d). This relaxation enables a more strict description of the region of unfalsified controllers. Finally, conclusions and recommendations are presented in Chapter 8 and Chapter 9, respectively.

Chapter 2

Unfalsification

U*NFALSIFIED* control is used as the framework for data-driven control design in this thesis. In this chapter, the philosophy of unfalsification is briefly recalled and its use in *Unfalsified Control* is explained. Then, the key elements that form an Adaptive Unfalsified Controller are defined.

2.1 Unfalsification of hypotheses

As a reaction to classical empiricism, the philosopher Karl Popper embraced the idea of falsification (Popper, 2002). In his book, Popper argues that scientific theories can never be proven, merely tested and accordingly ratified or falsified. Clearly, this view is in contradiction to deductionism, which tries to deduce universal theories from observations. A famous example of this perspective is given by Popper's swan argument (Popper, 2002, p. 4): no matter how many *white swans* one may have observed, the statement "all swans are white" is easily falsified by the observation of a single *black swan* (see Fig. 2.1).

2.2 Unfalsified Control

In Unfalsified Control, the ability of controllers to meet the given performance requirement is considered. The theory of unfalsification of hypothesis is used to



Figure 2.1: Illustration of Popper's swan argument: the observation of a single black swan falsifies the statement "all swans are white."

distinguish between controller that are *demonstrably unable* to meet the given performance requirement by measurement data and controllers that are not: the first set defines the falsified controllers, whereas the second set contains the unfalsified controllers. Instead of trying to find *the* best controller (at a certain time), this adaptive control concept finds the set of controllers that is good enough. Since no assumptions are made on future behavior, unfalsified controllers might get falsified by future measurement data.

Definition 2.1 (Controller Unfalsification) *A controller is said to be falsified by measurement information if this information is sufficient to deduce that the performance requirement would be violated if that controller were in the feedback loop. Otherwise, the controller is said to be unfalsified. (Safonov and Tsao, 1997)*

The concept of controller unfalsification is schematically depicted in Fig. 2.2. Measurement data is used to evaluate if controllers are able to meet the performance requirement. The set of controllers is then divided in two sets: the set with controllers whose ability to satisfy the performance requirement is falsified by measurement data and the set with controllers whose ability is unfalsified. In fact, the first set could be compartmentalized for instance by the number of times the controllers are falsified or the last time that falsification occurred, which could then be used for the re-enabling of candidate controllers, as is proposed in Section 2.3.3.

¹Photo courtesy of S. Brosen

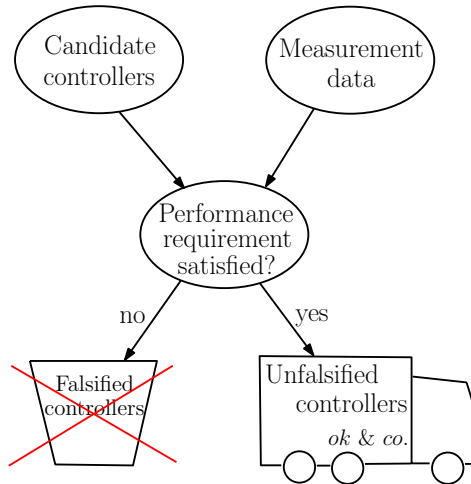


Figure 2.2: Schematic representation of controller unfalsification.

2.3 Elements of Adaptive Unfalsified Control

Actually, in the construction of an Adaptive Unfalsified Controller, controller unfalsification is just one element. The elements to obtain an Adaptive Unfalsified Controller are discussed next.

2.3.1 Performance inference

A straight forward method to determine the performance of candidate controllers would be to implement all controllers one-by-one. However, this would lead to poor transient behavior, especially if a switching strategy with a predefined sequence ('pre-routed') as in (Mårtensson, 1985; Fu and Barmish, 1986) were to be adopted, since it might take long before even a stabilizing controller is inserted. Transients can be improved by online selection of the 'optimal' candidate controller to be inserted. In (Narendra and Balahrishnan, 1994) the controllers are designed with accompanying models, and the errors between the modeled output and the measured output is the selection criterion for the controllers to be implemented. A similar approach is followed in Multiple Model Adaptive Controller, see for instance (Athans et al., 2005).

Instead of following the two-step procedure of model-matching and performance inference, in Unfalsified Control the performance of controllers is directly determined from measurement data. The application of the ‘fictitious reference signal’ allows the deduction of the performance of controllers without the need to implement them and without the need of an accompanying model.

The application of the fictitious reference inevitably also has some drawbacks. As discussed in Section 3.3.1 on page 23, the fictitious reference excites different dynamics than the actual reference. Consequently, the inference of the performance might be inaccurate, resulting in the wrongly (un-)falsification of candidate controllers. This property might hamper the achievable performance with the proposed method. Nevertheless, despite this drawback, the fictitious reference is used in this thesis to directly infer the candidate controllers’ performance.

2.3.2 Controller unfalsification

The inferred performance of the candidate controllers is compared to the requirement. In this thesis, a deterministic check is used, i.e., the controller either meets or does not meet the requirement. Non-deterministic checks might be used, as was already observed in (Safonov and Tsao, 1994), for instance to handle outliers and sensor faults. However, the deterministic method fits naturally in the framework that from data it is concluded that a controller is either good or bad, without assumptions on the process or noise distributions. In the current work, outliers and sensor faults are handled by a weighting filter. (Of course, preliminary information is needed to predict the probability of outliers and sensor faults and to design the weighting filter accordingly.)

In contrast to works that perform an *optimization* of the performance, here a predefined performance requirement is explicitly used. This is in accordance with the philosophy of unfalsification, which ratifies or dismisses predefined hypotheses with data, in contrast to enforcing an ordering of the hypothesis based on the data.

2.3.3 Update of the set of unfalsified controllers

A set is constructed with all the controllers for which it is not shown that they do not meet the performance requirement. Hence, once a controller is falsified, it is removed from this set. As a result, the set is monotone non-increasing.

In this thesis, the set of unfalsified controllers is a continuous set that is recursively approximated with an ellipsoid. The approximation is outer-bounding to not wrongly dismiss unfalsified controllers, at the expense of wrongly retaining falsified controllers. Accordingly, controllers are in the ellipsoid that are not in the set of unfalsified controllers. Nevertheless, it is guaranteed that the final controller is chosen from the set of unfalsified controllers that is constructed with the measurement data since the last update of the ellipsoid.

To address time-varying performance requirements or time-varying plants, in some works a forgetting factor is proposed to re-enable controllers that were once falsified. Another, more ad hoc, option is to base re-enabling of controllers on their proximity to the current set of unfalsified controllers. If the set of falsified controller is compartmentalized as is proposed in Section 2.2, this subdivision can be used as a re-enabling criterion. De facto, these methods result in the expansion of the set of unfalsified controllers, thereby enabling a shift of the set of unfalsified controllers in the controller parameter space.

2.3.4 Controller adaptation

An adaptive controller is only achieved, if the unfalsification information is used to update the controller parameters. Once it is derived that the currently implemented controller is not able to meet the performance requirement, it should be replaced by a controller whose ability is not (yet) falsified. The currently implemented controller is maintained as long as it is able to meet the performance requirement, which minimizes switching. Consequently, a relaxed and barely exciting trajectory for which the performance requirement is easily met does not result in controller parameter drift.

The update of the controller parameters basically is arbitrary, as long as it is from the set of (up-to-then) unfalsified controllers. In this thesis, a deterministic switching algorithm is proposed that is used to enforce a limited number of controller switches.

An alternative to direct adaptation of the controller parameters is a batch-wise, or run-to-run, adaptation. With this method, the controller parameters are only updated after an entire batch of data is collected, irrespective of the intermediate falsification of the currently implemented controller.

The combination of the four elements performance inference, controller unfalsification, update of the set of unfalsified controllers and controller adaptation forms the Adaptive Unfalsified Controller. The method presented in the next sections is an Adaptive Unfalsified Controller that contains all four elements.

Chapter 3

Ellipsoidal Unfalsified Control

IN THIS chapter, *Ellipsoidal Unfalsified Control* is introduced. This theory uses the general framework of *Unfalsified Control* and appends this framework with a suitable choice for the performance requirement, the controller structure and the description of the set of unfalsified controllers. These choices guarantee an analytic solution to the update of the set of unfalsified controllers, which enables real-time online implementation on a motion system.

3.1 Preliminaries

In this thesis, discrete-time controllers are considered that are parameterized with a controller parameter vector $\theta \in \mathbb{R}^p$. The controllers are causal and time-invariant for a fixed θ . The structure of the controllers is fixed and defined a priori. The controller parameter vector θ , also called the controller parameter set θ , is used as a representation of the corresponding controller.

3.2 Performance requirement

A key issue in Unfalsified Control is the performance requirement. The ability of controllers to meet the predefined performance requirement directly determines whether a controller is unfalsified or not, see (Safonov and Tsao, 1997).

Let the performance requirement be defined as a (time-dependent) bound $0 < \Delta(t_k) < \infty$ on the tracking error plus a κ -weighted control effort, $\kappa(t_k) > 0$:

$$|W(q)e(t_k)| + \kappa(t_k)|u(t_k)| \leq \Delta(t_k) \quad (3.1)$$

with

$$e(t_k) = G_m(q)r(t_k) - y(t_k) \quad (3.2)$$

Here, q is the backward time-shift operator (i.e., $q * t_k = t_{k-1}$), $W(q)$ is a stable filter, e.g., a low-pass filter to reduce the effect of outliers, $G_m(q)$ is the desired closed loop dynamics and r , u and y are defined as in Fig. 3.1.

The performance requirement (3.1) contains both a condition on $y(t_k)$ and on $u(t_k)$ to guarantee that both signals remain bounded. Instead of simply $u(t_k)$, also a condition on $u(t_k) - u_{\text{ref}}(t_k)$ can be considered with $u_{\text{ref}}(t_k)$ the expected behavior of $u(t_k)$, however, this would require extended plant knowledge.

To perform the check (3.1) for all controllers would be a tedious job, all the more since it has to be done for all possible operating conditions. Therefore, the fictitious reference is considered to infer the performance of controllers that are not implemented.

3.3 Fictitious reference

The fictitious reference is a fictitious signal, used to infer the performance of controllers. For a given controller, the fictitious reference is defined as *the reconstructed reference signal* that would have resulted in *exactly the measured input and output* of the plant if that controller *would have been* implemented. A schematic representation of the construction of the fictitious reference is shown in Fig. 3.1. Measurement data $[u, y]$ is acquired with controllers $C_r(\tilde{\theta})$ and $C_y(\tilde{\theta})$ in the feedback loop. Then the fictitious reference $r_{\text{fict}}(\theta')$ is constructed for a general controller parameter set θ' , such that had $r_{\text{fict}}(\theta')$ been applied to the system with controllers $C_r(\theta')$ and $C_y(\theta')$ this would exactly have resulted in the measured $[u, y]$.

The concept of a fictitious reference enables the evaluation of controllers, even if they were not in the loop at the time of the measurement, for the fictitious error $e_{\text{fict}}(\theta, t_k)$ instead of the actual tracking error (3.2) can be used to evaluate (3.1), with

$$e_{\text{fict}}(\theta, t_k) = G_m(q)r_{\text{fict}}(\theta, t_k) - y(t_k) \quad (3.3)$$

This substitution enables the construction of a region containing the controllers that are unfalsified by current measurement data at time t_k :

$$\mathcal{U}(t_k) = \{\theta \mid |W(q)e_{\text{fict}}(\theta, t_k)| + \kappa(t_k)|u(t_k)| \leq \Delta(t_k)\} \quad (3.4)$$

$$= \{\theta \mid -\hat{\Delta}(t_k) \leq W(q)e_{\text{fict}}(\theta, t_k) \leq \hat{\Delta}(t_k)\} \quad (3.5)$$

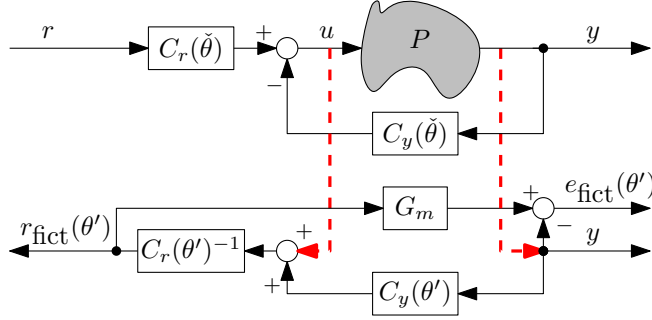


Figure 3.1: Schematic representation of the construction of the fictitious reference r_{fict} and fictitious error e_{fict} .

with

$$\hat{\Delta}(t_k) = \Delta(t_k) - \kappa(t_k)|u(t_k)| \quad (3.6)$$

It should be noted that $\mathcal{U}(t_k)$ is empty for $\hat{\Delta}(t_k) < 0$.

Note that with (3.4) not only controllers are falsified that, ultimately, do not meet the performance requirement, but also those that are not able to do that starting from the current controller states. This implies that switching control parameter set θ does not need any accompanying measures, like resetting the controller states, to guarantee a suitable transient.

3.3.1 Remark on the fictitious reference

The fictitious reference signal is used as a tool to infer the performance of controllers, thereby eliminating the need to implement all controllers. However, since this fictitious signal differs from the actual reference, the evaluation based on the fictitious reference might not hold for the actual reference. Different dynamics might be emphasized or, on the contrary, not excited (Engell et al., 2007), resulting in the erroneous falsification or unfalsification of controllers. Consider for instance Fig. 3.1, where the actual tracking error is defined as $e = G_m r - y$ and

next equations can be derived:

$$y = \frac{PC_r(\check{\theta})}{1 + PC_y(\check{\theta})}r \quad (3.7)$$

$$u = \frac{C_r(\check{\theta})}{1 + PC_y(\check{\theta})}r \quad (3.8)$$

$$e = \frac{G_m(1 + PC_y(\check{\theta})) - PC_r(\check{\theta})}{1 + PC_y(\check{\theta})}r \quad (3.9)$$

$$\begin{aligned} r_{\text{fict}}(\theta') &= C_r(\theta')^{-1}(u + C_y(\theta')y) \\ &= \frac{C_r(\theta')^{-1}C_r(\check{\theta})(1 + PC_y(\theta'))}{1 + PC_y(\check{\theta})}r \end{aligned} \quad (3.10)$$

$$\begin{aligned} e_{\text{fict}}(\theta') &= G_m r_{\text{fict}}(\theta') - y \\ &= \frac{G_m C_r(\theta')^{-1}C_r(\check{\theta})(1 + PC_y(\theta')) - PC_r(\check{\theta})}{1 + PC_y(\check{\theta})}r \end{aligned} \quad (3.11)$$

$$\neq \frac{G_m(1 + PC_y(\theta')) - PC_r(\theta')}{1 + PC_y(\theta')}r, \quad \text{for general } \theta' \neq \check{\theta} \quad (3.12)$$

For the evaluation of a general controller parameter set θ' , ideally (3.12) is used, since this equation represents the behavior of the controller when it is actually implemented. However, (3.11) is evaluated, which might result in the wrong (un-)falsification of controllers, due to other dynamics exited by $r_{\text{fict}}(\theta')$ than by r , as follows from (3.10).

Despite of the drawback described here, the evaluation of the fictitious reference is used in this thesis as the method to infer the performance of candidate controllers. To reduce the influence of the imperfect performance inference, a slowly decreasing performance bound is realized and a cautious parameter switching scheme is adopted, such that controllers are only falsified gradually.

3.4 Controller structure

The controller structure is chosen such that the fictitious reference generator, $r_{\text{fict}}(\theta, t_k)$, is affine in the control parameter set θ . Furthermore, $r_{\text{fict}}(\theta, t_k)$ depends on $u(t_k)$, $y(t_k)$ and filtered versions thereof and also possibly on nonlinear functions of $u(t_{k-1})$, $y(t_k)$ and past values thereof. Then, a general form for the

fictitious reference generator is given by

$$r_{\text{fict}}(\theta, t_k) = \begin{bmatrix} u(t_k) \\ \Lambda_u(q) \otimes u(t_{k-1}) \\ \Lambda_y(q) \otimes y(t_k) \\ f(u(t_{k-1}), y(t_k), q) \end{bmatrix}^T \begin{bmatrix} \theta_1 \\ \theta_2 \\ \theta_3 \\ \theta_4 \end{bmatrix} \quad (3.13)$$

$$= w(u(t_k), y(t_k), q)^T \theta, \quad (3.14)$$

where $\Lambda_u(q)$ and $\Lambda_y(q)$ are vectors of asymptotically stable linear filters and \otimes denotes the Kronecker product. The vector $f(u(t_{k-1}), y(t_k), q)$ contains globally asymptotically stable nonlinear functions that are bounded in amplitude for all $u(t_{k-1})$ and $y(t_k)$. Clearly, (3.14) defines the set of candidate controllers, as it follows that

$$u(t_k) = \begin{bmatrix} r(t_k) \\ \Lambda_u(q) \otimes u(t_{k-1}) \\ \Lambda_y(q) \otimes y(t_k) \\ f(u(t_{k-1}), y(t_k), q) \end{bmatrix}^T \begin{bmatrix} 1/\tilde{\theta}_1 \\ -\tilde{\theta}_2/\tilde{\theta}_1 \\ -\tilde{\theta}_3/\tilde{\theta}_1 \\ -\tilde{\theta}_4/\tilde{\theta}_1 \end{bmatrix} \quad (3.15)$$

Figure 3.2 shows a schematic representation of controller (3.15) and fictitious reference generator (3.13).

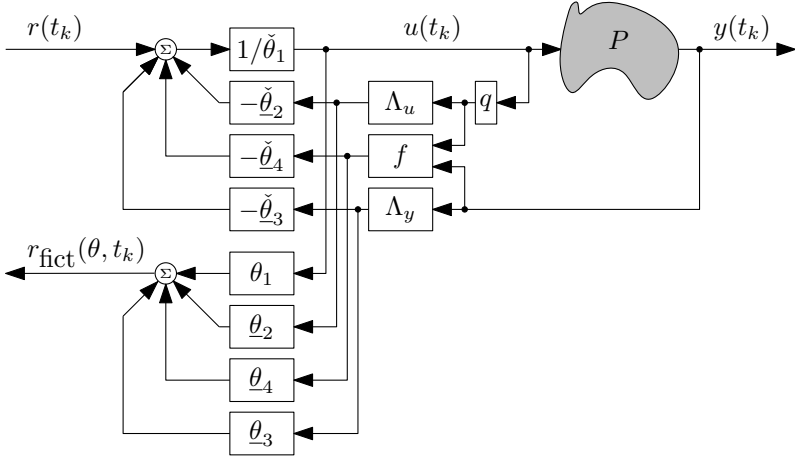


Figure 3.2: Schematic representation of controller (3.15) and fictitious reference generator (3.13).

Similar to (Paul, 2005), a controller is considered *Stably Causally-Left-Invertible (SCLI)* if the corresponding fictitious reference generator is causal and stable (Paul, 2005, Definition 9). These conditions ensure that the fictitious reference signal is uniquely determined by past and present measurement data and that the

relating system is stable. For controller (3.15) to be SCLI the requirement is that $\check{\theta}_1 \neq 0$.

The controller of Fig. 3.2 equals the controller of Fig. 3.1 by substitution of $C_r(\check{\theta}) = \frac{1}{\check{\theta}_1 + \check{\theta}_2^T \Lambda_u(q)}$, $C_y(\check{\theta}) = \frac{\check{\theta}_3^T \Lambda_y(q)}{\check{\theta}_1 + \check{\theta}_2^T \Lambda_u(q)}$ and $\check{\theta}_4 = 0$.

Controller structure (3.13) imposes the constraint that $C_r(\check{\theta})$ and $C_y(\check{\theta})$ have a shared parametrization of the denominator, however, the parametrization itself is free to choose. Furthermore, the numerator of $C_r(\check{\theta})$ does not depend on $\check{\theta}$, but it is influenced by the selection of the denominators of the filters in $\Lambda_u(q)$.

The region $\mathcal{U}(t_k)$, (3.5), defines two parallel half-spaces for $\hat{\Delta}(t_k) > 0$, as can be seen by substitution of (3.14) in (3.3):

$$\mathcal{U}(t_k) = \{\theta \mid -1 \leq \phi_k^T \theta - y_k \leq 1\} \quad (3.16)$$

with

$$\phi_k = \frac{W(q)G_m(q)w(u(t_k), y(t_k), q)}{\hat{\Delta}(t_k)} \quad (3.17)$$

$$y_k = \frac{W(q)y(t_k)}{\hat{\Delta}(t_k)} \quad (3.18)$$

Consequently, the application of the fictitious reference generator (3.14) together with the combined evaluation of $e_{\text{fict}}(t_k)$ and $u(t_k)$ in the performance requirement (3.4) results in two parallel half-spaces (3.16).

3.5 Noise analysis

Since Ellipsoidal Unfalsified Control does not employ any model of the plant, no distinction between plant output and noise can be made. At best a distinction can be made between a part of $y(t_k)$ that correlates with the reference and a part that does not, part of which may originate from noise. The influence of both parts of $y(t_k)$ on $e(t_k)$ and $u(t_k)$ is affected by their magnitude and by the controller, and has to be bounded, otherwise the controller is falsified.

Let the part of $y(t_k)$ that does not correlate with the reference be given by $d(t_k)$ and be bounded by \bar{d} . Let the influence of $d(t_k)$ on the tracking error $e(t_k)$ be bounded by $\bar{e}(\theta)$ and let the influence of $d(t_k)$ on the control effort $u(t_k)$ be bounded by $\bar{u}(\theta)$. Then the influence of $d(t_k)$ on the performance requirement (3.4) is bounded by $\bar{e}(\theta) + \kappa(t_k)\bar{u}(\theta)$.

Controllers for which the influence of $d(t_k)$ on $e(t_k)$ and $u(t_k)$ is too large are

falsified. Hence, by upperbounding the performance requirement (3.4) with $\Delta(t_k)$, simultaneously the transfers of $d(t_k)$ to the error and to the control effort are bounded.

The maximum influence of $d(t_k)$ on the performance requirement is $\bar{e}(\theta) + \kappa(t_k)\bar{u}(\theta)$ and the performance requirement of the ‘noisy’ case as compared to the ‘noise free’ case is as $|e(t_k)| + \kappa(t_k)|u(t_k)| \leq \Delta(t_k) - (\bar{e}(\check{\theta}) + \kappa(t_k)\bar{u}(\check{\theta}))$. So, the effect of $d(t_k)$ can be seen as a tightening of the performance requirement, thereby reducing the chance of feasibility. In the design of the adaptive control problem, a lower bound on $\Delta(t_k)$ should be included, to assure $\Delta(t_k) - (\bar{e}(\check{\theta}) + \kappa(t_k)\bar{u}(\check{\theta})) > 0$.

3.6 Unfalsified Set

The region $\mathcal{U}(t_k)$ defines the region of controllers that are unfalsified by measurement data at time t_k . To merge the unfalsification information with previous measurement data, consider first the definition of the True Unfalsified Set.

Definition 3.1 *The True Unfalsified Set E_{tus} is the set of controller parameter sets that are currently unfalsified by all available measurement data.*

In Ellipsoidal Unfalsified Control, the True Unfalsified Set is approximated by an ellipsoid in the controller parameter space. This ellipsoid is used as a representation for the True Unfalsified Set and will be denoted as the Unfalsified Set $\mathcal{E}(t_k)$.

The Unfalsified Set at time t_{k-1} is described by

$$\mathcal{E}(t_{k-1}) = \{\theta | (\theta - \theta_c(t_{k-1}))^T \Sigma^{-1}(t_{k-1})(\theta - \theta_c(t_{k-1})) \leq 1\} \quad (3.19)$$

with $\theta \in \mathbb{R}^p$ the controller parameters, $\theta_c(t_k) \in \mathbb{R}^p$ the center of the ellipsoid and $\Sigma(t_{k-1}) \in \mathbb{R}^{p \times p}$ the symmetric, positive definite matrix that describes the shape of the ellipsoid.

3.7 Unfalsification

The set of controller parameters that is approximately unfalsified by all measurement data is given by $\theta \in (\mathcal{E}(t_{k-1}) \cap \mathcal{U}(t_k))$, since it is both approximately unfalsified by past measurement data ($\theta \in \mathcal{E}(t_{k-1})$) and unfalsified by current measurement data ($\theta \in \mathcal{U}(t_k)$).

3.8 Update ellipsoidal Unfalsified Set

For compliance with new measurement data and, moreover, for preservation of the ellipsoidal shape of the Unfalsified Set, the intersection $\mathcal{E}(t_{k-1}) \cap \mathcal{U}(t_k)$ is approximated by a minimum-volume outer-bounding ellipsoid $\mathcal{E}(t_k)$. Since $\mathcal{U}(t_k)$ defines two parallel half-spaces, an analytic solution exists, as was shown by Pronzato and Walter (1994). Five cases are distinguished:

- (a) $\mathcal{E}(t_{k-1})$ and $\mathcal{U}(t_k)$ do not intersect: an empty intersection results (Fig. 3.3a).
- (b) $\mathcal{E}(t_{k-1})$ is intersected by only one hyper-plane of $\mathcal{U}(t_k)$ (Fig. 3.3b).
- (c) $\mathcal{E}(t_{k-1})$ is intersected by both hyper-planes of $\mathcal{U}(t_k)$ (Fig. 3.3c).
- (d) $\mathcal{E}(t_{k-1})$ is, symmetrically around the center, intersected by both hyper-planes of $\mathcal{U}(t_k)$ (Fig. 3.3d).
- (e) $\mathcal{E}(t_{k-1})$ is entirely contained in $\mathcal{U}(t_k)$: the intersection $\mathcal{E}(t_k)$ trivially is $\mathcal{E}(t_{k-1})$ (Fig. 3.3e).

3.8.1 Ellipsoid-with-Parallel-Cuts algorithm

Consider the ellipsoid $\mathcal{E}(t_{k-1})$, with its center defined by the vector $\theta_c(t_{k-1})$ and its shape by the matrix $\Sigma(t_{k-1})$, see (3.19). To compute $\mathcal{E}(t_k)$, define the variables

$$a_+ = \frac{y_k - \phi_k^T \theta_c(t_{k-1}) - 1}{\sqrt{g}} \quad (3.20)$$

$$a_- = \frac{-y_k + \phi_k^T \theta_c(t_{k-1}) - 1}{\sqrt{g}} \quad (3.21)$$

with

$$g = \phi_k^T \Sigma(t_{k-1}) \phi_k \quad (3.22)$$

and ϕ_k and y_k as defined in (3.17) and (3.18), respectively. The indicators a_+ and a_- correspond to the algebraic distance of $\theta_c(t_{k-1})$ to the bounds of $\mathcal{U}(t_k)$, in the metric defined by $\Sigma(t_{k-1})$.

In Table 3.1, the relations between the indicators a_+ and a_- and the five distinctive cases, as are discussed here, are summarized.

For case (a), $a_+ > 1$ or $a_- > 1$, and an empty intersection results. In this case, the algorithm should be terminated since the adaptive control problem is not feasible, or the requirement should be relaxed, e.g., by increasing $\Delta(t_k)$.

For case (b), $a_+ < -1$ or $a_- < -1$, and the corresponding bound does not cut the ellipsoid. To obtain the minimum volume ellipsoid, (3.20) and (3.21) are replaced

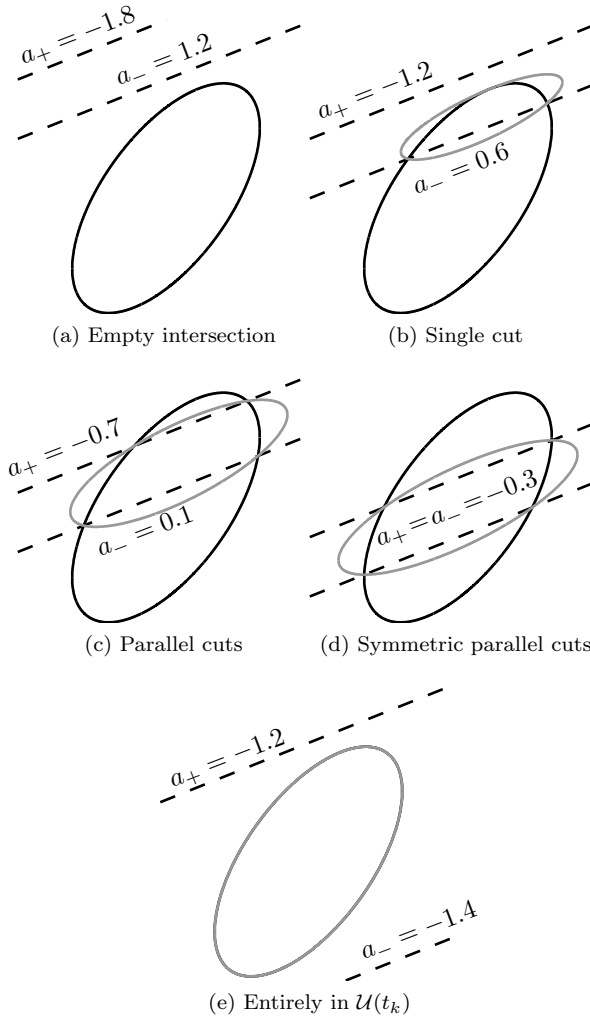


Figure 3.3: Examples (2 dimensional) of possible intersections of $\mathcal{E}(t_{k-1})$ (black, solid) and $\mathcal{U}(t_k)$ (black, dashed). Resulting minimum volume, outer-bounding ellipsoid $\mathcal{E}(t_k)$ is shown in grey. An indication is given of the values of a_+ (3.20) and a_- (3.21).

Table 3.1: Summary of cases (a) through (e) for conditions on a_+ and a_- . Note that the lower right part is inaccessible, since $a_+ + a_- = \frac{-2}{\sqrt{g}} < 0$.

	$a_- < -1$	$-1 \leq a_- \leq 1$	$a_- > 1$
$a_+ < -1$	(e)	(b) \rightarrow (c) or (d)	(a)
$-1 \leq a_+ \leq 1$	(b) \rightarrow (c) or (d)	$a_+ \neq a_-$: (c) $a_+ = a_-$: (d)	\times
$a_+ > 1$	(a)	\times	\times

by

$$a_+ = \max\left(\frac{y_k - \phi_k^T \theta_c(t_{k-1}) - 1}{\sqrt{g}}, -1\right) \quad (3.23)$$

$$a_- = \max\left(\frac{-y_k + \phi_k^T \theta_c(t_{k-1}) - 1}{\sqrt{g}}, -1\right) \quad (3.24)$$

Subsequently, the applicable case with the modified bounds is considered (case (c) or case (d)).

For case (c), it holds that $-1 \leq a_+ \leq 1 \wedge -1 \leq a_- \leq 1 \wedge a_+ \neq a_-$. Additionally, consider the inequality

$$a_+ a_- \leq 1/p \quad (3.25)$$

Recall from (3.19) that p is the number of controller parameters. If inequality (3.25) does *not* hold, then $\mathcal{E}(t_{k-1})$ is the minimum-volume outer-bounding ellipsoidal approximation of the intersection, hence, $\mathcal{E}(t_k) = \mathcal{E}(t_{k-1})$. Consequently, $\Sigma(t_k) = \Sigma(t_{k-1})$ and $\theta_c(t_k) = \theta_c(t_{k-1})$.

However, if inequality (3.25) holds, the intersection can be approximated by an ellipsoid of smaller volume, resulting in an update of $\mathcal{E}(t_k)$ as defined by (see (Pronzato and Walter, 1994))

$$\Sigma(t_k) = \delta \left(\Sigma(t_{k-1}) - \frac{\sigma}{g} \Sigma(t_{k-1}) \phi_k \phi_k^T \Sigma(t_{k-1}) \right) \quad (3.26)$$

$$\theta_c(t_k) = \theta_c(t_{k-1}) + \frac{\sigma(a_+ - a_-)}{2\sqrt{g}} \Sigma(t_{k-1}) \phi_k \quad (3.27)$$

with

$$\delta = \frac{p^2}{p^2 - 1} \left(1 - \frac{a_+^2 + a_-^2 - \rho/p}{2} \right) \quad (3.28)$$

$$\sigma = \frac{1}{p+1} \left(p + \frac{2}{(a_+ - a_-)^2} \left(1 - a_+ a_- - \frac{\rho}{2} \right) \right) \quad (3.29)$$

$$\rho = \sqrt{4(1 - a_+^2)(1 - a_-^2) + p^2(a_+^2 - a_-^2)^2} \quad (3.30)$$

For case (d), it holds that $-1 \leq a_+ \leq 1 \wedge -1 \leq a_- \leq 1 \wedge a_+ = a_- = a$. If, additionally, inequality (3.25) does not hold, then $\mathcal{E}(t_{k-1})$ is the minimum-volume outer-bounding ellipsoidal approximation of the intersection, hence, $\mathcal{E}(t_k) = \mathcal{E}(t_{k-1})$ (as with case (c)).

If, however, inequality (3.25) holds, $\mathcal{E}(t_k)$ is defined by

$$\Sigma(t_k) = \frac{p(1-a^2)}{p-1} \left(\Sigma(t_{k-1}) - \frac{1-pa^2}{(1-a^2)g} \Sigma(t_{k-1}) \phi_k \phi_k^T \Sigma(t_{k-1}) \right) \quad (3.31)$$

$$\theta_c(t_k) = \theta_c(t_{k-1}) \quad (3.32)$$

For case (e), $a_+ < -1 \wedge a_- < -1$, and, trivially, $\mathcal{E}(t_k) = \mathcal{E}(t_{k-1})$.

The ellipsoid $\mathcal{E}(t_k)$, as computed in this section, includes only points that are either in $\mathcal{E}(t_{k-1})$ or in $\mathcal{U}(t_k)$ and includes all points that are both in $\mathcal{E}(t_{k-1})$ and in $\mathcal{U}(t_k)$. Furthermore, the volume of $\mathcal{E}(t_k)$ is monotone non-increasing, since either $\mathcal{E}(t_{k-1})$ is kept or it is replaced by an ellipsoid of smaller volume.

3.9 Controller selection

A controller that is unfalsified by the available measurement data is to be inserted in the loop. Or, in other words, one controller inside $\mathcal{E}(t_{k-1}) \cap \mathcal{U}(t_k)$ is to be implemented.

The selection of the controller that is to be implemented can depend on several criteria or it might even be chosen randomly within $\mathcal{E}(t_{k-1}) \cap \mathcal{U}(t_k)$. Here, a deterministic selection is presented, which will be utilized in Section 4.5 to guarantee a limited number of switches per ellipsoid.

Consider the controller selection algorithm

$$\check{\theta}(t_k) = \begin{cases} \check{\theta}(t_{k-1}) & \text{if } |\gamma(t_k)| \leq 1 \\ \Gamma(t_k, \alpha) \check{\theta}(t_{k-1}) + (1 - \Gamma(t_k, \alpha)) \theta_c(t_k) & \text{if } |\gamma(t_k)| > 1 \end{cases} \quad (3.33)$$

with $\check{\theta}(t_{k-1})$ the currently implemented controller parameters and

$$\Gamma(t_k, \alpha) = \alpha \frac{\text{sign}(\gamma(t_k)) - \gamma_c(t_k)}{\gamma(t_k) - \gamma_c(t_k)} \quad (3.34)$$

$$\alpha \in [0, 1] \quad (3.35)$$

$$\gamma(t_k) = \phi_k^T \check{\theta}(t_{k-1}) - y_k \quad (3.36)$$

$$\gamma_c(t_k) = \phi_k^T \theta_c(t_k) - y_k \quad (3.37)$$

Note that for $|\gamma(t_k)| > 1$, $\check{\theta}(t_{k-1})$ is falsified by current measurement data (see (3.16)).

Parameter α , (3.35), determines the stepsize of the switching algorithm. Choosing $\alpha = 0$ corresponds to switching to the center of the Unfalsified Set, which is the point furthest from the bound of the Unfalsified Set, but which might be considered as aggressive switching. To decrease aggressiveness, up to $\alpha = 1$ might be chosen, which corresponds to a point on the boundary of the parallel half-spaces. In Fig. 3.4, the difference between $\alpha = 0$ and $\alpha = 1$ is schematically depicted.

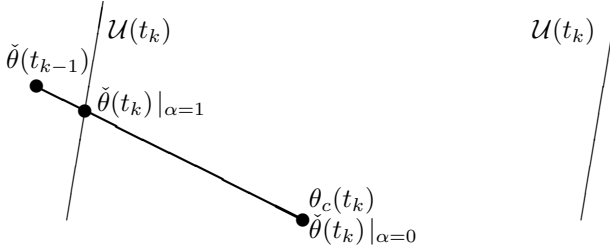


Figure 3.4: Example of cautious ($\alpha = 1$) versus aggressive ($\alpha = 0$) switching

It is now proven that with (3.33) indeed $\check{\theta}(t_k) \in \mathcal{E}(t_{k-1}) \cap \mathcal{U}(t_k)$.

Lemma 3.2a $\theta_c(t_k) \in \mathcal{E}(t_{k-1}) \cap \mathcal{U}(t_k)$

Proof: Ellipsoid $\mathcal{E}(t_k)$ is the minimum-volume outer-bounding ellipsoidal approximation of $\mathcal{E}(t_{k-1}) \cap \mathcal{U}(t_k)$ (Pronzato and Walter, 1994). Note that $\mathcal{E}(t_{k-1}) \cap \mathcal{U}(t_k)$ is a convex region. Suppose that $\theta_c(t_k) \notin \mathcal{E}(t_{k-1}) \cap \mathcal{U}(t_k)$, then two parallel half-spaces can be constructed with $a_+ = 0$, i.e., through $\theta_c(t_k)$, and $a_- = -1$, hence, $a_+ a_- = 0 < 1/p$, such that $\mathcal{E}(t_{k-1}) \cap \mathcal{U}(t_k)$ is entirely contained between these two parallel half-spaces. Next, an ellipsoid can be constructed that outer-bounds $\mathcal{E}(t_{k-1}) \cap \mathcal{U}(t_k)$ and, moreover, that is of smaller volume than $\mathcal{E}(t_k)$. However, this smaller ellipsoid is in contradiction to $\mathcal{E}(t_k)$ being the minimal-volume approximation. Consequently, $\theta_c(t_k) \in \mathcal{E}(t_{k-1}) \cap \mathcal{U}(t_k)$ has to hold. ■

Lemma 3.2b If $\check{\theta}(t_{k-1}) \in \mathcal{E}(t_{k-1})$, then $\check{\theta}(t_k) \in \mathcal{E}(t_{k-1}) \cap \mathcal{U}(t_k)$.

Proof: First, observe that $0 \leq \Gamma(t_k, \alpha) \leq 1$ for $|\gamma(t_k)| > 1$. Then, with (3.33) and Lemma 3.2a,

$$\check{\theta}(t_k) \in [\check{\theta}(t_{k-1}), \theta_c(t_k)] \subset \mathcal{E}(t_{k-1}) \quad (3.38)$$

Next, it is proven that also $\check{\theta}(t_k) \in \mathcal{U}(t_k)$. For $|\gamma(t_k)| \leq 1$, $\check{\theta}(t_{k-1}) \in \mathcal{U}(t_k)$, and hence, with (3.33), $\check{\theta}(t_k) \in \mathcal{U}(t_k)$. For $|\gamma(t_k)| > 1$, consider

$$\phi_k^T \check{\theta}(t_k) = \Gamma(t_k, \alpha) \phi_k^T \check{\theta}(t_{k-1}) + (1 - \Gamma(t_k, \alpha)) \phi_k^T \theta_c(t_k) \quad (3.39)$$

With (3.36) and (3.37), (3.39) can be rewritten as

$$\begin{aligned}\phi_k^T \check{\theta}(t_k) &= \Gamma(t_k, \alpha)(\gamma(t_k) + y_k) + (1 - \Gamma(t_k, \alpha))(\gamma_c(t_k) + y_k) \\ &= \alpha \text{sign}(\gamma(t_k)) + (1 - \alpha)\gamma_c(t_k) + y_k\end{aligned}$$

From Lemma 3.2a it follows that $\theta_c(t_k) \in \mathcal{U}(t_k)$, therefore $|\gamma_c(t_k)| \leq 1$ and, consequently, $|\phi_k^T \check{\theta}(t_k) - y_k| = |\alpha \text{sign}(\gamma(t_k)) + (1 - \alpha)\gamma_c(t_k)| \leq 1$ for all $\alpha \in [0, 1]$, from which with (3.16) it is concluded that

$$\check{\theta}(t_k) \in \mathcal{U}(t_k) \quad \forall \alpha \in [0, 1] \quad (3.40)$$

Combination of (3.38) and (3.40) results in

$$\check{\theta}(t_k) \in \mathcal{E}(t_{k-1}) \cap \mathcal{U}(t_k) \quad \forall \alpha \in [0, 1] \quad (3.41)$$

■

Corollary 3.3 *If $\check{\theta}(t_0) \in \mathcal{E}(t_0)$, then $\check{\theta}(t_{k-1}) \in \mathcal{E}(t_{k-1})$.*

Proof: Since $\mathcal{E}(t_k) \supseteq \mathcal{E}(t_{k-1}) \cap \mathcal{U}(t_k)$, (3.41) is sufficient to deduce that $\check{\theta}(t_k) \in \mathcal{E}(t_k)$. The corollary follows by repetition of Lemma 3.2b for t_1 up to t_{k-1} .

■

If the ellipsoid is not adapted, it can be shown that $\check{\theta}(t_k)$ is even in a tighter intersection:

Lemma 3.4 *If $\mathcal{E}(t_n) = \mathcal{E}(t_m)$ for some $t_n > t_m$, then $\check{\theta}(t_n) \in \mathcal{E}(t_{m-1}) \cap \mathcal{U}(t_m) \cap \dots \cap \mathcal{U}(t_n)$*

Proof: The ellipsoid is not adapted at $t_k \in [t_{m+1}, t_n]$, which implies that $\mathcal{E}(t_k) = \mathcal{E}(t_{k-1})$ and, consequently, $\theta_c(t_k) = \theta_c(t_{k-1})$. With Lemma 3.2a and 3.2b, $\theta_c(t_k) \in \mathcal{E}(t_{k-1}) \cap \mathcal{U}(t_k)$ and $\check{\theta}(t_k) \in \mathcal{E}(t_{k-1}) \cap \mathcal{U}(t_k)$. Then for $t_k = t_{m+1}$

$$\begin{aligned}\begin{cases} \theta_c(t_{m+1}) \in \mathcal{E}(t_m) \cap \mathcal{U}(t_{m+1}) \\ \theta_c(t_{m+1}) = \theta_c(t_m) \in \mathcal{E}(t_{m-1}) \cap \mathcal{U}(t_m) \end{cases} &\Rightarrow \\ \theta_c(t_{m+1}) \in \mathcal{E}(t_{m-1}) \cap \mathcal{E}(t_m) \cap \mathcal{U}(t_m) \cap \mathcal{U}(t_{m+1}) &\end{aligned}$$

and, with (3.33),

$$\begin{aligned}\begin{cases} \check{\theta}(t_{m+1}) \in \mathcal{E}(t_m) \cap \mathcal{U}(t_{m+1}) \\ \check{\theta}(t_{m+1}) \in [\check{\theta}(t_m), \theta_c(t_{m+1})] \subset \mathcal{E}(t_{m-1}) \cap \mathcal{U}(t_m) \end{cases} &\Rightarrow \\ \check{\theta}(t_{m+1}) \in \mathcal{E}(t_{m-1}) \cap \mathcal{E}(t_m) \cap \mathcal{U}(t_m) \cap \mathcal{U}(t_{m+1}) &\end{aligned}$$

Ellipsoid $\mathcal{E}(t_m)$ does not contribute to the intersection, because $\mathcal{E}(t_m) \supseteq \mathcal{E}(t_{m-1}) \cap \mathcal{U}(t_m)$.

The Lemma follows by repetition for t_k up to t_n .

■

From Lemma 3.4 it follows that $\check{\theta}(t_n)$ is in the strict intersection of $\mathcal{E}(t_{m-1}) \cap \mathcal{U}(t_m) \cap \dots \cap \mathcal{U}(t_n)$ even though $\mathcal{E}(t_n)$ is an outer-bounding approximation. As a consequence, if a controller is in the falsified region \mathcal{U} for any given time after convergence of the Unfalsified Set, it is ineligible for implementation, even if it still resides in \mathcal{E} . This guarantees that the final controller is selected from the polytope within the half-spaces after convergence of the Unfalsified Set \mathcal{E} , which typically is a tighter approximation of the True Unfalsified Set than \mathcal{E} .

To prevent the selection of $\check{\theta}_1(t_k) = 0$, as is required to satisfy the SCLI property of the controller structure (3.15), additional measures have to be taken. In the case that coincidentally $\check{\theta}_1(t_k) = 0$ results from controller selection (3.33), a controller parameter set corresponding to a different $\alpha \in [0, 1]$ should be chosen. This always results in $\check{\theta}_1(t_k) \neq 0$, because the line segment connecting $\check{\theta}_1(t_{k-1})$ and $\theta_{c,1}(t_k)$ has at most 1 point of intersection with $\theta_1 = 0$, which follows from the condition that $\check{\theta}_1(t_{k-1}) \neq 0$ (which by repetition is enforced by selection of $\check{\theta}_1(t_0) \neq 0$).

3.10 Summary and remarks

Several design choices are explicitly specified for Ellipsoidal Unfalsified Control, such that a fast evaluation of an infinite number of candidate controllers is feasible. First, the performance requirement (3.5) is adopted, which, in combination with the fictitious reference generator (3.13) and controller structure (3.14), results in two parallel half-spaces. Second, the Unfalsified Set is specified by an ellipsoid that describes a continuous region of control parameter sets. The intersection of the ellipsoid and the two parallel half-spaces is approximated by a minimum-volume outer-bounding ellipsoidal Unfalsified Set, which can be computed analytically, and which is used as the Unfalsified Set in the next time step. Accordingly, the same arithmetics can be used every time step. An algorithm for the deterministic selection of the controller parameters to be implemented is given.

If desired, other choices can be made for the performance requirement, the performance inference and the controller structure than explained in this chapter. The same arithmetics can be used, if an ellipsoidal Unfalsified Set is considered and if the region $\mathcal{U}(t_k)$ is defined by two parallel half-spaces. The latter is realized if the combination of the performance requirement, the performance inference and the controller structure result in a region $\mathcal{U}(t_k)$ that is affine in the controller parameters.

The controller selection presented here is just one choice to select a $\check{\theta}(t_k) \in \mathcal{E}(t_{k-1}) \cap \mathcal{U}(t_k)$ and that guarantees a limited number of controller switches. Dif-

ferent choices are valid if they also contain these properties.

With the current algorithm, the control parameter set can be adapted even if the Unfalsified Set remains unchanged. Also the opposite is true, that is, the Unfalsified Set can be adapted while the control parameter set remains unchanged.

Chapter 4

Stability of Ellipsoidal Unfalsified Control

IN THE previous chapter, the Ellipsoidal Unfalsified Control algorithm was introduced. In this chapter, the stability of the Ellipsoidal Unfalsified Control adaptive system is addressed. It is shown that, with some extensions, the stability of the adaptive control system can be guaranteed. At the end of this chapter, the results are summarized in a theorem.

4.1 Preliminaries

Following the definitions used by Åström and Wittenmark (1995), an *adaptive controller* is defined as a controller with adjustable parameters and a mechanism for adjusting the parameters. An *adaptive control system* is a control system with an adaptive controller.

The *candidate controller set* is the set composed by time-invariant controllers with any of the possible parameters (Wang et al., 2005).

4.2 BIBO stability

Ellipsoidal Unfalsified Control only considers the external, or input-output, behavior of a plant, in contrast to the internal, or state-space, behavior. This naturally

leads to the stability concept of bounded-input bounded-output (BIBO) stability. In this thesis, unless stated otherwise, BIBO stability is considered.

Definition 4.1 (BIBO stability) *A system S with input $u(t_k)$ and output $y(t_k)$ is bounded-input bounded-output (BIBO) stable if for any finite, positive constant β there exists a finite, positive constant ε such that the following property holds for any t_0 . If the input signal satisfies*

$$\|u(t_k)\|_\ell \leq \beta, \quad t_k \geq t_0$$

then the corresponding response satisfies

$$\|y(t_k)\|_\ell \leq \varepsilon, \quad t_k \geq t_0$$

where ε depends on β , but also ε can depend on t_0 , on the particular input signal $u(t_k)$ or on the initial conditions. (Based on (Rugh, 1996, Ch. 27 and Note 12.1 on p. 216)).

In this thesis, for $\|\cdot\|_\ell$ the ℓ_∞ discrete-time signal norm is considered, which is denoted by $\|\cdot\|_\infty$.

$$\|x(t_k)\|_\infty = \max_j \sup_{t_k \geq t_i \geq t_0} |x_j(t_i)|$$

where $x_j(t_k)$ is the j^{th} element of $x(t_k)$.

Stability is a system property that is based on infinite-time information. With limited information, such as a sequence of measurement data, it can only be concluded if the system is demonstrably unstable.

Definition 4.2 (Demonstrably unstable) *The system S is demonstrably unstable, if at some time t_k it can be deduced from data $u_{t_0}^{t_k} = [u(t_0), \dots, u(t_k)]$, $y_{t_0}^{t_k} = [y(t_0), \dots, y(t_k)]$ that $\|y_{t_0}^{t_k}\|_\infty = \infty$ for $\|u_{t_0}^{t_k}\|_\infty < \infty$.*

Definition 4.3 (Demonstrably destabilizing) *A controller is demonstrably destabilizing, if it renders the closed loop control system demonstrably unstable.*

Consider the definition of feasibility, as is derived from (Stefanovic et al., 2005):

Definition 4.4 (Feasibility) *The adaptive control problem is said to be feasible if the set of candidate controllers contains at least a polytope E in the controller parameter spaces \mathbb{R}^P with controllers that fulfill the performance requirement at all times. Region E has a volume $e > 0$, but is unknown otherwise.*

The region E is subject to the sequence of the implemented controller parameter sets $\check{\theta}$, since the implemented controllers determine the experimental data that is observed. Furthermore, the region E is constructed with the fictitious reference, which might lead to inaccurate performance inference, see Section 3.3.1. Therefore, a different region E might result for different initial conditions and different experiments.

Although stability is not guaranteed for a single controller in this data-driven context, sufficient conditions are given in (Stefanovic et al., 2005) and (Wang et al., 2005) for an adaptive control system to be stable. In short, these boil down to the following lemma.

Lemma 4.5 *Sufficient plant-model-free conditions to guarantee stability of an adaptive control system are:*

1. *the adaptive control problem is feasible,*
2. *controllers that are demonstrably destabilizing without assumptions on the plant are discarded from the candidate controller set,*
3. *the number of controller switches is limited.*

In the remainder of this section, the three conditions from Lemma 4.5 will be elaborated upon for Ellipsoidal Unfalsified Control. It should be noted that all considerations regard BIBO stability, with as input the reference and the output noise $\begin{bmatrix} r(t_k) \\ d(t_k) \end{bmatrix}$ and as output the plant output and the control effort $\begin{bmatrix} y(t_k) \\ u(t_k) \end{bmatrix}$.

4.3 Feasibility

The feasibility condition is only fulfilled by assumption. The controller structure is chosen rich enough, such that it is likely that this assumption will be fulfilled. No information is available (to the authors' knowledge) that predicts the feasibility of an adaptive control system if no plant-model is available. Nevertheless, the chances of feasibility might be improved by consideration of some known characteristics of the plant in the design of the adaptive problem, such as a low-pass characteristic, approximate low-frequency phase lag, relative degree or dissipativity of the plant.

4.4 Discarding of demonstrably destabilizing controllers

For the physical systems, as are considered in this thesis, the output will typically not be able to grow unbounded in finite time and with discrete-time measurements, for instance due to saturation levels and a constrained stroke. As a consequence, for these systems it is impossible to actually become BIBO unstable as defined by Definition 4.1, not to speak of demonstrably unstable. Nevertheless, controllers that hypothetically render the system unstable are discarded before they would become demonstrably destabilizing.

In this section, it is established that controllers are discarded before they are demonstrably destabilizing, by application of performance requirement (3.4) in combination with SCLI candidate controllers. The controller structure (3.13) is SCLI for $\check{\theta}_1 \neq 0$, since $\Lambda_u(q)$, $\Lambda_y(q)$ and $f(u(t_{k-1}), y(t_k), q)$ are stable. For a relaxation on the SCLI property, see (Zhang and Ioannou, 2006; Manuelli et al., 2007).

Theorem 4.6 *Restriction of the candidate controllers to $\mathcal{E}(t_{k-1}) \cap \mathcal{U}(t_k)$ is sufficient to discard demonstrably destabilizing controllers.*

Proof: Selecting a controller from $\mathcal{E}(t_{k-1}) \cap \mathcal{U}(t_k)$ guarantees that the controller fulfills the performance requirement (3.4) and that the controller is approximately unfalsified by past measurement data. Remains to establish that if a controller is demonstrably destabilizing, that it is not in $\mathcal{U}(t_k)$, which is sufficient for it to not be in $\mathcal{E}(t_{k-1}) \cap \mathcal{U}(t_k)$.

Recall that for $\theta = \check{\theta}$, it holds that $r_{\text{fict}}(\theta, t_k) = r(t_k)$. Only when $\theta \neq \check{\theta}$, e.g., when switching controller parameters, $r_{\text{fict}}(\theta, t_k) \neq r(t_k)$. As a consequence, for an unfalsified controller parameter set $\check{\theta}$, $G_m(q)r_{\text{fict}}(\check{\theta}, t_k)$ converges to $G_m(q)r(t_k)$ for a stable reference model $G_m(q)$ and a stable fictitious reference generator, and the fictitious tracking error $e_{\text{fict}}(\check{\theta}, t_k) = G_m(q)r_{\text{fict}}(\check{\theta}, t_k) - y(t_k)$, (3.3), converges to the true tracking error $G_m(q)r(t_k) - y(t_k)$.

Suppose that $\check{\theta}$ is destabilizing, however, it is not (yet) demonstrably destabilizing.

I.e., $\left\| \begin{bmatrix} y(t_k) \\ u(t_k) \end{bmatrix} \right\|_{\infty} \uparrow \infty$ for some $\left\| \begin{bmatrix} r(t_k) \\ d(t_k) \end{bmatrix} \right\|_{\infty} \leq \beta < \infty$. Then, if $|u(t_k)| \uparrow \infty$, directly (3.4) is violated. And for $|y(t_k)| \uparrow \infty$, $|e_{\text{fict}}(\check{\theta}, t_k)| \uparrow \infty$ because $G_m(q)r_{\text{fict}}(\check{\theta}, t_k)$ converges to $G_m(q)r(t_k)$, which also violates (3.4). If (3.4) is violated, the current controller is falsified and thereby discarded from the candidate controller set, even though it is not (yet) demonstrably destabilizing. ■

The discarding of demonstrably destabilizing controllers with performance requirement (3.4) has a resemblance with the cost-detectability property, as found for instance in (Paul et al., 2005; Wang et al., 2007). The cost-detectability property implies that the destabilizing behavior of a candidate controller is reflected in its performance index. However, cost-detectability defines a necessary and sufficient condition to discard demonstrably destabilizing controllers, whereas here only a sufficient condition is presented.

4.5 Limited number of switches

Ellipsoidal Unfalsified Control uses an ellipsoidal description of the Unfalsified Set, which is a continuous region in the controller parameter space. Hence, an infinite number of candidate controllers is considered. To prove that condition 3 of Lemma 4.5 is fulfilled for Ellipsoidal Unfalsified Control, the condition is split in two parts: first it is shown that, with a minor constraint, a finite number of distinctive ellipsoidal Unfalsified Sets can be guaranteed. Then it is shown that, again with a minor constraint, a finite number of controller switches per ellipsoid can be guaranteed. Hence, by combining these two parts, a finite number of overall controller switches can be guaranteed.

4.5.1 Limited number of ellipsoids

The volume of the ellipsoidal Unfalsified Set is monotone non-increasing. Furthermore, the volume is lower bounded by e , the volume of the polytope E by assumption of feasibility, see Section 4.3. Here, it is shown that a maximum volume ratio between two consecutive distinctive ellipsoids implies a limited number of ellipsoids.

Decrease of volume

To address the decrease in volume of two consecutive distinctive ellipsoids, consider the volume ratio.

Lemma 4.7 *The volume ratio $\delta_V(t_k)$ between two consecutive distinctive ellipsoids for $a_+ \neq a_-$ is given by*

$$\delta_V(t_k) = \sqrt{\delta^p(1 - \sigma)} \quad (4.1)$$

with δ and σ as in (3.28) and (3.29), respectively, and p the number of parameters as in (3.19).

Proof: The volume $V(t_{k-1})$ of the Unfalsified Set $\mathcal{E}(t_{k-1})$ is given by

$$V(t_{k-1}) = \text{vol}(\mathcal{E}(t_{k-1})) = V_p \sqrt{\det(\Sigma(t_{k-1}))} \quad (4.2)$$

with V_p the volume of the unit ball in \mathbb{R}^p and $\Sigma(t_{k-1})$ from (3.19). The volume ratio $\delta_V(t_k)$ between two consecutive distinctive ellipsoids is given by

$$\delta_V(t_k) = \frac{\text{vol}(\mathcal{E}(t_k))}{\text{vol}(\mathcal{E}(t_{k-1}))} = \sqrt{\frac{\det(\Sigma(t_k))}{\det(\Sigma(t_{k-1}))}} \quad (4.3)$$

Consider $a_+ \neq a_-$. Using (3.22) and (3.26), $\det(\Sigma(t_k))$ can be expressed in terms of $\det(\Sigma(t_{k-1}))$:

$$\begin{aligned} \det(\Sigma(t_k)) &= \det\left(\delta\left(\Sigma(t_{k-1}) - \frac{\sigma}{g}\Sigma(t_{k-1})\phi_k\phi_k^T\Sigma(t_{k-1})\right)\right) \\ &= \delta^p \det(\Sigma(t_{k-1})) \det\left(\mathbb{I} - \frac{\sigma}{g}\phi_k\phi_k^T\Sigma(t_{k-1})\right) \\ &= \delta^p \det(\Sigma(t_{k-1})) \left(1 - \text{Tr}\left(\frac{\sigma}{g}\phi_k\phi_k^T\Sigma(t_{k-1})\right)\right) \\ &= \delta^p(1 - \sigma) \det(\Sigma(t_{k-1})) \end{aligned} \quad (4.4)$$

$$\Rightarrow \delta_V(t_k) = \sqrt{\frac{\det(\Sigma(t_k))}{\det(\Sigma(t_{k-1}))}} = \sqrt{\delta^p(1 - \sigma)}$$

■

Corollary 4.8 *The volume ratio $\delta_V(t_k)$ between two consecutive distinctive ellipsoids is given by*

$$\delta_V(t_k) = \sqrt{\delta^p \left(1 - \frac{1 - pa^2}{1 - a^2}\right)} \quad (4.5)$$

for $a_+ = a_- = a$.

Proof: The result for $a_+ = a_- = a$ is obtained by using (3.31) to evaluate $\det(\Sigma(t_k))$ in (4.3). The remainder of the derivation is similar to the proof of Lemma 4.7

■

From Lemma 4.7 and Corollary 4.8 it can be concluded that the volume of the ellipsoids decreases when $\delta^p(1 - \sigma) < 1$ or $\delta^p \left(1 - \frac{1 - pa^2}{1 - a^2}\right) < 1$.

Intermezzo: two limit cases

Two limit cases are considered, which bound the operating area of $\delta_V(t_k)$:

- $a_+ = -a_- \Rightarrow \sigma = 1$

As can be seen from Lemma 4.7, the volume ratio $\delta_V(t_k)$ is 0 for $\sigma = 1$. Physically, this corresponds to the situation where the two parallel half-spaces, defined by the performance requirement, connect to each other, hence, no unfalsified set can exist. This, however, contradicts the assumption that there exists a polytope E of some volume $e > 0$ that is unfalsified at all times.

- $a_+ a_- = 1/p \Rightarrow \sigma = 0 \wedge \delta = 1$

As can be seen from Lemma 4.7, the volume ratio $\delta_V(t_k)$ is 1 for $\sigma = 0 \wedge \delta = 1$. This corresponds to the situation where the minimum-volume outer-bounding ellipsoidal approximation of the intersection, $\mathcal{E}(t_k)$, coincides with the previous ellipsoid $\mathcal{E}(t_{k-1})$.

Remark 4.9 *The two limit cases discussed above also hold for $a_+ = a_-$ (limit cases: $a_+ = a_- = 0$ and $a_+ = a_- = -\sqrt{1/p}$).*

In Fig. 4.1, a plot is shown of $\delta_V(t_k)$ as a function of a_+ and a_- for $p = 10$, together with the two limit cases as are discussed here. As can be seen, in the area between these two bounds it holds that $0 < \delta_V(t_k) < 1$.

Conditions for a finite number of ellipsoids

The volume ratio between two consecutive distinctive ellipsoids is given in (4.1) and (4.5). Consider a constraint $0 < \nu < 1$ on the maximum volume ratio

$$\delta_V < \nu \tag{4.6}$$

A sufficient condition to ensure (4.6) is to impose

$$a_+ a_- \leq \epsilon(\nu)/p \tag{4.7}$$

between two consecutive distinctive ellipsoids, for some $0 < \epsilon(\nu) < 1$. If $\epsilon(\nu)/p < a_+ a_- \leq 1/p$, the additionally falsified region is neglected and the Unfalsified Set is not changed. This maximum volume ratio is enforced in the Ellipsoidal Unfalsified Control algorithm, by using (4.7) instead of (3.25).

The value of $\epsilon(\nu)$ can be derived from (4.1) and (4.5). It is observed, that for $\epsilon(\nu)$ close to 1,

$$\arg \max_{a_+ = \frac{\epsilon(\nu)}{p a_-}} \delta_V(t_k) = -1 \wedge -\epsilon(\nu)/p \tag{4.8}$$

for a fixed p .

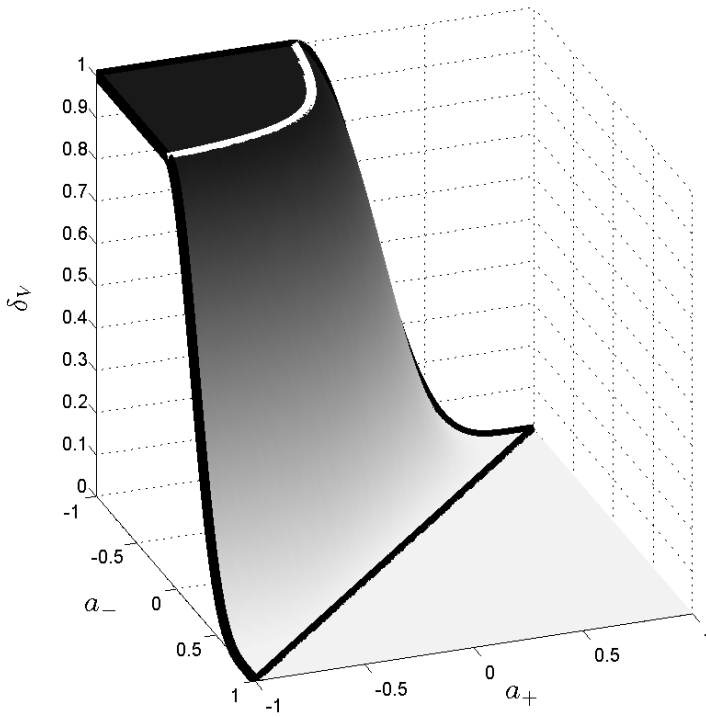


Figure 4.1: Plot of δ_V as a function of a_+ and a_- for $p = 10$.

To express the maximum number of ellipsoidal Unfalsified Sets, consider the volume $V(t_0)$ of the initial Unfalsified Set, which is the largest possible volume of the Unfalsified Set. The volume of the n^{th} ellipsoid is upperbounded by $V(t_0)\nu^n$. Next, consider the smallest possible volume e of the Unfalsified Set, which is given by the volume of polytope E . Then the number of ellipsoidal updates n_e is limited by

$$\begin{aligned} \nu^{n_e} &= \frac{e}{V(t_0)} \Rightarrow \\ n_e &= \left\lceil \frac{\log(e/V(t_0))}{\log(\nu)} \right\rceil \end{aligned} \quad (4.9)$$

4.5.2 Limited number of switches per ellipsoid

In the previous subsection, it is shown that a finite number of updates of the ellipsoid is guaranteed. However, multiple controllers per ellipsoid might still result before the ellipsoid has to be updated. Therefore, in this subsection it is shown that the number of controller switches per ellipsoid can be limited.

First observe that several controllers can be chosen consecutively within the same ellipsoid, as a function of the location of $\mathcal{U}(t_k)$. However, this can only continue while $a_+a_- > \epsilon(\nu)/p$, for otherwise the ellipsoid is to be updated. Next, observe that for the controller selection algorithm (3.33), all consecutive controllers for a given ellipsoid are on the same line segment $[\tilde{\theta}(t_{k-1}), \theta_c(t_k)]$. By enforcing a minimum stepsize on the controller adjustments, this line segment can be divided in a maximum number of adjustments. Therefore, instead of (3.35) consider the condition

$$\alpha \in [0, \epsilon_\alpha] \quad (4.10)$$

for some

$$0 < \epsilon_\alpha < 1 \quad (4.11)$$

Then the maximum number of controller switches per ellipsoid n_{ce} is given by

$$\begin{aligned} \epsilon_\alpha^{n_{ce}} &= \epsilon(\nu)/p \Rightarrow \\ n_{ce} &= \left\lceil \frac{\log(\epsilon(\nu)/p)}{\log(\epsilon_\alpha)} \right\rceil \end{aligned} \quad (4.12)$$

Remark 4.10 *The maximum numbers of updates of the ellipsoidal Unfalsified Sets and controller switches per ellipsoid, as derived above, are not an accurate prediction of the actual attainable number of controller switches. They merely serve as a demonstration of the upperbound on the number of controller switches.*

Typically, the convergence is much faster, so less switches are used.

(For the simulation example in Chapter 5, $n_e = \left\lceil \frac{\log(4.2 \cdot 10^{-34})}{\log(0.999989)} \right\rceil = 7.0 \cdot 10^6$, $n_{ce} = \left\lceil \frac{\log(0.99/5)}{\log(0.9)} \right\rceil = 16$, whereas the number of controller switches is $69 \ll (n_e + 1)(n_{ce} + 1) - 1$.)

4.6 Summary and remarks

From Lemma 4.5 and Section 4.3 through 4.5, the following theorem can be deduced

Theorem 4.11 (Stability Ellipsoidal Unfalsified Control) *An Ellipsoidal Unfalsified Control adaptive system is BIBO stable, if*

1. *the adaptive control problem is feasible,*
2. *the SCLI candidate controllers of (3.14) are considered, in combination with the ℓ_∞ performance requirement (3.4),*
3. *the number of controller switches is limited, by imposing $a_+ a_- \leq \epsilon(\nu)/p$, $0 < \epsilon(\nu) < 1$, on the update of the ellipsoid (3.25) and $\alpha \in [0, \epsilon_\alpha]$, $0 < \epsilon_\alpha < 1$, on the controller update (3.35).*

Proof: In Section 4.4 it is shown, that demonstrably destabilizing controllers are discarded, when considering the Ellipsoidal Unfalsified Control controller structure (3.14) and the ℓ_∞ performance requirement (3.4). From the feasibility of the adaptive control problem, it follows that there exists at all times an Unfalsified Set $\mathcal{E}(t_k) \supseteq E_{\text{tus}} \supseteq E$ of candidate controllers, which is unfalsified. As the number of controller switches is limited by imposing $\epsilon(\nu) < 1$ and $\epsilon_\alpha < 1$, switching will eventually stop, resulting in a fixed controller that is unfalsified $\forall t_k$, hence, that is stable $\forall t_k$.

Since the preceding is true for any bounded $r(t_k)$ and $d(t_k)$ for which the adaptive control problem is feasible, it can be concluded that the stability of the Ellipsoidal Unfalsified Control adaptive system is unfalsified for all bounded $r(t_k)$ and $d(t_k)$ for which the conditions of Theorem 4.11 are fulfilled, and, hence, that the Ellipsoidal Unfalsified Control adaptive system is stable. ■

Chapter 5

Application of Ellipsoidal Unfalsified Control

IN THIS chapter, the results of the application of Ellipsoidal Unfalsified Control to motion systems are presented. Both a simulation study and an experimental implementation are discussed. Both applications incorporate characteristics often encountered in motion systems, such as a high sample rate of 1 kHz and a low-frequent rigid-body mode.

5.1 Simulation: Plant

In simulation, the applicability of Ellipsoidal Unfalsified Control has been evaluated. Consider the plant, as shown in Fig. 5.1. The continuous time state-space model is given by

$$\dot{x} = Ax + Bu \tag{5.1}$$

$$y = Cx \tag{5.2}$$

with

$$\begin{aligned}
 x &= [x_1 \quad \dot{x}_1 \quad x_2 \quad \dot{x}_2]^T \\
 y &= x_2 \\
 A &= \begin{bmatrix} 0 & 1 & 0 & 0 \\ -c/J_1 & -d/J_1 & c/J_1 & d/J_1 \\ 0 & 0 & 0 & 1 \\ c/J_2 & d/J_2 & -c/J_2 & -d/J_2 \end{bmatrix} \\
 B &= [0 \quad 1/J_1 \quad 0 \quad 0]^T \\
 C &= [0 \quad 0 \quad 1 \quad 0]
 \end{aligned}$$

The parameter-values are chosen as $J_1 = 1.56 \cdot 10^{-4}$, $J_2 = 1.95 \cdot 10^{-4}$, $d = 0.9 \cdot 10^{-3}$ and $c = 8.64$. The plant is sampled at 1 kHz with a zero-order hold and a pseudo-white noise d with power 10^{-8} and bounded to $[-0.015, 0.015]$ is added to the sampled output y . A Bode plot of the plant is shown in Fig. 5.2.

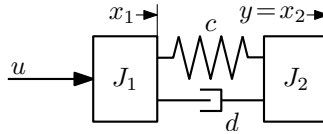


Figure 5.1: Schematic representation of fourth order motion system.

5.2 Simulation: Design

5.2.1 Goals

The desired closed loop behavior $G_m(q)$ of the controlled system is prescribed by a 2nd order low-pass reference model, to impose low-frequent tracking and high-frequent noise suppression.

$$G_m(q) = \frac{2 \cdot 10^{-4}(q + q^2)}{1 - 1.96q + 0.9604q^2} \quad (5.3)$$

The reference model has a low-pass characteristic with at low-frequent gain of 1 and is shown in Fig. 5.3.

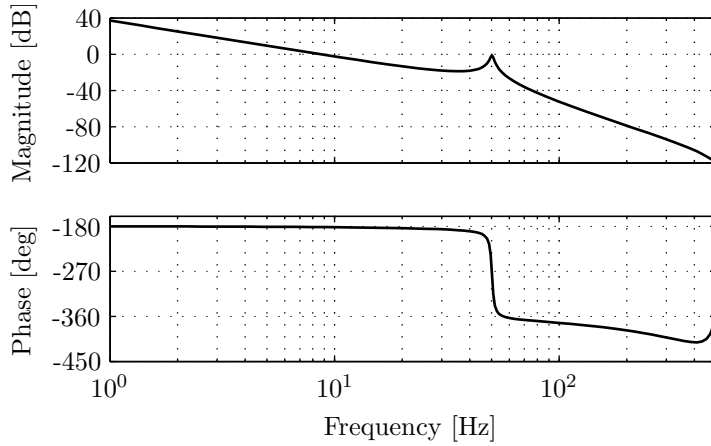


Figure 5.2: Bode plot (magnitude top, phase bottom) of the plant of Fig. 5.1, with zero-order hold sampling at 1 kHz.

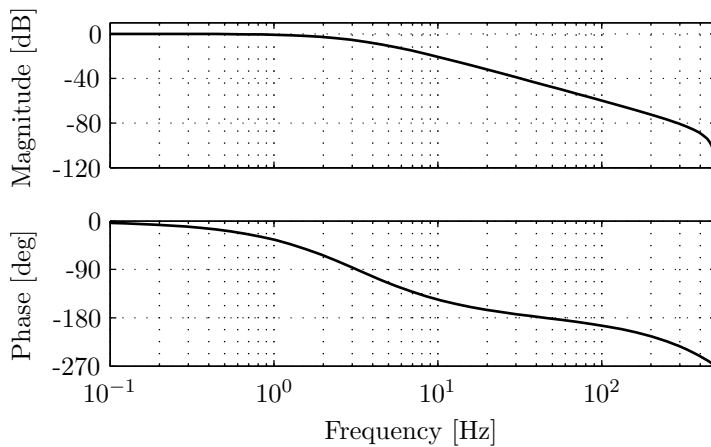


Figure 5.3: Bode plot (magnitude top, phase bottom) of the reference model $G_m(q)$.

The reference trajectory is a square wave of 4 seconds with amplitude 1, as is given by

$$r(t_k) = \text{sign}(\sin(0.5\pi t_k)) \quad (5.4)$$

The reference $r(t_k)$ and desired output $G_m(q)r(t_k)$ are shown in Fig. 5.4, the frequency content of $r(t_k)$ is shown in Fig. 5.5.

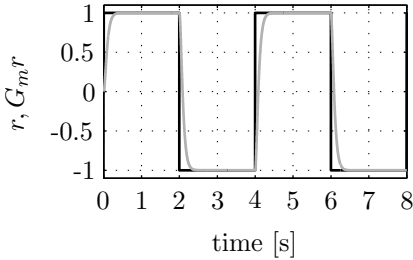


Figure 5.4: Plot of the reference $r(t_k)$ (black) and the desired output $G_m(q)r(t_k)$ (grey) as a function of time.

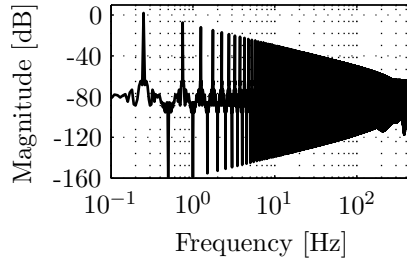


Figure 5.5: Plot of the frequency content of the reference $r(t_k)$.

The performance bound $\Delta(t_k)$ is given by

$$\Delta(t_k) = 0.018 + 0.5e^{-0.1t_k} \quad (5.5)$$

The lower bound on $\Delta(t_k)$ is included to guarantee feasibility in the presence of the output noise, whereas the exponential term is included to limit the influence of transient behavior. The volume of the polytope with stabilizing and performing controllers E is directly influenced by the magnitude of $\Delta(t_k)$.

The factor $\kappa(t_k) = 0.018$ is chosen such that the control effort at $t_k = 100$ s is bounded by $|u(100)| < \frac{\Delta(100)}{\kappa(100)} = 1.0$. The weighting filter $W(q)$ is set to 1.

5.2.2 Controller structure

The controller structure $w(u(t_k), y(t_k), q)$ is chosen as

$$w(u(t_k), y(t_k), q) = \begin{bmatrix} u(t_k) \\ \frac{1}{1-0.99q}u(t_{k-1}) \\ y(t_k) \\ \frac{1}{1-0.99q}y(t_{k-1}) \\ y^2(t_k) \end{bmatrix} \quad (5.6)$$

This controller structure incorporates dependencies on $u(t_k)$, $y(t_k)$ and low-pass terms. With (5.6), a first order controller results, which is sufficient to generate the phase lead needed for a stable closed loop system.

For perfect tracking of a given reference by Plant Inversion, a controller structure is required that can realize $C_r = (P^{-1} + C_y)G_m$, where C_r and C_y are defined as in Fig. 3.1. Despite the shared parametrization of C_r and C_y , for a given linear minimum-phase plant $P(q) = \frac{b_0 + b_1q + b_2q^2}{1 + a_1q + a_2q^2}$, $b_0 \neq 0$, perfect tracking is achieved for instance with reference model $G_m(q) = 1$ and controller

$$r(t_k) = \begin{bmatrix} u(t_k) \\ u(t_{k-1}) \\ u(t_{k-2}) \\ y(t_k) \\ y(t_{k-1}) \\ y(t_{k-2}) \end{bmatrix}^T \begin{bmatrix} b_0 \\ b_1 \\ b_2 \\ 0 \\ -a_1 \\ -a_2 \end{bmatrix}$$

for which C_r and C_y are given by

$$C_r = \frac{1}{b_0 + b_1q + b_2q^2}$$

$$C_y = -\frac{a_1q + a_2q^2}{b_0 + b_1q + b_2q^2}$$

Perfect disturbance attenuation can be realized with the Internal Model Principle for a C_y of high enough order, since the parameters of the controller C_y can be adapted independently. However, due to the restricted order of the controller structure and the output noise in the simulation example presented in this chapter, perfect tracking can not be achieved for the current setting. Nevertheless, with the current controller structure tracking within a bound $\pm\Delta(t_k)$ can be achieved.

The last, nonlinear, element of $w(u(t_k), y(t_k), q)$ is chosen to underline that Ellipsoidal Unfalsified Control is not limited to linear controllers, even though its presence is not required for adequate control of the plant.

5.2.3 Initialization

The algorithm is initialized at $t_k = 0$ with

$$\Sigma(0) = 10^3 \mathbb{I}_{5 \times 5} \quad (5.7)$$

$$\check{\theta}(0) = \theta_c(0) = [100 \ 0 \ 1 \ 0 \ 0]^T \quad (5.8)$$

The initial value $\check{\theta}(0)$ corresponds to a P-controller with gain 0.01 ($1/\check{\theta}_1$) that, in fact, destabilizes the system due to the phase lag caused by the zero order hold. The stepsize of the controller parameter update is set to $\alpha = 0.9$. The maximum volume ratio is constrained by setting $\epsilon(\nu) = 0.99 < 1$. This corresponds to $\nu = 0.999989$, which is close to, but still smaller than, 1.

5.3 Simulation: Results

5.3.1 Time domain

Figure 5.6 shows the tracking error $G_m(q)r(t_k) - y(t_k)$ of the Ellipsoidal Unfalsified Control adaptive system. Due to the destabilizing controller $C(\check{\theta}(0))$, initially the tracking error grows rapidly and crosses the unfalsification bound after 0.4 s (not visible in the plot, due to clipping of the y-axis). Therefore, the current controller parameters are falsified and they are updated. This process is repeated whenever the performance requirement is not met by the current controller. In Fig. 5.7, the controller parameters $\check{\theta}(t_k)$ are shown as a function of time, together with the center of the ellipsoidal Unfalsified Set $\theta_c(t_k)$. If the current controller is unfalsified, the controller parameters are unchanged. The center $\theta_c(t_k)$ on the other hand changes almost continuously. The values of $\check{\theta}(t_k)$ and $\theta_c(t_k)$ after 100 s are given by

$$\check{\theta}(100) = \begin{bmatrix} 7.2523 \\ 0.2840 \\ 1.9974 \\ -0.0099 \\ -0.0000 \end{bmatrix}, \quad \theta_c(100) = \begin{bmatrix} 7.1492 \\ 0.2850 \\ 1.9961 \\ -0.0099 \\ 0.0007 \end{bmatrix}$$

The edges of \mathcal{E} for the separate variation per parameter ($\theta_{c,i} \pm \Sigma_{i,i}^{-1/2}$) are also shown in Fig. 5.7. Over time, the orientation of \mathcal{U} changes, which is inherited in \mathcal{E} due to the outer-bounding update, resulting in the ‘lobes’ on the edges of \mathcal{E} . Nevertheless, still the volume of \mathcal{E} is monotone non-increasing, see Fig. 5.8.

Even though $\alpha = 0.9$, the controller selection (3.33) results in a $\check{\theta} \in \mathcal{E}(t_{k-1}) \cap \mathcal{U}(t_k)$ that is closer to θ_c than to the edges of $\mathcal{E}(t_k)$ for this example, because the bounds of $\mathcal{E}(t_{k-1}) \cap \mathcal{U}(t_k)$ are tighter than the bounds of $\mathcal{E}(t_k) \supseteq \mathcal{E}(t_{k-1}) \cap \mathcal{U}(t_k)$ (outer-bounding approximation).

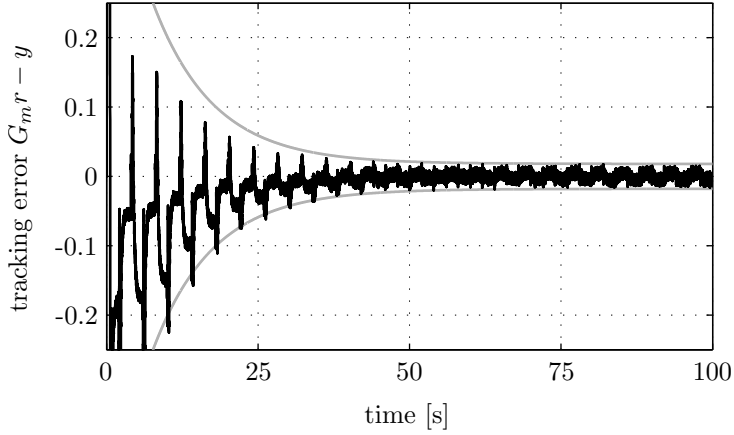


Figure 5.6: Tracking error (black, clipped to ± 0.25) of plant Fig. 5.1 with Ellipsoidal Unfalsified Control with control structure (5.6), together with the bounds $\pm \Delta(t_k)$ (grey).

5.3.2 Frequency domain

Besides a time domain analysis, also a frequency domain analysis is performed to investigate the behavior of the linear part of the obtained controller. The nonlinear part is neglected in this analysis, supported by $\check{\theta}_5(100) \approx 0$ and its minimal influence compared to the other elements.

For this simulation example with known plant, the root loci of the poles and zeros of the linearized control system with the currently implemented controllers are computed. These root loci are used to evaluate the properties of the system with the implemented controllers. The nonlinear effect of the controller switching is neglected in this analyses as if the controllers were not adapted. In Fig. 5.9, a selection of the root loci of the poles and zeros of the linearized control system are shown with the currently implemented controllers. Not shown are a complex pole pair at $[0.9457, 0.9460] \pm [0.3076, 0.3088]i$ and a complex zero pair at $0.9457 \pm 0.3089i$. A controller that stabilizes the closed loop system is inserted within 1 s. The stepsize parameter α directly influences the coarseness of the root loci, nevertheless, for all admissible values a similar shape results.

The frequency responses of the obtained controller after 100 s are shown in Fig. 5.10 and Fig. 5.11. Here, the same factorization is used as in Fig. 3.1, i.e., $u = C_r(\check{\theta})r - C_y(\check{\theta})y$. Since $C_r(\check{\theta}(100), q)$ and $C_y(\check{\theta}(100), q)$ have a shared parametrization, their shapes are similar. Both filters show a first order lead filter, which is needed by $C_y(\check{\theta}(t_k), q)$ to generate the phase lead to result in a stable control system. In the plot of the open loop $PC_y(\check{\theta}(100), q)$, shown in Fig. 5.12, ample

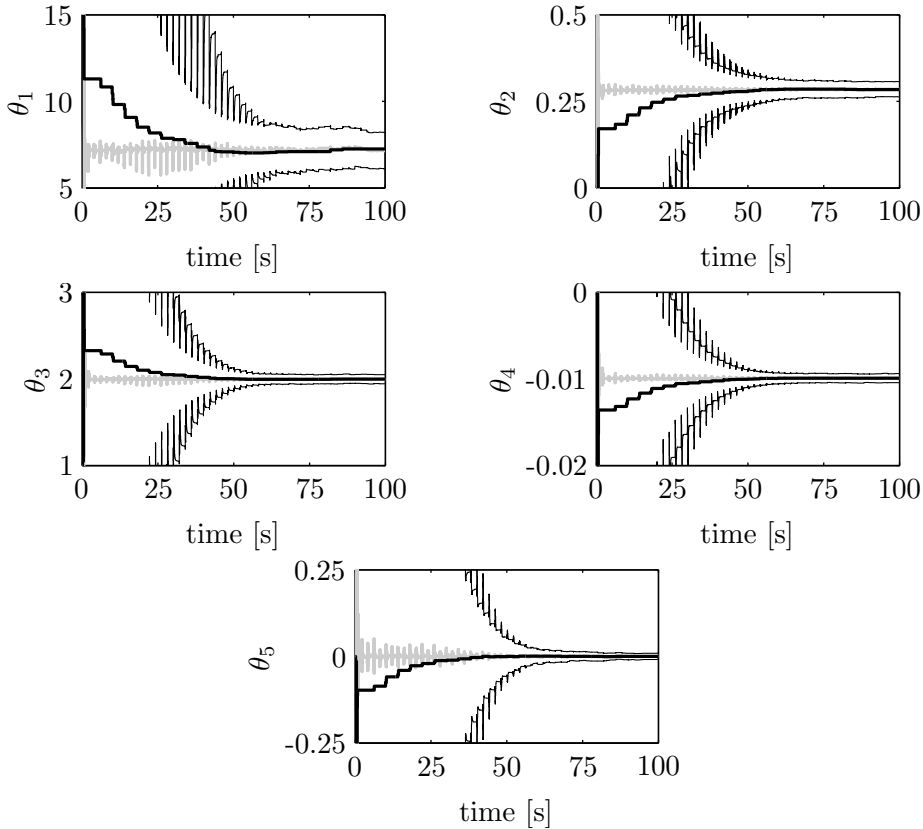


Figure 5.7: Plot of the controller parameters $\check{\theta}(t_k)$ (bold black line) as a function of time, together with the center of the ellipsoidal Unfalsified Set $\theta_c(t_k)$ (grey). The upper and lower thin black lines denote the edges of $\mathcal{E}(t_k)$ ($\theta_{c,i} \pm \Sigma_{i,i}^{-1/2}$).

amplitude and phase margins are observed in the controlled system.

In Fig. 5.13, the frequency responses of the closed loop system and of the reference model $G_m(q)$ are shown. At low frequencies, both responses are similar, however, around the resonance frequency of the plant differences occur. The first order controller is not able to suppress the resonance of the plant. Although this deviation causes an error in $G_m(q)r(t_k) - y(t_k)$, from the evaluation of the frequency content of the error with the controller after 100 s, shown in Fig. 5.14, it is concluded that the deviation around the resonance frequency only has a limited contribution to the overall error. Apparently, the basis frequency of the reference at 0.25 Hz accounts for the majority of the tracking error. Even so, the performance requirement is met with the controller after 100 s.

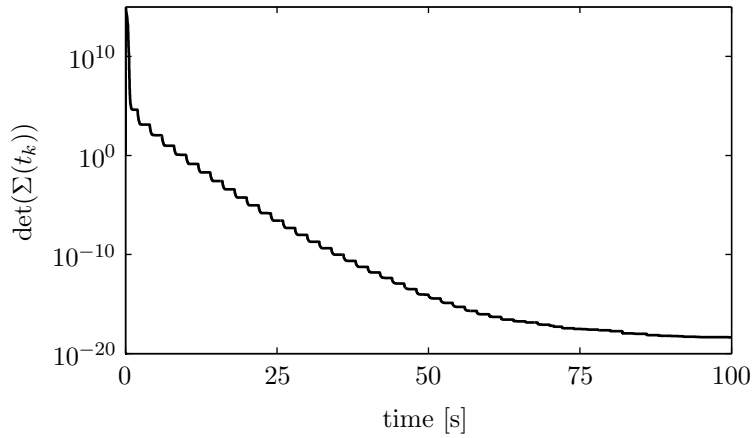


Figure 5.8: Determinant of $\Sigma(t_k)$, which is proportional to the volume of $\mathcal{E}(t_k)$, see (4.2), as a function of time.

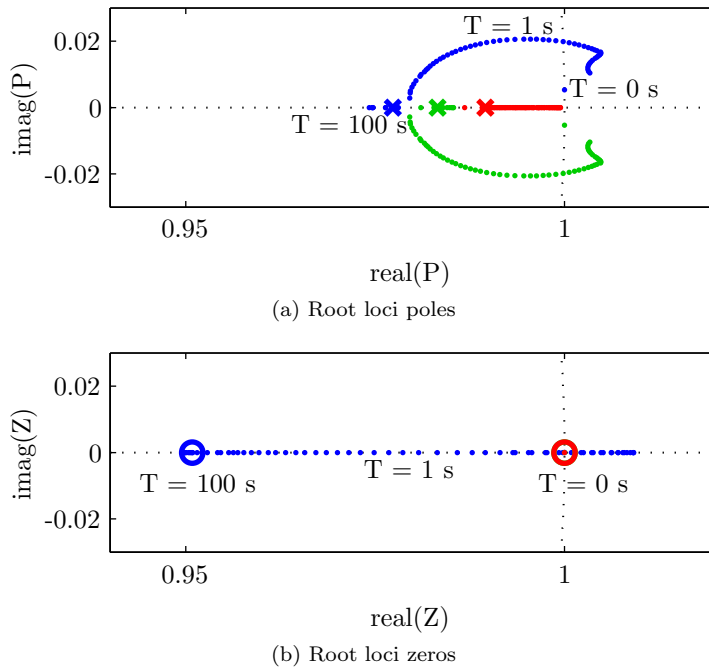


Figure 5.9: Plot of the root loci of the linearized control system with the implemented controllers of a selection of poles (top) and zeros (bottom). Locations of the poles and zeros with the controller after 100 s are denoted with \times and \odot respectively.

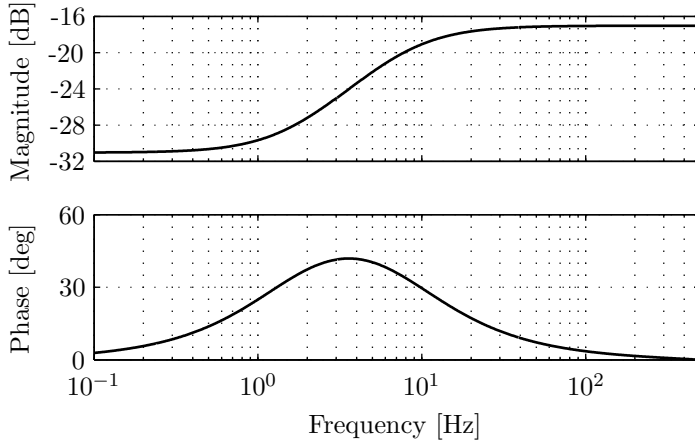


Figure 5.10: Bode plot (magnitude top, phase bottom) of $C_r(\check{\theta}(100), q)$.

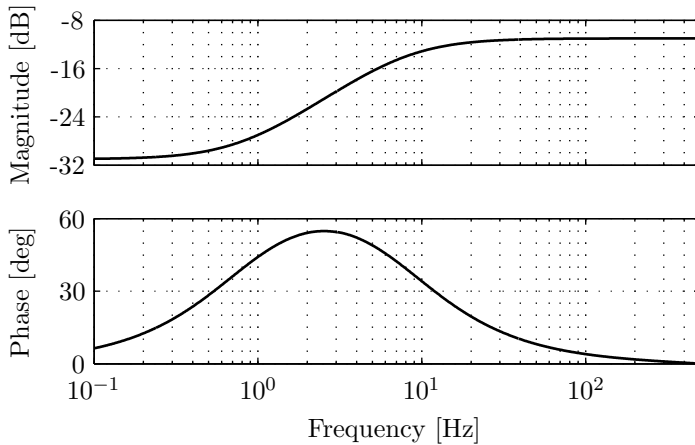


Figure 5.11: Bode plot (magnitude top, phase bottom) of $C_y(\check{\theta}(100), q)$.

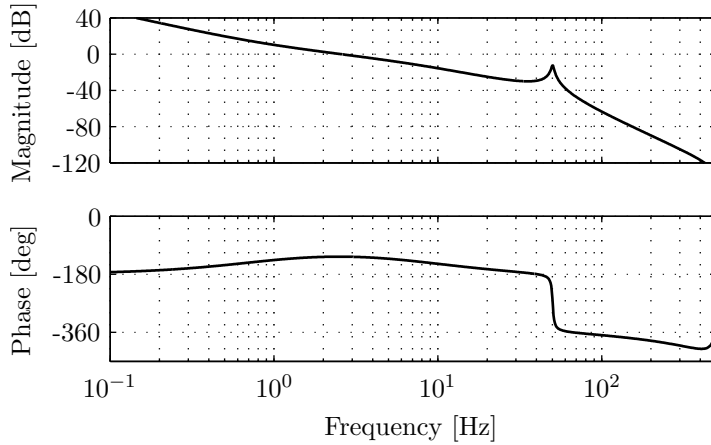


Figure 5.12: Bode plot (magnitude top, phase bottom) of the open loop $PC_y(\hat{\theta}(t_k), q)$ with the controller after 100 s.

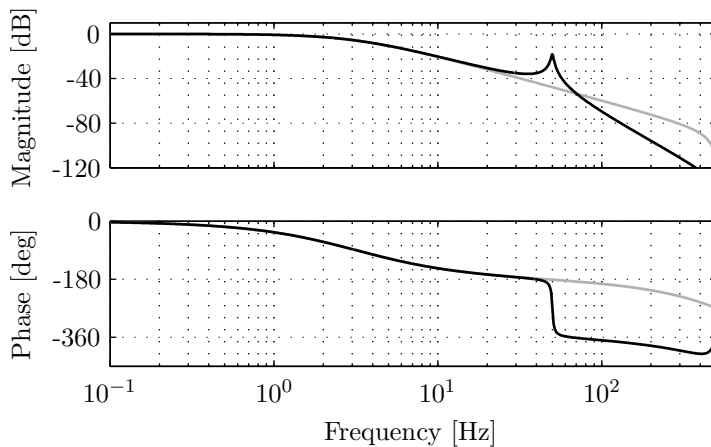


Figure 5.13: Bode plot (magnitude top, phase bottom) of the closed loop system with the controllers after 100 s (black) and the reference model $G_m(q)$ (grey).

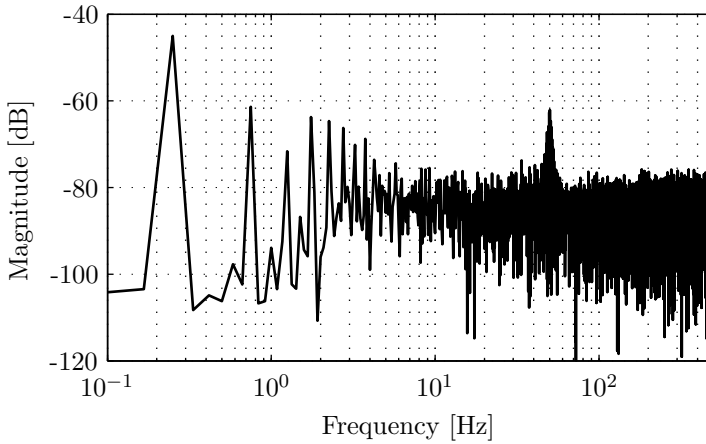


Figure 5.14: Plot of the frequency content of the error $G_m(q)r(t_k) - y(t_k)$ with the final controller.

5.3.3 Evaluation

The results of this simulation demonstrate that the proposed method is able to derive the controller parameters that are able to meet the performance requirement. The implemented parameters are adapted if they violate the performance requirement, whereas the Unfalsified Set is adapted almost continuously.

With the resulting controller, even though it is only of first order, a large similarity is observed between desired and achieved closed loop behavior. It should be noted, however, that the control problem presented in this simulation is not very challenging. The difficulty might be increased, for instance by increasing the bandwidth of the reference model or by decreasing the lower bound on $\Delta(t_k)$. Nonetheless, applicability of the proposed adaptive control method is proven here, which was the goal of this simulation. In the remainder of this chapter, a more challenging application is considered in the implementation on an experimental setup.

5.4 Experiment: Plant

Besides simulations, also experiments have been performed on a motion system to illustrate the effectiveness of the method. In the experiment, phenomena as friction, quantization and computational delays are present. The realtime environment strictly requires that the adaptive algorithm is evaluated within one sample time.

As a benchmark testbed, a stripped-down industrial inkjet printer is utilized, which is depicted in Fig. 5.15. The carriage for the printheads moves along a guidance rail and is driven by a DC-motor through a belt transmission. The position of the carriage is measured by a linear optical encoder, with an increment size of $4.26 \cdot 10^{-5}$ m/inc. The system is sampled at 1 kHz.

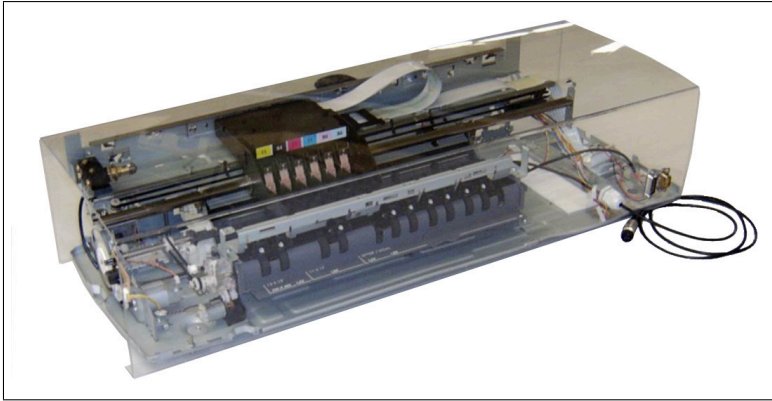


Figure 5.15: Photo of the stripped-down inkjet printer setup. The transparent cover is attached for safety.

5.4.1 Coulomb friction

The first characteristic, observed when conducting experiments on the printer setup, is a high level of Coulomb friction. This parasitic effect is induced by the sleeve bearing between the carriage and the guidance rail. The effort consumed for this effect accounts for roughly 40% of the available input.

5.4.2 Frequency response

To obtain an estimate of the frequency response function of the printer setup, a measurement is conducted of the sensitivity function $S = (1 + CP)^{-1}$. This frequency response will not be used in the design of the controllers, but only to evaluate the controllers and to provide insight in the dynamics of the system at hand. For the sensitivity measurement, a rudimentary feedback controller is implemented that achieves a stable closed loop with attenuation of low-frequent disturbances, such as e Coulomb friction. To further limit the influence of friction, the level of Coulomb friction is estimated and roughly compensated with a

feedforward signal. Moreover, a constant velocity trajectory is imposed, to assure that the carriage is not in the stick region of the friction. A pseudo-random signal is added to the controller output and the influence on the plant input is captured. This way, the sensitivity function $S = (1 + CP)^{-1}$ is computed. Since C is known (transfer of the implemented feedback controller), the only unknown is the plant P .

A Bode plot of the transfer of the input voltage of the amplifier of the DC-motor to the position of the carriage (in encoder increments), computed from the sensitivity measurement, is shown in Fig. 5.16. This transfer shows the characteristic low-frequent rigid body mode ($1/(Ms^2)$) of motion systems, with a phase shift due to time delay and a resonance at higher frequencies.

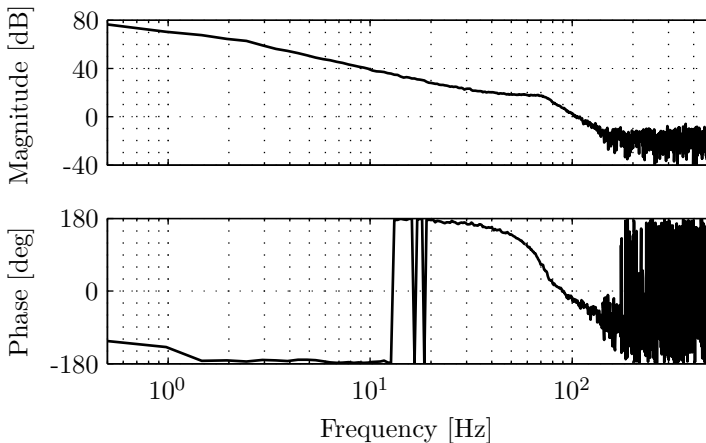


Figure 5.16: Bode plot (magnitude top, phase bottom) of the transfer of the input voltage of the amplifier of the motor to the position of the carriage, for the experimental setup as shown in Fig. 5.15.

5.4.3 Remark on the obtained frequency response

The frequency response, as obtained with the sensitivity measurement, is a good starting point for controller design. However, the frequency response function for similar setups might differ, a phenomenon that is not captured in this single measurement. To cover variations induced, e.g., by the production process or by wear, an uncertainty model might be included. The construction of such an uncertainty model is not a straightforward procedure and might end up in an overly conservative design. Therefore, we apply Ellipsoidal Unfalsified Control to

this setup, since it adapts to the actual system at hand and to the disturbances present during operation.

5.5 Experiment: Design

5.5.1 Goals

Characteristic for an inkjet printer is the repetitive nature of the motion of the carriage. To deliver the ink to the paper, the carriage moves over the paper in multiple strokes. During a stroke, the carriage ideally moves with constant velocity, and the turn at the end of a stroke is as fast as possible. To accomplish a maximum region of constant velocity, a triangular wave is chosen as the trajectory $r(t_k)$ of the carriage. The amplitude is representative for printing of an A4/letter size page.

If the carriage is in the printing area, the performance requirement is strict. However, if the carriage is not in the printing area, the requirements with regard to accuracy are less strict. Therefore, different levels are chosen for the performance requirement Δ . The relaxation of the performance requirement outside the printing area allows fast reversal of the carriage.

The desired closed loop behavior $G_m(q)$ of the controlled system is prescribed by a 2nd order low-pass reference model, to impose low-frequent tracking and high-frequent noise suppression.

$$G_m(q) = \mathcal{Z} \left(\frac{\omega_n^2}{s^2 + 2\zeta\omega_n s + \omega_n^2} \right) \quad (5.9)$$

with

$$\omega_n = 100 \quad (5.10)$$

$$\zeta = 0.8 \quad (5.11)$$

Here, $\mathcal{Z}(\cdot)$ denotes the Zero-Order-Hold transformation from the s -domain to the q -domain. A Bode plot of the reference model is shown in Fig. 5.17.

The triangular reference is given by

$$r(t) = 2fA \int_0^t \text{sign}(\sin(2\pi ft)) dt \quad (5.12)$$

with $f = 0.75$ Hz and $A = 7050$ inc. and sampled at 1kHz with a zero-order-hold. The reference $r(t_k)$ is shown in Fig. 5.18 and the frequency content of $r(t_k)$ is shown in Fig. 5.19.

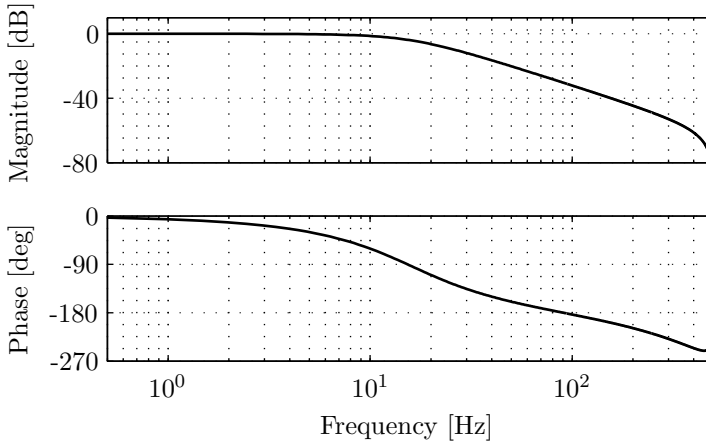


Figure 5.17: Bode plot (magnitude top, phase bottom) of the reference model $G_m(q)$.

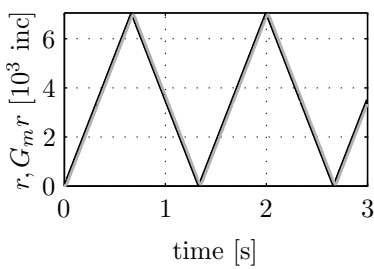


Figure 5.18: Plot of the reference $r(t_k)$ (black) and the desired output $G_m(q)r(t_k)$ (grey).

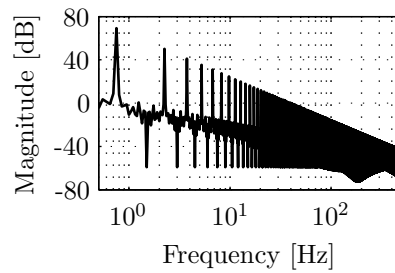


Figure 5.19: Plot of the frequency content of the triangular reference $r(t_k)$. The magnitude of the peaks (at odd multiples of 0.75 Hz) decreases for increasing frequency.

The performance requirement is chosen to decay exponentially, and is 10 times larger if the carriage is not in the printing area:

$$\Delta(t_k) = \begin{cases} 10 + 1000e^{-0.1t_k} & \text{for } 500 \leq r(t_k) \leq 6550 \\ 10(10 + 1000e^{-0.1t_k}) & \text{otherwise} \end{cases} \quad (5.13)$$

The initial value $\Delta(0)$ is determined from preliminary experiments, by investigation of the error with the initial controller. The final value $\Delta(t_\infty)$ is determined by repeatedly performing the experiment with diminishing $\Delta(t_\infty)$. The exponential decay is included to prescribe a gradually improving tracking performance and to allow for transient behavior.

The influence of $u(t_k)$ on the performance requirement is only marginally weighted, by setting its weighting factor to $\kappa(t_k) = 10^{-3}$. The maximum observed value of $u(t_k)$ is 5.1935.

The filter to reduce the effect of noise and outliers $W(q)$, (3.1), is set to 1.

5.5.2 Controller structure

The controller structure is chosen as a collection of low-pass and high-pass filters, and a nonlinear element of $r(t_k)$.

$$w(u(t_k), y(t_k), r(t_k), q) = \begin{bmatrix} u(t_k) \\ \frac{q-0.25q^2}{1-0.99q} u(t_k) \\ \frac{q-0.99q^2}{1-0.25q} u(t_k) \\ q u(t_k) \\ y(t_k) \\ \frac{q-0.25q^2}{1-0.99q} y(t_k) \\ \frac{q-0.99q^2}{1-0.25q} y(t_k) \\ q y(t_k) \\ \text{sign}((1-q)r(t_k)) \end{bmatrix} \quad (5.14)$$

The linear filters are chosen such that a lead-filter and a lag-filter are in the candidate controller set. Furthermore, symmetry between $u(t_k)$ and $y(t_k)$ is introduced. Typically, for motion systems a $1/(Ms^2)$ trend is observed at low-frequencies, with some additional delay. This implies that a lead-lag filter suffices to result in a stable control system with sufficient margins. It is therefore expected that the combination of lead- and lag-filters results in a feasible adaptive control problem. The breakpoints of the filters are chosen well below and above the breakpoint of $G_m(q)$.

The nonlinear element represents the direction of motion and is included to compensate the high level of Coulomb friction, as encountered in the experimental

setup. It is not included in the definition of $r_{\text{fict}}(\theta, t_k)$, (3.14), so it is regarded as an exogenous signal, which is plausible because it only depends on the direction of movement of $r(t_k)$. Nonetheless, it might introduce an offset in the fictitious reference, especially at the reversal of the carriage motion. Yet, the benefit that the carriage starts moving even with the initial controller, despite the high level of Coulomb friction, is eminent with this setup.

Note that the controller structure is not designed to achieve perfect tracking. Perfect tracking is not an issue here, merely tracking within the user defined bounds $\pm\Delta(t_k)$.

5.5.3 Initialization

Several parameters at $t_k = 0$ need to be defined a priori, which will be discussed here.

As initial controller, a P-controller is constructed with a very small gain plus a unit compensation for the Coulomb friction:

$$\check{\theta}(0) = [1000 \ 0 \ 0 \ 0 \ 1 \ 0 \ 0 \ 0 \ -1000]^T \quad (5.15)$$

The resulting control effort is given by

$$u(t_k) = \frac{1}{1000}(r(t_k) - y(t_k)) + \text{sign}((1 - q)r(t_k)) \quad (5.16)$$

The center $\theta_c(0)$ of the initial ellipsoidal Unfalsified Set is chosen identical to the initial candidate controller set $\check{\theta}(0)$. The initial ellipsoid is chosen as a sphere with radius 100:

$$\Sigma(0) = 10^4 \mathbb{I}_{9 \times 9} \quad (5.17)$$

The stepsize of the controller switching algorithm is chosen $\alpha = 0.9$, which is at some distance from the bounds of the Unfalsified Set. This choice enforces a moderate stepsize of the controller parameters, thereby limiting transient behavior, while still guaranteeing a finite number of controller switches.

The maximum volume ratio is constrained by setting $\epsilon(\nu) = 0.99 < 1$.

5.6 Experiment: Results

In this section, the results of the experimental implementation of Ellipsoidal Unfalsified Control are shown, and an evaluation of the results is provided.

5.6.1 Time domain

In Fig. 5.20, the tracking error $e(t_k) = G_m(q)r(t_k) - y(t_k)$ is shown as a function of time, together with the bound $\pm\Delta(t_k)$. Since the performance bound $\Delta(t_k)$ switches between two values, see (5.13), two distinctive levels are observed. Because the control effort is only weighted marginally, the two signals shown in Fig. 5.20 give a good indication on the unfalsification of the currently implemented controller. Namely, if the tracking error is outside the bounds $\pm\Delta(t_k)$, the currently implemented controller is falsified.

The initial controller (5.16) results in a large tracking error. Every time that the currently implemented controller is falsified, the controller parameters are adapted. In Fig. 5.21, the tracking error is shown after 70 s. During reversal of the carriage motion, peaks in the tracking error are observed. However, due to relaxation of the performance requirements outside the printable area, these peaks are not restrictive. Nevertheless, the tracking error crosses the bounds $\pm\Delta(t_k)$ on three instances, which result in an update of the implemented controller parameter set.

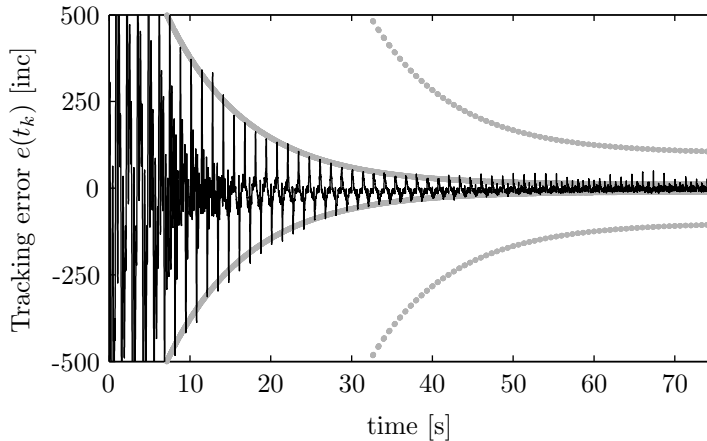


Figure 5.20: Tracking error as a function of time (black line) and bounds $\pm\Delta(t_k)$ (grey dots). Due to the switching of the bound $\Delta(t_k)$, see (5.13), two distinctive levels are observed.

The evolution of the controller parameters $\check{\theta}(t_k)$ is shown in Fig. 5.22. This figure also shows the center of the ellipsoid, $\theta_c(t_k)$, as well as the bounds of $\mathcal{E}(t_k)$ in the direction of the parameter, $\theta_{c,i} \pm \Sigma_{i,i}^{-1/2}$. Because the currently implemented controller parameters are frequently falsified, see Fig. 5.20, the parameters are also adapted many times.

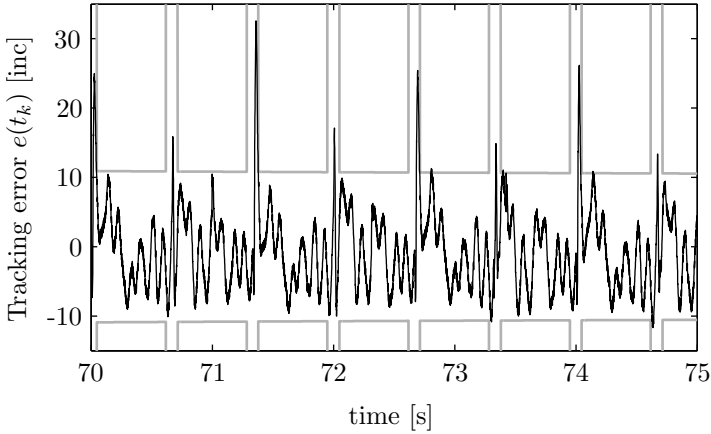


Figure 5.21: Zoom of tracking error after 70 s (black) and bounds $\pm\Delta(t_k)$ (grey). Peaks in the tracking error are observed during reversal of the carriage motion.

Initially, the bounds for θ_6 decrease rapidly, whereas simultaneously the bounds of the other parameters increase. This increase results from the outer bounding ellipsoidal approximation. Nonetheless, the volume of the Unfalsified Set is monotone non-increasing, as can be seen from Fig. 5.23, which shows the evolution of $\det(\Sigma(t_k))$ over time. The combination of a simultaneous increase in some directions and decrease in others is also visible in the lobes on $\theta_{c,i} \pm \Sigma_{i,i}^{-1/2}$, which result from a changing orientation of $\mathcal{U}(t_k)$ over time, combined with the outer-bounding approximation.

The values of the controller parameters $\check{\theta}(75)$ and the center of the Unfalsified Set $\theta_c(75)$ are

$$\check{\theta}(75) = \begin{bmatrix} 653.4618 \\ -6.5962 \\ 0.8944 \\ -351.3421 \\ -67.4793 \\ -0.0024 \\ 109.4123 \\ 67.2029 \\ -656.9903 \end{bmatrix}, \quad \theta_c(75) = \begin{bmatrix} 653.3262 \\ -6.6972 \\ 0.9075 \\ -351.4874 \\ -67.4075 \\ -0.0025 \\ 109.6084 \\ 67.1313 \\ -656.9457 \end{bmatrix}$$

Note that the parameters $\check{\theta}(75)$ are just one selection from the Unfalsified Set at $t_k = 75$ s, and that the distance to the center of the Unfalsified Set differs per parameter. Furthermore, the resulting controller parameter set $\check{\theta}(75)$ is not in the initial ellipsoid $\mathcal{E}(0)$. This remarkable phenomenon is allowed by the outer-bounding approximations that let the ellipsoid extend in some directions.

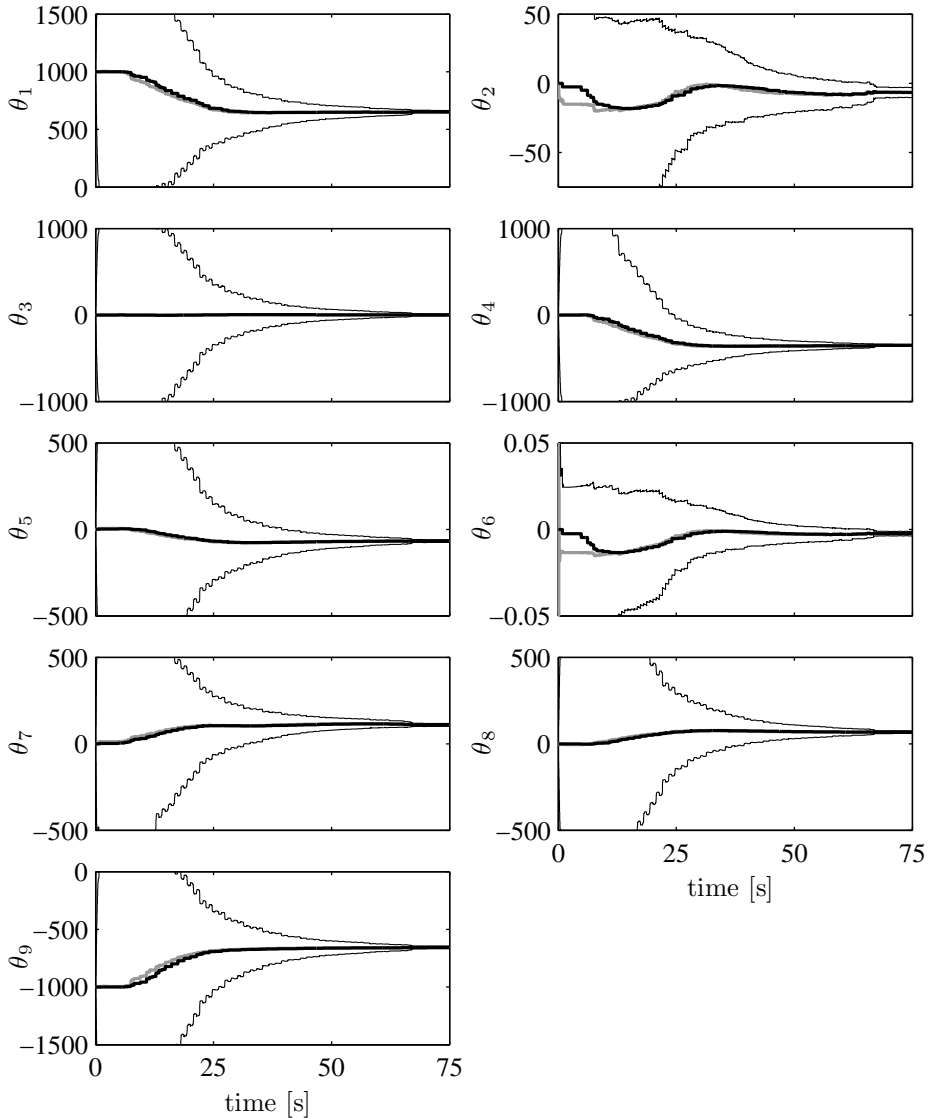


Figure 5.22: Evolution of controller parameters $\check{\theta}(t_k)$ over time (black pronounced line). Also shown is the center of the ellipsoid $\theta_c(t_k)$ (grey) and the bounds $\theta_{c,i} \pm \Sigma_{i,i}^{-1/2}$ (thin black lines).

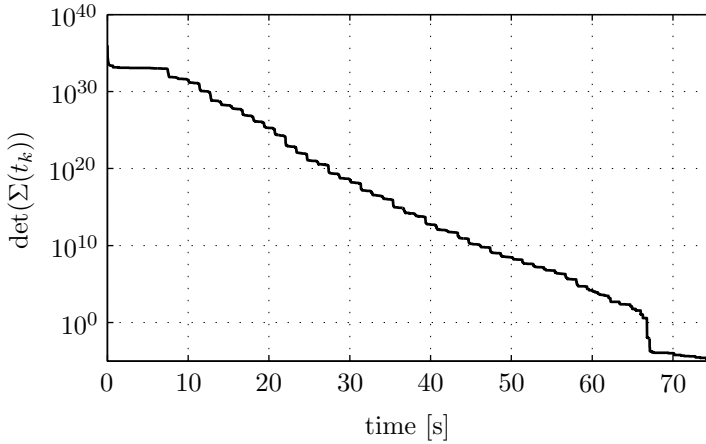


Figure 5.23: Evolution of $\det(\Sigma(t_k))$ over time, which is proportional to the volume of the Unfalsified Set $\mathcal{E}(t_k)$.

5.6.2 Frequency domain

The measured frequency response of the experimental setup (which is *not* used in the Ellipsoidal Unfalsified Control algorithm), as derived in Section 5.4.2, is used to construct the frequency response of the open loop of the controlled system. The Bode plot of the controller $C_y(\check{\theta}(75), q)$ is shown in Fig. 5.24, and the Bode plot of the open loop is shown in Fig. 5.25. The controller $C_y(\check{\theta}(75), q)$ exhibits a phase lead of maximally 50 degrees, required to result in a stable control system. Furthermore, the controller has a pole and a zero outside the unit circle. Nevertheless, the resulting closed loop is stable, as can also be seen from the Nyquist plot in Fig. 5.26.

For the evaluation of the closed loop system from r to y , first only the linear filters of $w(\cdot)$, (5.14), are considered. The resulting frequency response is shown in Fig. 5.27. Most striking observation is the lower gain of the closed loop frequency response compared to the frequency response of the reference model $G_m(q)$, (5.9). In Fig. 5.28, the frequency content is shown of the achieved output $y(t_k)$ and the desired output $G_m(q)r(t_k)$. The low-frequency deviation, as predicted by Fig. 5.27, is not observed. Actually, the frequency content matches up to 15 Hz in the peaks, where the signal-to-noise ratio is largest. At frequencies higher than 15 Hz, the

achieved output $y(t_k)$ even contains more energy than $G_m(q)r(t_k)$. Therefore, an extension to the analysis as performed above is proposed.

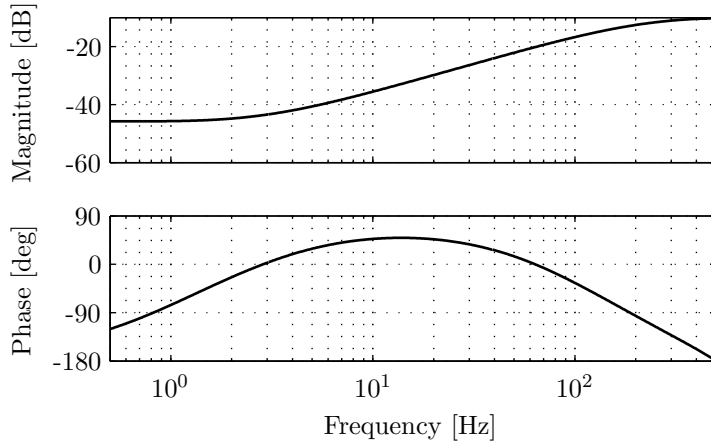


Figure 5.24: Bode plot (magnitude top, phase bottom) of the controller $C_y(\check{\theta}(75), q)$.

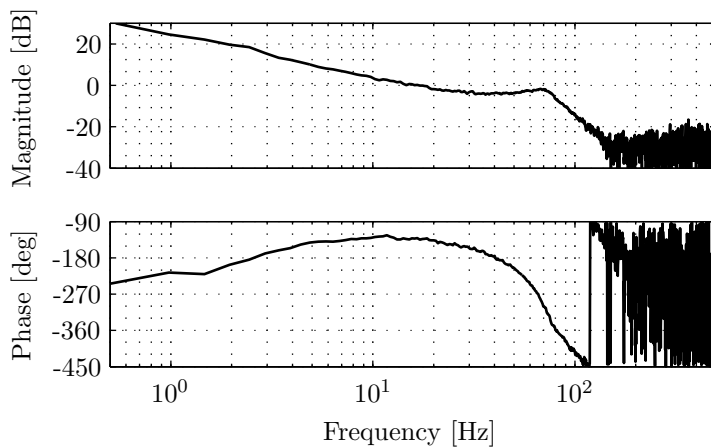


Figure 5.25: Bode plot (magnitude top, phase bottom) of the open loop $PC_y(\check{\theta}(75), q)$.

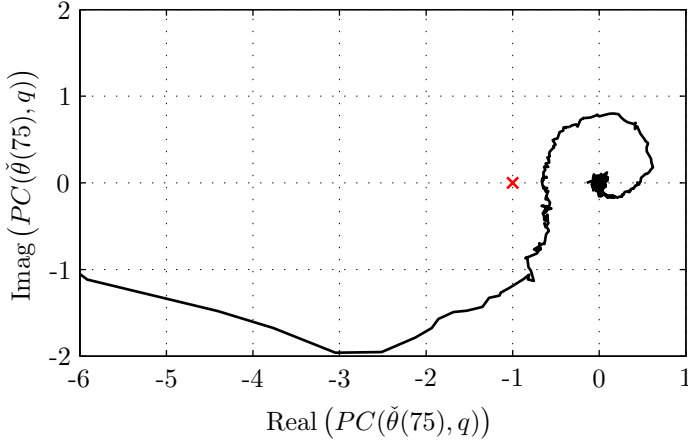


Figure 5.26: Nyquist plot of the controlled system with $\check{\theta}(75)$ for positive frequencies. For decreasing frequencies outside this plot, the response goes clockwise to the positive real-axis.

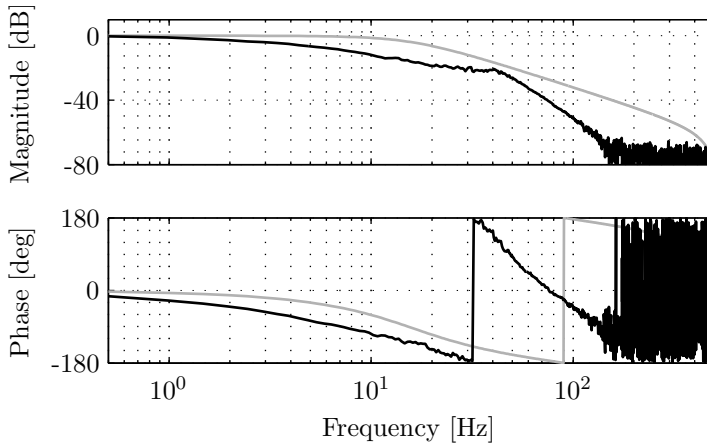


Figure 5.27: Bode plot (magnitude top, phase bottom) of the closed loop system from r to y with $\check{\theta}(75)$ (black) and of the reference model $G_m(q)$ (grey). Only the linear filters of $w(\cdot)$ are regarded.

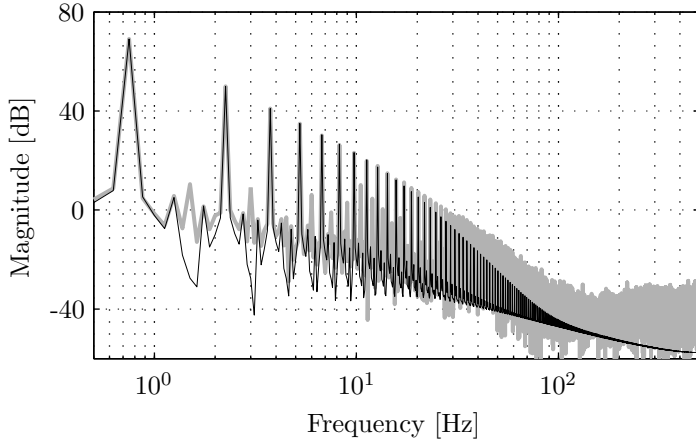


Figure 5.28: Estimated frequency content of $G_m(q)r(t_k)$ (black) and $y(t_k)$ with $\theta(75)$ (grey).

In the frequency response analysis above, the influence of the nonlinear element of $w(\cdot)$, (5.14), is neglected. To incorporate the influence of this element, it is observed that the output signal of the nonlinear filter $\text{sign}((1-q)r(t_k))$ is exactly duplicated by the linear filter $\frac{f_s}{2fA}(1-q)r(t_k)$ for the reference defined in (5.12) and zero initial conditions, with f and A as in (5.12) and f_s the sample frequency (1000 Hz for this setup). Since both filters produce exactly the same output signal for this specific $r(t_k)$, the control output is not changed if the nonlinear filter was replaced by the linear filter. For the frequency domain analyses, the linear filter can therefore be substituted for the nonlinear filter, and an analysis can be made of the frequency content of the output relative to the frequency content of the input of the closed loop system incorporating the influence of the additional filter. This ratio of the frequency contents is shown in Fig. 5.29, and the gain of the closed loop transfer function increased drastically for frequencies larger than 1 Hz by incorporation of the filter.

The ratio of the frequency contents predicts good tracking for frequencies up to 12 Hz, whereas the frequency response with the purely linear filters already showed a considerable deviation for frequencies larger than 2 Hz. In the frequency contents, shown in Fig. 5.28, no large low frequent deviation is observed, therefore it is concluded that the extended frequency response is more consistent with the observed behavior.

The analysis as performed above only holds for the specific triangular reference as is applied in the experiment. But then again, the resulting controller is specifically designed using the conditions as encountered in the experiment.

The Bode plots of the controller $C_r(\check{\theta}(75), q)$ are shown in Fig. 5.30. The influence of the nonlinear filter can be observed as the increase of the gain of the controller at frequencies higher than 2 Hz.

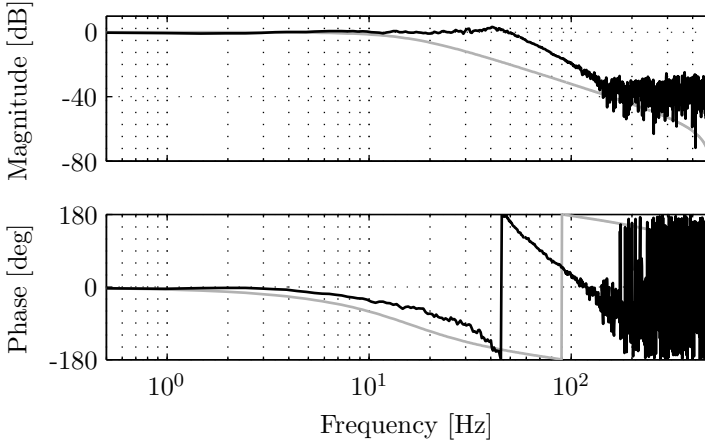


Figure 5.29: Frequency content of the output relative to the frequency content of the input of the closed loop system from r to y with $\check{\theta}(75)$ with substituted contribution of the nonlinear filter of $w(\cdot)$ (black) and of the reference model $G_m(q)$ (grey).

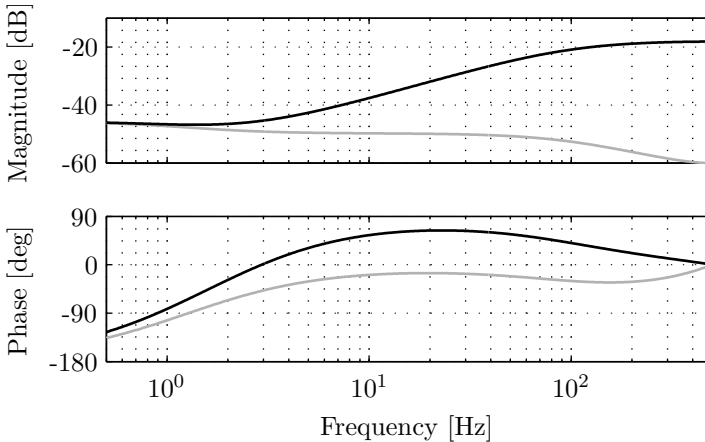


Figure 5.30: Bode plot (magnitude top, phase bottom) of controller $C_r(\check{\theta}(75), q)$, with only the linear filters of $w(\cdot)$ (grey) and with substituted contribution of the nonlinear filter of $w(\cdot)$ (black).

5.6.3 Evaluation

Based on the results from the experiment, it is assessed that the Ellipsoidal Unfalsified Algorithm achieves appropriate adaptation of the controller parameters. Even under the influence of the disturbances, as encountered in the experiment, this plant-model-free controller design method with realtime adaptation correctly adapted the Unfalsified Set and the implemented controller. This demonstrates the applicability of Ellipsoidal Unfalsified Control to a real-life motion system, with as constraint a high sample frequency of 1 kHz.

The little plant knowledge that was available from some preliminary experiments is used in the design of the controller structure and the performance requirement, for instance in the selection of $G_m(q)$, $w(\cdot)$, $\Delta(t_k)$, $\kappa(t_k)$ and $r(t_k)$. No further plant knowledge is needed, since the controller parameters are adapted using measured input/output data. During the experiment, the controlled system satisfied the predefined performance requirement, except at the instances that the currently implemented controller was falsified and a new controller was inserted in the loop. Because not much effort is needed in the design of the initial controller, only limited tuning effort is needed in the entire control design. Furthermore, this data-driven method is applied under normal operating conditions, i.e., no especially designed experiment is required. Accordingly, the method is very versatile.

Chapter 6

Multivariable Ellipsoidal Unfalsified Control

IN THIS chapter, the methodology of Ellipsoidal Unfalsified Control is extended to cover general multivariable controllers. The conditions that are imposed on the control law are analyzed, and a controller structure that fulfills these conditions is proposed. It is shown how the new controller structure fits in the Ellipsoidal Unfalsified Control framework and how the same arithmetics can be used to update the Unfalsified Set.

6.1 Plant properties

Consider the general Multiple-Input Multiple-Output plant in Fig. 6.1. Plant P has inputs $\underline{u}(t_k) \in \mathbb{R}^m$, outputs $\underline{y}(t_k) \in \mathbb{R}^n$ that are available to the controller and outputs $\underline{z}(t_k) \in \mathbb{R}^l$ that are used in the performance criterion. Note that $\underline{z}(t_k)$ are the plant outputs that are not required to be small in this setting. For clarity, $\underline{u}(t_k)$ and $\underline{y}(t_k)$ are used in this chapter, in contrast to $u(t_k)$ and $y(t_k)$, to stress that vector signals are considered here.

The desired multivariable closed loop dynamics of the controlled system are defined by the reference model $G_m(q)$. The reference model $G_m(q)$ might for instance be diagonal, if a decoupled closed-loop system is desired. $G_{m,i}(q)$ denotes the i^{th} row of $G_m(q)$.

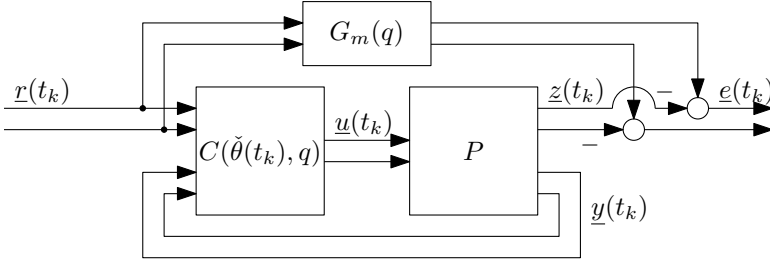


Figure 6.1: Schematic representation of general MIMO plant P with controller $C(q)$ and reference model $G_m(q)$.

It is assumed that the controller $C(q)$ has access to all plant outputs $\underline{y}(t_k)$ and references $\underline{r}(t_k) \in \mathbb{R}^l$. The error $\underline{e}(t_k)$ is defined as $\underline{e}(t_k) = G_m(q)\underline{r}(t_k) - \underline{z}(t_k)$; $\underline{e}(t_k) \in \mathbb{R}^l$.

6.2 Controller structure

As in the SISO case (3.14), let the controller structure be chosen such that its inverse to the reference $\underline{r}(t_k)$ is affine in the controller parameters $\check{\theta}(t_k)$:

$$\underline{r}(t_k) = w(\underline{u}(t_k), \underline{y}(t_k), q)\check{\theta}(t_k) \quad (6.1)$$

A further restriction is that $\underline{u}(t_k)$ has to be uniquely defined by (6.1), for given $\check{\theta}(t_k)$, $\underline{r}(t_k)$ and measured inputs and outputs. Therefore, consider the controller structure

$$\underline{r}(t_k) = \check{\Theta}_u(t_k)\underline{u}(t_k) + \Lambda(\underline{u}(t_{k-1}), \underline{y}(t_k), q)\check{\theta}_l(t_k) \quad (6.2)$$

$$= [\mathbb{I} \otimes \underline{u}^T(t_k) \quad \Lambda(\underline{u}(t_{k-1}), \underline{y}(t_k), q)] \begin{bmatrix} \check{\theta}_u(t_k) \\ \check{\theta}_l(t_k) \end{bmatrix} \quad (6.3)$$

Here, \otimes denotes the Kronecker product. The matrix $\check{\Theta}_u(t_k)$ is constructed from the elements of $\check{\theta}(t_k)$ that correspond to $\underline{u}(t_k)$ and the vector $\check{\theta}_u(t_k)$ contains the concatenated transposed rows of $\check{\Theta}_u(t_k)$. The matrix Λ contains (stably filtered) measured input/output data. From (6.2), it can be seen that $\underline{u}(t_k)$ is well defined, if $\check{\Theta}_u$ is invertible. The resulting controller has an ARMA structure, with basis functions defined by the elements of Λ .

The controller structure (6.3) defines Stably Causally-Left-Invertible (SCLI) controllers for $\Lambda(\cdot)$ stable and $\check{\Theta}_u$ invertible.

From (6.1) the fictitious reference $\underline{r}_{\text{fict}}(\theta, t_k)$ is easily derived, by considering general parameters θ

$$\underline{r}_{\text{fict}}(\theta, t_k) = w(\underline{u}(t_k), \underline{y}(t_k), q)\theta \quad (6.4)$$

6.3 Performance requirement

Consider the l_∞ performance requirement (3.4), as prescribed by Ellipsoidal Unfalsified Control. For multivariable systems, this translates to the vector requirement (6.5) that has to hold elementwise.

$$|W(q)(G_m(q)\underline{r}_{\text{fict}}(\theta, t_k) - \underline{z}(t_k))| + |K(t_k)\underline{u}(t_k)| \leq \underline{\Delta}(t_k) \quad (6.5)$$

where $W(q)$ is a square MIMO weighting filter, $\underline{\Delta} \in \mathbb{R}_+^l$ is a (time-dependent) bound and $K(t_k)$ is a full rank matrix of appropriate size $\forall t_k$, to ensure that $K(t_k)\underline{u}(t_k) = \underline{0}$ only if $\underline{u}(t_k) = \underline{0}$.

6.4 Unfalsified Set

The Unfalsified Set at time t_{k-1} is described by the ellipsoid $\mathcal{E}(t_{k-1})$, (3.19). The region of parameters that is unfalsified by the current measurement data, $\mathcal{U}(t_k)$, is defined by

$$\mathcal{U}(t_k) = \left\{ \theta \mid -\hat{\underline{\Delta}}(t_k) \leq W(q)G_m(q)w(\underline{u}(t_k), \underline{y}(t_k), q)\theta - W(q)\underline{z}(t_k) \leq \hat{\underline{\Delta}}(t_k) \right\} \quad (6.6)$$

with $\hat{\underline{\Delta}}(t_k) = \underline{\Delta}(t_k) - |K(t_k)\underline{u}(t_k)|$.

Equation (6.6) has to hold for all rows and, therefore, is evaluated row-wise. As a consequence, (6.6) defines l sets of parallel half-spaces.

The Unfalsified Set at time t_k , $\mathcal{E}(t_k)$, is constructed from the intersection $\mathcal{E}(t_{k-1}) \cap \mathcal{U}(t_k)$. However, current analytical results to approximate the intersection only exist for the intersection of an ellipsoid with 1 set of parallel half-spaces. Therefore, the intersection is approximated by considering the parallel half-spaces (6.6) sequentially. The ordering in this sequential procedure can be chosen arbitrarily, although a different ordering might lead to different results.

The sequential update of the Unfalsified Set is in many ways analogous to the update of the Unfalsified Set in consecutive time-steps, where only the parallel half-spaces of the last measurement are regarded. However, with time-steps the ordering is fixed, given by the order the measurements become available.

Theorem 6.1 demonstrates that the new ellipsoidal Unfalsified Set $\mathcal{E}(t_k)$ outer-bounds the region of currently unfalsified controllers $\mathcal{E}(t_{k-1}) \cap \mathcal{U}(t_k)$. The outer-bounding property assures that unfalsified controllers are not wrongly dismissed.

Theorem 6.1 *Sequential application of the update with the individual sets of parallel half-spaces guarantees $\mathcal{E}(t_k) \supseteq \mathcal{E}(t_{k-1}) \cap \mathcal{U}(t_k)$.*

Proof: Let $\mathcal{U}_i(t_k)$ be defined as the i^{th} set of parallel half-spaces of $\mathcal{U}(t_k)$, $i = 1, \dots, l$, and let $\mathcal{E}_i(t_k)$ be the ellipsoid after the sequential update with $\mathcal{U}_i(t_k)$. From Section 3.8 it follows that

$$\mathcal{E}_i(t_k) \supseteq (\mathcal{E}_{i-1}(t_k) \cap \mathcal{U}_i(t_k)) \quad (6.7)$$

since $\mathcal{E}_i(t_k)$ is the outer-bounding ellipsoidal approximation of the intersection. Consequently, it holds that

$$\mathcal{E}_{i+1}(t_k) \supseteq (\mathcal{E}_i(t_k) \cap \mathcal{U}_{i+1}(t_k)) \supseteq (\mathcal{E}_{i-1}(t_k) \cap \mathcal{U}_i(t_k) \cap \mathcal{U}_{i+1}(t_k)) \quad (6.8)$$

By expanding (6.7) and (6.8) for $i = 1, \dots, l$, it follows that

$$\mathcal{E}_l(t_k) \supseteq (\mathcal{E}_0(t_k) \cap \mathcal{U}_1(t_k) \cap \dots \cap \mathcal{U}_l(t_k)) \quad (6.9)$$

Next, consider that at some time t_k , $\mathcal{E}_0(t_k) = \mathcal{E}(t_{k-1})$ and $\mathcal{E}_l(t_k) = \mathcal{E}(t_k)$. Furthermore, $\mathcal{U}(t_k) = \mathcal{U}_1(t_k) \cap \dots \cap \mathcal{U}_l(t_k)$. The theorem follows by substitution of $\mathcal{E}(t_{k-1})$, $\mathcal{E}(t_k)$ and $\mathcal{U}(t_k)$ in (6.9). ■

The sequential update procedure results in a sub-optimal approximation of the Unfalsified Set, since consecutive outer-bounding approximations are made. Nevertheless, the volume of the Unfalsified Set is monotone non-increasing, as follows from Section 3.8 and the observation of the analogy with consecutive time-steps.

6.5 Controller selection

For multivariable Ellipsoidal Unfalsified Control, the controller selection (3.33) is maintained. However, the controller update is applied after every sequential update with \mathcal{U}_i , $i = 1, \dots, l$. Then, $\check{\theta}(t_k)$ is the controller after the last sequential update at time t_k .

A condition on the selection of $\check{\theta}(t_k)$ is that $\Theta_u(t_k)$ has to be invertible. If the condition is not met for current α , a different $\alpha \in [0, 1)$ is to be selected for which $\Theta_u(t_k)$ is invertible.

With the proposed controller selection, it is not guaranteed that $\check{\theta}(t_k) \in \mathcal{E}(t_{k-1}) \cap \mathcal{U}(t_k)$. As alternative, consider to first update the ellipsoidal Unfalsified Set for all sets of parallel half-spaces, before applying the controller update. With this alternative, if $\theta_c(t_k) \in \mathcal{U}(t_k)$, then $\check{\theta}(t_k) \in \mathcal{U}(t_k)$. However, if the condition that $\theta_c(t_k) \in \mathcal{U}(t_k)$ is not fulfilled, it can not be guaranteed with controller selection algorithm (3.33) that $\check{\theta}(t_k) \in \mathcal{U}(t_k)$ for any $\Gamma(t_k, \alpha)$. Therefore, the proposed controller selection algorithm is maintained, for which controller selection algorithm (3.33) can always be used.

Although $\check{\theta}(t_k) \in \mathcal{E}(t_{k-1}) \cap \mathcal{U}(t_k)$ can not be guaranteed in general, it can be guaranteed if $\mathcal{E}(t_k) = \mathcal{E}(t_{k-1})$ by application of Lemma 3.4 for the sequential update with $\mathcal{U}_i(t_k)$ for $i = 1, \dots, l$.

6.6 Stability

Ellipsoidal Unfalsified Control only considers the external, or input-output, behavior of the plant. This naturally leads to the stability concept of bounded-input bounded-output (BIBO) stability, see Definition 4.1 on page 38.

Theorem 6.2 (Stability multivariable Ellipsoidal Unfalsified Control)

The multivariable Ellipsoidal Unfalsified Control adaptive system is BIBO stable, if the adaptive control problem is feasible.

Proof: In Chapter 4, sufficient conditions are derived for the stability of SISO Ellipsoidal Unfalsified Control, based on the stability conditions in (Stefanovic et al., 2005; Wang et al., 2005). The conditions can be summarized as: 1) feasibility of the adaptive control problem, 2) discarding of demonstrably destabilizing controllers, and 3) a limited number of controller switches.

From the analogy to consecutive time-steps as observed in Section 6.4, it directly follows that the number of distinctive ellipsoids is limited and that the number of controller switches per ellipsoids is limited. Thereby, the number of overall controller switches is limited and condition 3) is satisfied. For details, see Chapter 4.

The controllers with the controller structure of multivariable Ellipsoidal Unfalsified Control (6.3) are SCLI by construction, for $\check{\Theta}_u(t_k)$ invertible and because $\Lambda(\cdot)$ contains only stable filters. Then, from Theorem 4.6 it follows that a sufficient condition to discard demonstrably destabilizing controllers is that controllers that do not meet the performance requirement (3.4) are discarded from the candidate

controller set. However, for multivariable Ellipsoidal Unfalsified Control with a sequential update of the controller parameter set $\check{\theta}$, it is not guaranteed that indeed $\check{\theta}(t_k) \in \mathcal{E}(t_{k-1}) \cap \mathcal{U}(t_k)$, i.e., that the new implemented controller set indeed satisfies performance requirement (3.4). Nevertheless, the number of occurrences that $\check{\theta}(t_k) \notin \mathcal{E}(t_{k-1}) \cap \mathcal{U}(t_k)$ is limited, since it requires that $\mathcal{E}(t_{k-1}) \neq \mathcal{E}(t_k)$. Because the number of distinctive ellipsoids is limited, see Section 4.5.1, this implies that eventually $\check{\theta}(t_k) \in \mathcal{E}(t_{k-1}) \cap \mathcal{U}(t_k)$, which is sufficient to discard demonstrably destabilizing controllers, see Theorem 4.6. So, although it might not hold on every single timestep, eventually the sufficient condition to meet condition 2) is fulfilled.

Condition 1) is only fulfilled by assumption. If no plant information is available a priori, it is impossible to guarantee feasibility. If some plant information is available, though, it should be used in the design of the controller structure to maximize the chance of feasibility.

Concluding, with the assumption of feasibility, multivariable Ellipsoidal Unfalsified Control is stable. ■

6.7 Simulation

6.7.1 Plant

Ellipsoidal Unfalsified Control has been applied to the 2×2 plant shown in Fig. 6.2. The plant is sampled at 1 kHz with a zero-order-hold and the Ellipsoidal Unfalsified Control algorithm is applied every sample time. The computational load of the algorithm is such that an online implementation is feasible at this sample rate. An uncorrelated, bounded noise $\underline{d}(t_k)$ with power 10^{-10} [m²] and a maximum of 10^{-3} [m] is added to the plant outputs y . The plant inputs \underline{u} are in [kN]. The Bode magnitude plot of the plant, shown in Fig. 6.3, shows a high degree of interaction in the plant, with the off-diagonal terms similar in magnitude to the diagonal terms.

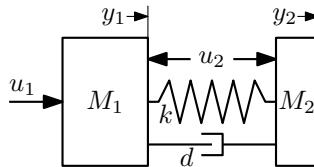


Figure 6.2: Schematic representation of the dual-stage motion system, with $M_1 = 1$ [kg], $M_2 = 0.1$ [kg], $k = 0.9$ [N/m] and $d = 0.1$ [Ns/m].

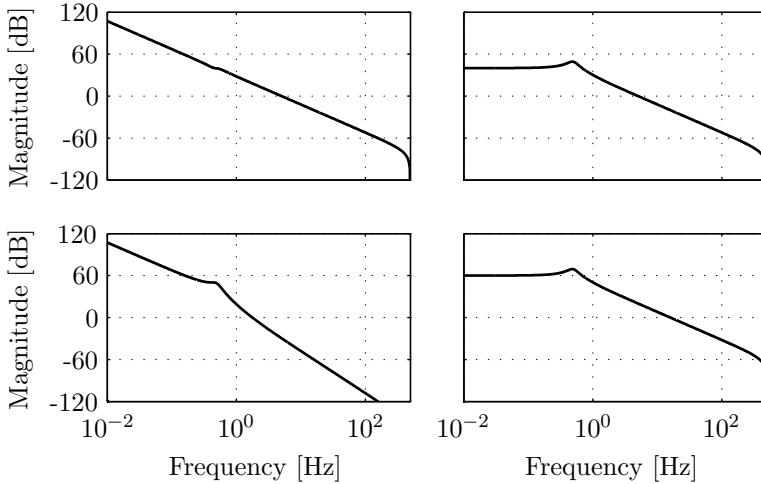


Figure 6.3: Bode magnitude-plot of the plant of Fig. 6.2.

6.7.2 Goals

The reference model G_m is given by

$$G_m(s) = \begin{bmatrix} \frac{10^2}{s^2 + 2 \cdot 10s + 10^2} & 0 \\ 0 & \frac{40^2}{s^2 + 2 \cdot 40s + 40^2} \end{bmatrix} \quad (6.10)$$

Reference model G_m is given here in continuous time solely for ease of perception. The performance outputs \underline{z} are the displacements of both masses: $\underline{z}(t_k) = \underline{y}(t_k)$. The trajectory for $z_1(t_k)$ is a square wave of amplitude 5 [m] every 5 [s], starting at $t_k = 0.5$ [s]. The trajectory for $z_2(t_k)$ is a square wave of amplitude 1 [m] every 2 [s], starting at $t_k = 0$ [s]. Plots of the trajectories $\underline{r}(t_k)$ and the corresponding desired outputs $G_m(q)\underline{r}(t_k)$ are shown in Fig. 6.4.

The bounds on the tracking errors are given by

$$\underline{\Delta}(t_k) = \begin{bmatrix} 10e^{-0.15t_k} + 0.005 \\ 10e^{-0.20t_k} + 0.0012 \end{bmatrix} \quad (6.11)$$

An offset is included in $\underline{\Delta}(t_k)$ to guarantee feasibility in the presence of output noise, whereas the exponential decay is included to allow for transients. The bound $\underline{\Delta}(t_k)$ is tighter for the second output than for the first output, both in the offset and in the exponential decay. The offset for the second output is just slightly larger than the maximum amplitude of the output noise of 0.001. The weighting function $W(q)$ is defined as $W(q) = \mathbb{I}_{2 \times 2}$. The matrix $K(t_k)$ is chosen as a constant matrix

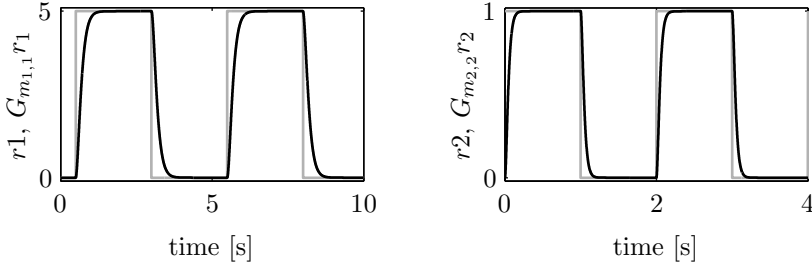


Figure 6.4: Plots of trajectories (grey) and filtered trajectories (black) (Note the different scales).

such that $|\underline{u}(t_k \rightarrow \infty)| \leq [5, 5]^T$:

$$K = \frac{1}{5} \begin{bmatrix} 0.005 & 0 \\ 0 & 0.0012 \end{bmatrix} \quad (6.12)$$

6.7.3 Controller structure

The controller structure is given by

$$w(u, y, q) = \mathbb{I}_{2 \times 2} \otimes \left[\underline{u}^T(t_k) \frac{1}{1 - 0.8q^{-1}} \underline{u}^T(t_{k-1}) \quad \underline{y}^T(t_k) \quad \underline{y}^T(t_{k-1}) \right] \quad (6.13)$$

This controller structure requires 16 parameters, the first group of 8 is used in the construction of $r_{\text{fict},1}(t_k)$, the second group of 8 is used in the construction of $r_{\text{fict},2}(t_k)$. Although both fictitious reference generators have an individual parametrization, the structure in $w(\cdot)$ is the same for both. Furthermore, the relations for $u_1(t_k)$ and $u_2(t_k)$, as well as for $y_1(t_k)$ and $y_2(t_k)$, are identical, such that a full-block multivariable controller can result without prejudice for a certain directionality.

To result in a stable control system, lead/lag filters are contained in the candidate controller set for all combinations of the inputs and outputs of the controller.

6.7.4 Initialization

The controller is initialized at $t_0 = 0$ with the parameter set

$$\check{\theta}(0) = [1 \ 0 \ 0 \ 0 \ 1 \ 0 \ 0 \ 0 \ 0 \ 1 \ 0 \ 0 \ 0 \ 1 \ 0 \ 0] \quad (6.14)$$

which is equivalent to $\underline{u}(t_k) = \underline{r}(t_k) - \underline{y}(t_k)$. This initial controller is destabilizing the plant. The initial ellips $\mathcal{E}(0)$ is defined by $\theta_c(0) = \check{\theta}(0)$, $\Sigma(0) = 10^4 \mathbb{I}_{16 \times 16}$.

The parameter α that influences the controller selection is set to $\alpha = 0.99$, and the parameter $\epsilon(\nu)$ that influences omissions in the update of the Unfalsified Set is set to $\epsilon(\nu) = 0.99$.

6.7.5 Time domain results

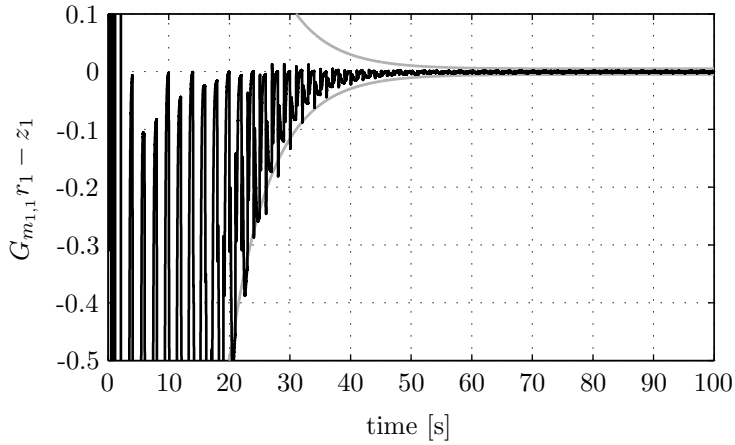
In Fig. 6.5 and Fig. 6.6, the errors of both performance channels are shown as a function of time, together with the performance bounds. When the performance requirement is not met, the current controller parameter set is falsified and replaced by a new controller parameter set. Both tracking errors have to be within the bounds simultaneously for the controller to be unfalsified. Remarkably, for $t_k < 24$ s, the currently implemented controller is falsified by the tracking error of performance channel 1 that crosses the bounds. However, for $t_k > 32$ s, the roles have changed and the currently implemented controller is only falsified because the tracking error of performance channel 2 crosses the bounds.

In Fig. 6.7, the evolution of the implemented controller parameters $\check{\theta}_i(t_k)$ is shown as a function of time, for $i = 1, \dots, 16$. The final values of the controller parameters are shown in Table 6.1. As already mentioned in Section 3.9, these parameters are just one selection from the Unfalsified Set. However, since it is in the Unfalsified set, this set fulfills the performance requirement.

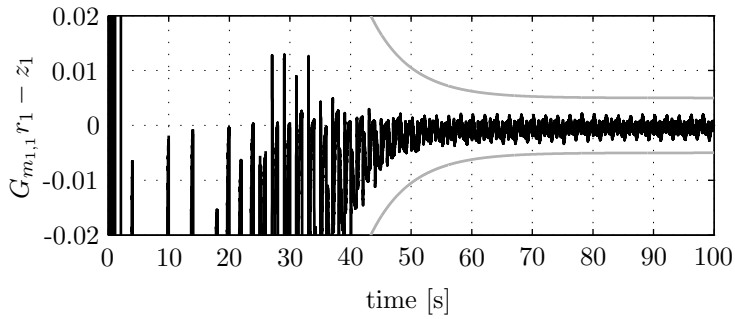
Table 6.1: Parameter values at $t_k = 100$ s.

$\check{\theta}_1$	10.1442	$\check{\theta}_5$	200.4127	$\check{\theta}_9$	-0.0001	$\check{\theta}_{13}$	0.6815
$\check{\theta}_2$	-9.1482	$\check{\theta}_6$	1.4528	$\check{\theta}_{10}$	6.6789	$\check{\theta}_{14}$	50.7923
$\check{\theta}_3$	0.0108	$\check{\theta}_7$	-199.4222	$\check{\theta}_{11}$	0.0001	$\check{\theta}_{15}$	-0.6754
$\check{\theta}_4$	-0.2962	$\check{\theta}_8$	-1.4442	$\check{\theta}_{12}$	0.0142	$\check{\theta}_{16}$	-49.7983
$\theta_{c,1}$	10.1840	$\theta_{c,5}$	200.4598	$\theta_{c,9}$	0.0003	$\theta_{c,13}$	0.6836
$\theta_{c,2}$	-9.1372	$\theta_{c,6}$	1.3921	$\theta_{c,10}$	6.6912	$\theta_{c,14}$	50.8086
$\theta_{c,3}$	0.0027	$\theta_{c,7}$	-199.4691	$\theta_{c,11}$	0.0002	$\theta_{c,15}$	-0.6775
$\theta_{c,4}$	-0.2467	$\theta_{c,8}$	-1.3829	$\theta_{c,12}$	0.0118	$\theta_{c,16}$	-49.8147

In Fig. 6.8, the evolution of the determinant of $\Sigma(t_k)$, which is proportional to the volume of the Unfalsified Set $\mathcal{E}(t_k)$, is shown over time. The determinant is monotone non-increasing and converges to a stationary value. By comparing the times at which changes occur in Fig. 6.7 and Fig. 6.8, it is established that the ellipsoid does not need to change for the currently implemented controller to be falsified, nor vice versa.

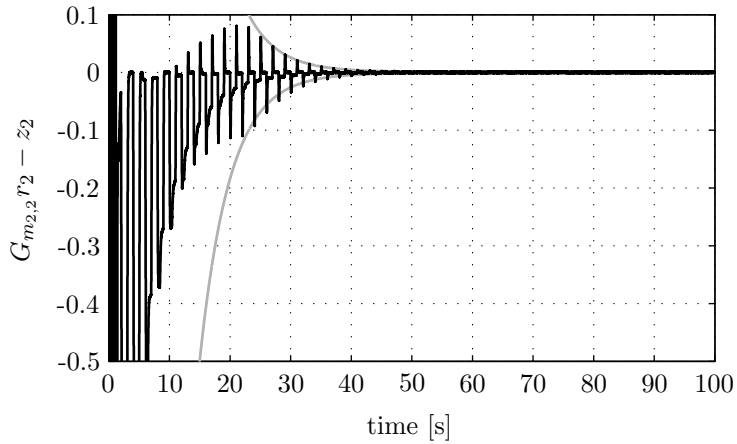


(a) performance channel 1

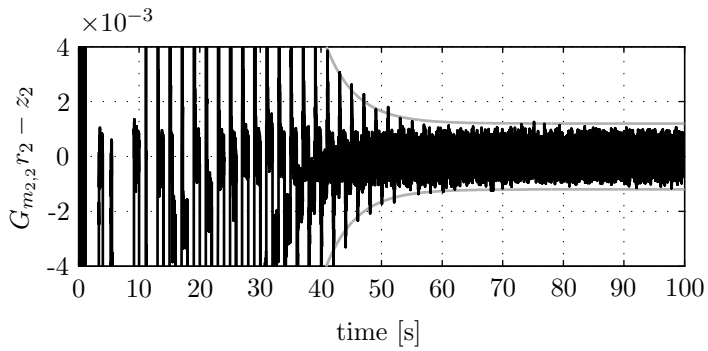


(b) closer zoom of performance channel 1

Figure 6.5: Plots of tracking error $G_{m_{1,1}}(q)r_1(t_k) - z_1(t_k)$ (black) of controlled system and bounds $\pm\Delta(t_k)$ (grey) as a function of time.



(a) performance channel 2



(b) closer zoom of performance channel 2

Figure 6.6: Plots of tracking error $G_{m_{2,2}}(q)r_2(t_k) - z_2(t_k)$ (black) of controlled system and bounds $\pm \Delta(t_k)$ (grey) as a function of time.

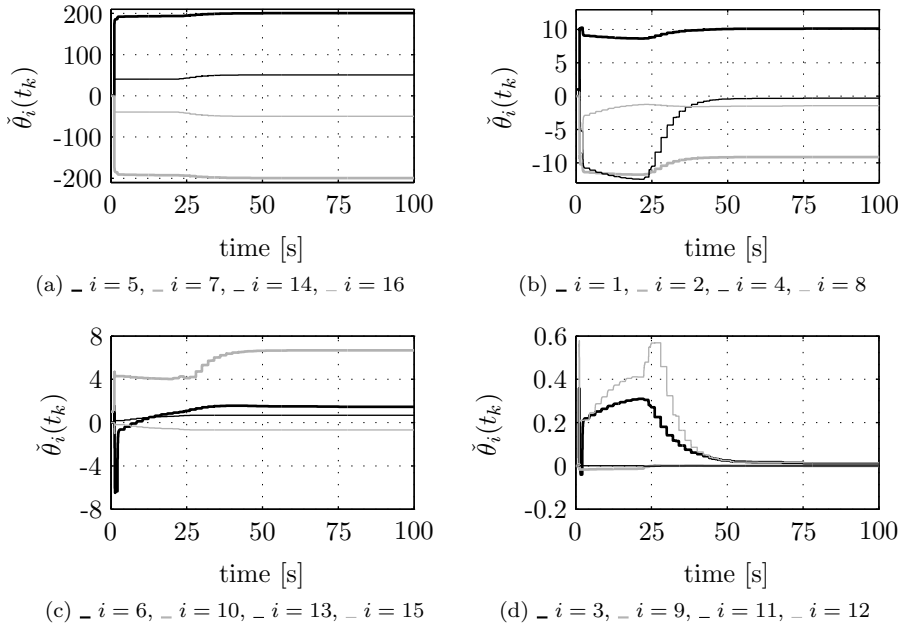


Figure 6.7: Plot of $\check{\theta}_i(t_k)$ as a function of time, for $i = 1, \dots, 16$. The parameters are grouped by their magnitude.

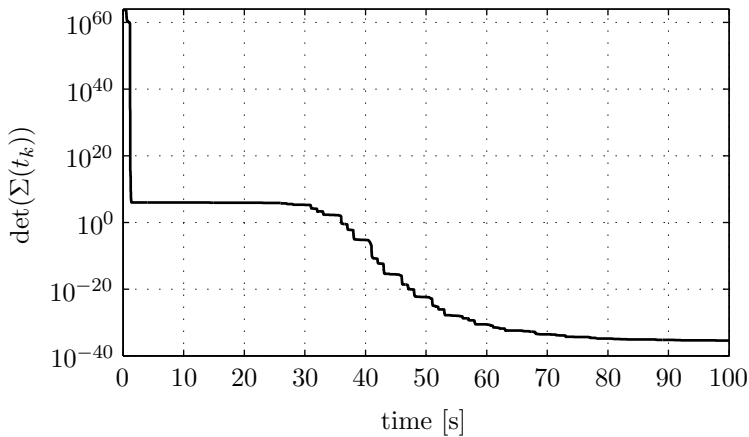


Figure 6.8: Evolution of $\det(\Sigma(t_k))$ over time, which is proportional to the volume of the Unfalsified Set $\mathcal{E}(t_k)$.

6.7.6 Frequency domain results

The frequency response functions of the closed loop system are investigated a posteriori. In Fig. 6.9, the closed loop transfer function is shown from r_i to z_i . The diagonal terms resemble the reference model (6.10), whereas the non-diagonal terms have peak values of -51.7 dB and -99.8 dB for the transfer of r_2 to z_1 and r_1 to z_2 , respectively.

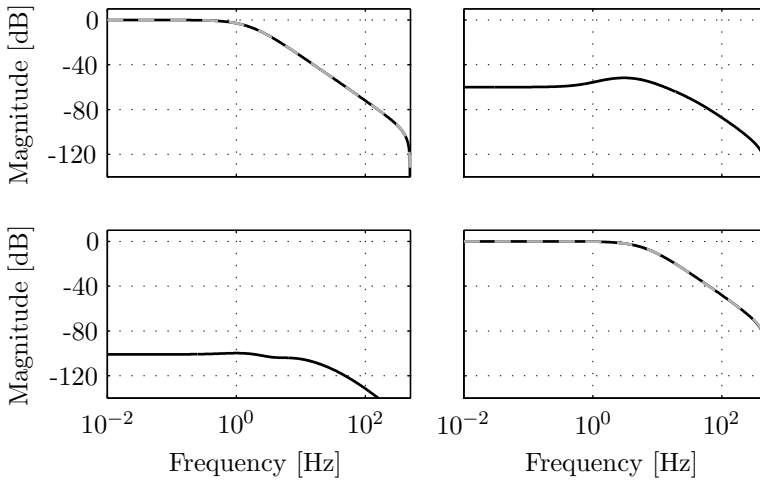


Figure 6.9: Bode magnitude-plot of the closed loop frequency response function (black) and the diagonal terms of the reference model G_m (grey dashed).

6.8 Summary and remarks

The extensions as proposed in this chapter cover a general multivariable controller, with an arbitrary number of inputs, outputs and performance channels. Inherent to the Ellipsoidal Unfalsified Control method, the controllers have a fixed, predefined structure. A reference model is prescribed to enforce a desired closed loop behavior (e.g., decoupling). An l_∞ performance requirement is imposed on the tracking performance of the performance channels. The extensions consist of a proposal for the controller structure and an update procedure of the ellipsoidal Unfalsified Set that considers the intersection with the parallel half-spaces of $\mathcal{U}(t_k)$ sequentially. The effectiveness of the proposed method to find a decoupling controller is shown in a simulation example.

Chapter 7

Batch Adaptive Unfalsified Control

IN *BATCH* adaptation, first n samples of measurement data are collected, before the adaptation algorithm is initiated. This implies that the computational demand per update is higher, however, the hard constraint on the maximum computation time is relaxed. As a consequence, in batch adaptation there is no need to approximate the region of unfalsified controllers.

7.1 Introduction

In (Woodley et al., 1999), a batch implementation of unfalsified control is proposed. It is shown how the exact description of the region of unfalsified controllers is written as a polytope, which enables to write the controller synthesis as a Linear Program. This convex optimization problem can be solved efficiently.

The drawback of the method described in (Woodley et al., 1999) is that it minimizes a filtered error, where the employed filter is a result of the optimization. More precisely, it is required that the error is filtered with the numerator of the resulting controller. As a consequence, the filtered error might be small whereas the true error is still arbitrarily large. This is in contradiction to the unfalsified philosophy, where the error is supposed to meet a predefined performance requirement, possibly filtered with a predefined filter.

In this chapter, a controller structure is proposed that ensures that the resulting fictitious error fulfills the predefined performance requirement. The error can be filtered, e.g., to penalize certain frequency ranges, but with this new method the filter can be chosen a priori instead of being a result of the optimization procedure. The applicability of the proposed method is shown on an experimental setup.

7.2 Direct unfalsified controller design - Solution via convex optimization

In this section, the approach as presented in (Woodley et al., 1999) is summarized and discussed.

7.2.1 Summary

Consider a plant P with input $u(t_k)$ and output $y(t_k)$. A controller is defined that outputs $u(t_k)$ as a function of $y(t_k)$ and a reference signal $r(t_k)$. The desired output of the plant is given by $G_m(q)r(t_k)$, with $G_m(q)$ the desired behavior of the controlled system.

The controller structure in (Woodley et al., 1999) is given by a numerator $N(\theta, q) = b_0 + b_1q + \dots + b_mq^m$ and a denominator $D(\theta, q) = 1 + a_1q + \dots + a_mq^m$. Here, q is the backward time-shift operator. Let the controller be parameterized by controller parameter set $\theta = [a_1, \dots, a_m, b_0, b_1, \dots, b_m]^T$. The currently implemented controller parameter set is denoted by $\check{\theta}$. The controller output is given by

$$u(t_k) = \frac{N(\check{\theta}, q)}{D(\check{\theta}, q)}(r(t_k) - y(t_k)) \quad (7.1)$$

Equation (7.1) can be rewritten as

$$r(t_k) = \frac{D(\check{\theta}, q)}{N(\check{\theta}, q)}u(t_k) + y(t_k) \quad (7.2)$$

If (7.2) is evaluated for a general controller parameter set θ instead of the currently implemented controller parameter set $\check{\theta}$, the fictitious reference generator results:

$$r_{\text{fict}}(\theta, t_k) = \frac{D(\theta, q)}{N(\theta, q)}u(t_k) + y(t_k) \quad (7.3)$$

The fictitious reference $r_{\text{fict}}(\theta, t_k)$ is that reference signal that, when applied to the system with the controller with parameter set θ , would have resulted in exactly

the measured $u(t_k)$ and $y(t_k)$. Although neither the controller with parameter set θ nor the fictitious reference $r_{\text{fict}}(\theta, t_k)$ are presented in (Woodley et al., 1999) as such, they are included here to conform with the extensions as introduced in Section 7.3.

The performance requirement is given by

$$\|W(q)(y(t_k) - G_m(q)r_{\text{fict}}(\theta, t_k))\|_{\infty} \leq \alpha \quad \forall t_k \in [t_0, t_{n-1}] \quad (7.4)$$

with $W(q)$ an LTI weighting function and α the maximum allowed weighted tracking error for a batch of data of length n . The use of an ℓ_{∞} -norm assures that the check of the performance requirement for the entire batch of data is sufficient to assure that any subinterval also fulfills the performance requirement, in contrast to, e.g., the ℓ_2 -norm, for which every subinterval is to be checked.

The optimal controller θ^* is derived from the batch of measurement data by minimization of α from (7.4)

$\theta^* = \arg \min_{\theta} \alpha$ subject to

$$\left\| W(q) \left(y(t_k) - G_m(q) \left(\frac{D(\theta, q)}{N(\theta, q)} u(t_k) + y(t_k) \right) \right) \right\|_{\infty} \leq \alpha \quad \forall t_k \in [t_0, t_{n-1}] \quad (7.5)$$

The minimization (7.5) can be written as a Linear Programming (LP) problem by selecting

$$W(q) = N(q) \quad (7.6)$$

Additional to the optimization discussed here, in (Woodley et al., 1999) arbitrary initial conditions are explicitly included in the optimization. These are omitted in this review for simplicity and because in the investigated setup in this research zero initial conditions can be assumed.

7.2.2 Discussion

Since the optimization of (7.5) with substitution (7.6) is a convex problem, efficient methods exist to compute θ^* . However, the computation time still exceeds the sample time for systems with a fast sample rate and a large batch length n , thereby restricting this method to off-line, batch-wise evaluation.

The drawback of substitution (7.6) is that there is no free choice for filter $W(q)$. Moreover, the output filter $W(q)$ is a result of the optimization. The coupling of $W(q)$ to the optimization is undesirable, because the optimization can result in a small minimized weighted error, whereas the real tracking error still is very large. This happens for instance if the low-frequent gain of $N(q)$ goes to zero. In this work, an alternative structure for the controller is proposed to eliminate the forced

selection of $W(q)$, as will be shown in the next section.

Although the method could be applied repeatedly, in (Woodley et al., 1999) it is specifically used as a single-shot method. In the next Section, a repetitive use is explicitly addressed.

7.3 Batch Adaptive Unfalsified Control

To avoid the drawback of substitution (7.6) in (Woodley et al., 1999), a different controller structure is considered. In this section, the alternative controller structure is introduced and applied to the adaptive algorithm, eliminating the restriction on filter $W(q)$. In subsequent sections, the results with the new algorithm are shown in an experiment.

7.3.1 Notation

Let the time in batch number l of batch-length n be denoted by $t_k \in [t_0^l, t_{n-1}^l]$, with t_0^l the start time of batch l and t_{n-1}^l the end time. As shorthand notation, in Section 7.4 t_k^l is used.

7.3.2 Controller structure

Consider a controller parameter set θ and implemented controller parameter set $\tilde{\theta}^l$. Also consider the performance requirement

$$\|W^l(q)(G_m(q)r_{\text{fict}}(\theta, t_k) - y(t_k))\|_\infty \leq \alpha \quad \forall t_k \in [t_0^l, t_{n-1}^l] \quad (7.7)$$

Weighting function $W^l(q)$ is defined a priori and is fixed for each batch. For instance, it could be chosen as a low-pass filter or integrator to penalize a steady-state error, or it could be chosen $W^l(q) = 1$ to directly address the unweighted tracking error $G_m(q)r(t_k) - y(t_k)$. Although constant per batch, the filter $W^l(q)$ might be adapted between batches by a supervisory loop to address, e.g., changing performance requirements or disturbance conditions.

If $r_{\text{fict}}(\theta, t_k)$ is affine in the controller parameters θ , then (7.7) can directly be used in a convex optimization without restrictions on $W^l(q)$. Therefore, consider the controller structure

$$r(t_k) = w(u(t_k), y(t_k), q)^T \tilde{\theta}^l \quad (7.8)$$

and fictitious reference generator

$$r_{\text{fict}}(\theta, t_k) = w(u(t_k), y(t_k), q)^T \theta \quad (7.9)$$

The condition for the derivation of the controller output $u(t_k)$ from (7.8) is that $w(u(t_k), y(t_k), q)^T \tilde{\theta}^l$ is invertible for $u(t_k)$. We propose as general formulation for $w(\cdot)$, see also Chapter 3,

$$w(u(t_k), y(t_k), q) = \begin{bmatrix} u(t_k) \\ \Lambda_u(q) \otimes u(t_{k-1}) \\ y(t_k) \\ \Lambda_y(q) \otimes y(t_k) \\ f(u(t_{k-1}), y(t_k), q) \end{bmatrix} \quad (7.10)$$

Here, $\Lambda_u(q)$ and $\Lambda_y(q)$ are vectors of asymptotically stable linear filters and \otimes denotes the Kronecker product. The vector $f(u(t_{k-1}), y(t_k), q)$ contains globally asymptotically stable nonlinear functions that are bounded in amplitude for all $u(t_{k-1})$ and $y(t_k)$. With (7.10), the control effort $u(t_k)$ is well defined if $[1, 0, \dots, 0] \tilde{\theta}^l \neq 0$. In Section 7.4 an example is shown that fits (7.10).

7.3.3 Controller selection

The controllers that are unfalsified by the measurement data of batch l are given by the set \mathcal{U}^l

$$\mathcal{U}^l = \left\{ \theta \mid \left\| W^l(q) \left(G_m(q) w(u(t_k), y(t_k), q)^T \theta - y(t_k) \right) \right\|_{\infty} \leq \alpha, \forall t_k \in [t_0^l, t_{n-1}^l] \right\} \quad (7.11)$$

In contrast to (Woodley et al., 1999), the performance bound α is defined a priori and will not be minimized to select a controller. In line with the theory of Unfalsification, all controllers $\theta \in \mathcal{U}$ are unfalsified by the measurement data and they are therefore eligible for implementation. As a deterministic choice for the selection of one controller, here the selection of the center of the maximum volume inscribed ellipsoid (MVIE) in \mathcal{U} is proposed. Additional benefit is that the MVIE provides information on the shape of \mathcal{U} , and can therefore be used as a purely data-driven coordinate transformation of the controller structure.

To compute the MVIE and its center, (7.11) is rewritten as

$$\begin{aligned}
\mathcal{U}^l &= \left\{ \theta \left\| W^l(q) \left(G_m(q) w(u(t_k), y(t_k), q)^T \theta - y(t_k) \right) \right\|_\infty \leq \alpha, \forall t_k \in [t_0^l, t_{n-1}^l] \right\} \\
&= \left\{ \theta \mid -\alpha \leq W^l(q) G_m(q) w(\cdot)^T \theta - W^l(q) y(t_k) \leq \alpha, \forall t_k \in [t_0^l, t_{n-1}^l] \right\} \\
&= \left\{ \theta \mid -W^l(q) G_m(q) w(\cdot)^T \theta \leq \alpha - W^l(q) y(t_k), \right. \\
&\quad \left. W^l(q) G_m(q) w(\cdot)^T \theta \leq \alpha + W^l(q) y(t_k), \forall t_k \in [t_0^l, t_{n-1}^l] \right\}
\end{aligned} \tag{7.12}$$

With (7.12), the maximum volume inscribed ellipsoid is computed with the optimization problem (Boyd and Vandenberghe, 2004, p. 414)

$$\begin{aligned}
\check{\theta}^{l+1} &= \arg \max_{\theta, B} \log \det B \quad \text{subject to} & (7.13) \\
&- W^l(q) G_m(q) w(\cdot)^T \theta + \| -W^l(q) G_m(q) w(\cdot)^T B \|_2 \leq \alpha - W^l(q) y(t_k) \\
&W^l(q) G_m(q) w(\cdot)^T \theta + \| W^l(q) G_m(q) w(\cdot)^T B \|_2 \leq \alpha + W^l(q) y(t_k) \\
&\forall t_k \in [t_0^l, t_{n-1}^l]
\end{aligned}$$

with B a symmetric positive definite matrix.

Optimization (7.13) is not a Linear Program. However, if the matrix B is used as the coordinate transformation $\zeta = B^{-1}\theta$ for later batches, (7.13) can approximately be solved with the computationally cheaper linear program

$$\begin{aligned}
\check{\zeta} &= \arg \max_{\zeta} r \quad \text{subject to} & (7.14) \\
&- W^l(q) G_m(q) w(\cdot)^T B \zeta + r \| -W^l(q) G_m(q) w(\cdot)^T B \|_2 \leq \alpha - W^l(q) y(t_k) \\
&W^l(q) G_m(q) w(\cdot)^T B \zeta + r \| W^l(q) G_m(q) w(\cdot)^T B \|_2 \leq \alpha + W^l(q) y(t_k) \\
&\forall t_k \in [t_0^l, t_{n-1}^l]
\end{aligned}$$

Here, r is the radius of the largest inscribed ball in the coordinates ζ . The matrix B can be used for trial $l+1$, under the assumption that B is constant for every trial. This assumption is plausible if \mathcal{U} does not change shape significantly, which happens for instance if the system is time invariant, the signal-to-noise ratio is large, the noise is stationary and the performance specification does not change per batch.

7.3.4 Stability

Although the stability results of (Stefanovic et al., 2005; Wang et al., 2005) can be used to guarantee the stability of an adaptive system, they do not guarantee stability for a specific individual controller. So, at a certain time, a destabilizing controller might be inserted in the loop. For continuous adaptation, this is only a minor problem since the controller parameters are adapted as soon as the performance requirement is violated, as follows from the property of discarding of demonstrably destabilizing controllers of the adaptive system. For batch adaptation, however, the controller is only changed after an entire batch. So if now a destabilizing controller is inserted, this poses a major problem in practice, since the response of the system might be very large and even exceed the range of operation. Furthermore, if the achieved output is far ($\gg \alpha$) from the desired output, then the fictitious reference of the unfalsified controllers is far from the actual reference, which compromises the derivation of the Unfalsified Set, see Chapter 3.3.1. Therefore, for batch adaptive systems, stability should be guaranteed not only for the adaptive system but also for individual controllers.

Some check should be performed on the selected controller, whether it will result in a stable closed loop system. One possibility might be to use the ν -gap metric (Vinnicombe, 1993) for the old and the new controller with the plant, however, this would require a frequency response “model” of the plant. See also (De Bruyne and Kammer, 1999) for the application of the ν -gap to the data-driven batch control design of Iterative Feedback Tuning. The ν -gap metric might even be employed in the selection of $\check{\theta}^{l+1}$. However, this is a topic for more thorough investigation.

Besides, to apply the stability results of (Stefanovic et al., 2005; Wang et al., 2005), some modifications of the performance requirement and of the construction of the Unfalsified Set are required. After all, the performance requirement (7.7) does not discard controllers for which $u(t_k)$ is too large. Therefore, to assure discarding of demonstrably destabilizing controllers, $u(t_k)$ should be appended to the performance requirement. Additionally, the Unfalsified Set is reinitiated for every batch, without accounting for the unfalsification information of previous batches. Consequently, controllers that were discarded because they did not fulfill the performance requirement are re-enabled every batch. This implies that the implicit cost function does not change monotonically and that the number of switches is not limited. By incorporating (an approximation of) the unfalsification information of previous batches, a decrease of the volume of the Unfalsified Set can be enforced and the number of switches can be limited.

7.4 Experiment

The Batch Adaptive Unfalsified Control approach is applied to a motion system in an experiment to demonstrate the applicability of the proposed method.

7.4.1 Plant

The experimental setup is a dual rotary fourth order motion system, as shown in Fig. 7.1. It consists of a load connected to a motor by a flexible bar. The transfer from the motor input to the angular position of the motor is considered. The sample frequency is 1 kHz. The measured frequency response function of the motor input to the angular position of the motor is shown in Fig. 7.2.

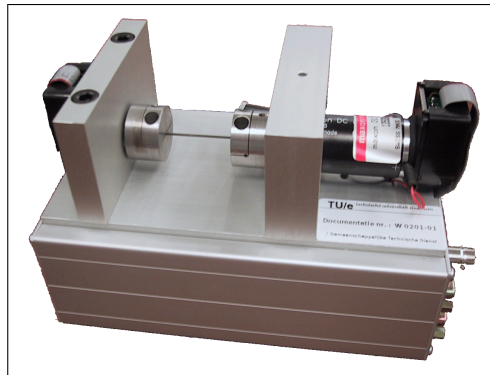


Figure 7.1: Photo of the motion system, with load (left) connected to a motor (right) by a flexible bar.

7.4.2 Goals

The desired closed loop behavior from r to y , G_m , is given by a second order low-pass filter. At low frequencies, the gain goes to 1 to impose that tracking of the typically low-frequent reference signal is achieved. At high frequencies a roll-off is imposed, to assure that potentially high-frequent noise is not amplified. These control goals are representative for most motion systems. In continuous

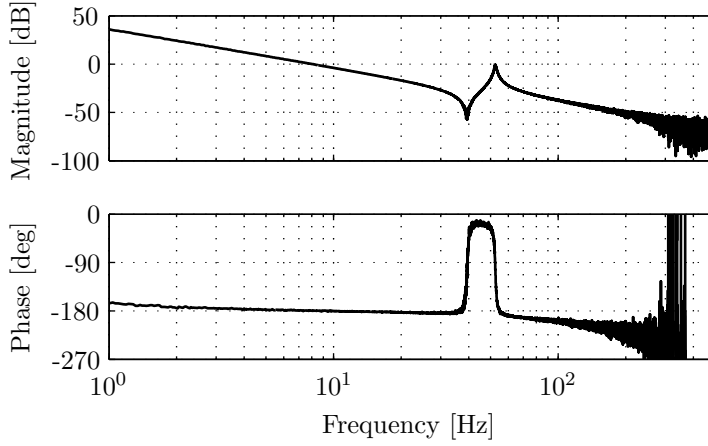


Figure 7.2: Bode plot (magnitude top, phase bottom) of the frequency response of the motor input to the angular motor position.

time, $G_m(s)$ is defined as:

$$G_m(s) = \frac{\omega_n^2}{s^2 + 2\xi\omega_n s + \omega_n^2} \quad (7.15)$$

with $\omega_n = 4\pi$ [rad/s] and $\xi = 1$ [-]. Equation (7.15) transformed to the q -domain with a zero-order-hold is given by

$$G_m(q) = \frac{(7.83q + 7.765q^2) \cdot 10^{-5}}{1 - 1.975q + 0.9752q^2} \quad (7.16)$$

The Bode plot of $G_m(q)$ is shown in Fig. 7.3.

As a reference trajectory, a step of magnitude 10 [rad] at time $t_k = 0.1$ s is imposed. A plot of the reference $r(t_k)$ and the desired output of the closed loop system $G_m(q)r(t_k)$ are shown in Fig. 7.4. The batch time is 2 seconds, which, together with the sample rate of 1 kHz, results in a batch length of $n = 2001$.

The performance requirement is an ℓ_∞ -norm, given by

$$\|W^l(q)(G_m(q)r_{\text{fict}}(\theta, t_k) - y(t_k))\|_\infty \leq \alpha \quad \forall t_k \in [t_0^l, t_{n-1}^l] \quad (7.17)$$

Herein, $G_m(q)$ is defined by (7.16), $W^l(q) = 1$ and $\alpha = 0.2$ [rad].

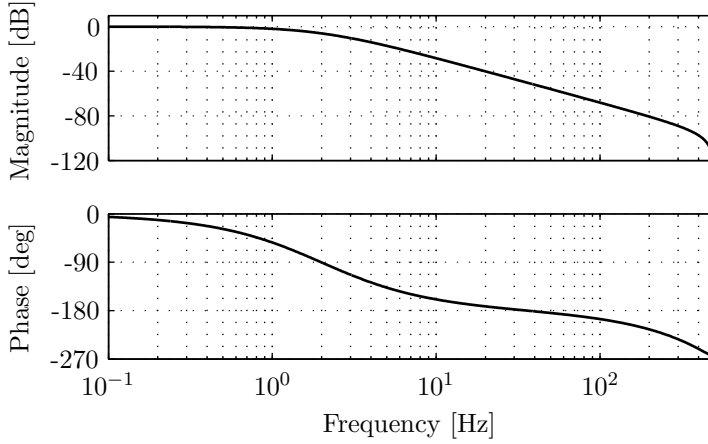


Figure 7.3: Bode plot (magnitude top, phase bottom) of the desired closed loop behavior $G_m(q)$.

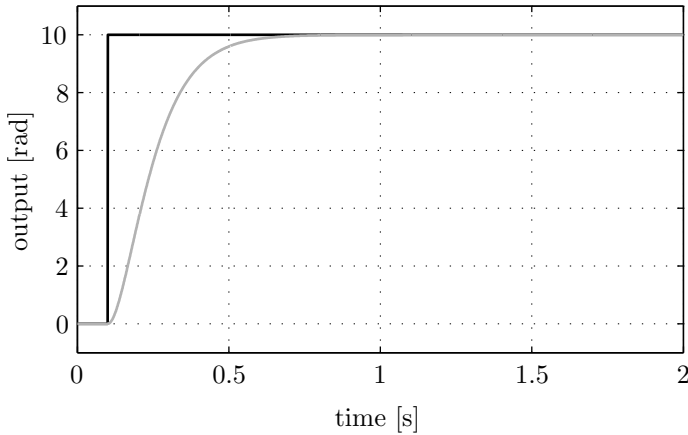


Figure 7.4: Reference $r(t_k)$ (black) and desired output $G_m(q)r(t_k)$ (grey).

7.4.3 Controller structure

The controller structure $w(u(t_k), y(t_k), q)$ is given by

$$w(u(t_k), y(t_k), q) = \begin{bmatrix} u(t_k) \\ \frac{q}{1-\gamma q} u(t_k) \\ y(t_k) \\ \frac{1+q}{1-\gamma q} y(t_k) \end{bmatrix} \quad (7.18)$$

with γ a design variable that determines the poles of the filters, which is chosen here to be $\gamma = 0.9$. The filters in $w(u(t_k), y(t_k), q)$ are asymptotically stable for $|\gamma| < 1$, for $\gamma = 0.9$ the breakpoints are at approximately 16 Hz. The resulting control force is defined as

$$u(t_k) = \underbrace{\frac{1-\gamma q}{\tilde{\theta}_1^l + (\tilde{\theta}_2^l - \gamma \tilde{\theta}_1^l)q}}_{C_r(\tilde{\theta}^l, q)} r(t_k) - \underbrace{\frac{(\tilde{\theta}_3^l + \tilde{\theta}_4^l) + (\tilde{\theta}_4^l - \gamma \tilde{\theta}_3^l)q}{\tilde{\theta}_1^l + (\tilde{\theta}_2^l - \gamma \tilde{\theta}_1^l)q}}_{C_y(\tilde{\theta}^l, q)} y(t_k) \quad (7.19)$$

with $\tilde{\theta}_i^l$ the i^{th} element of $\tilde{\theta}^l$. The controller has a first order numerator and denominator, which typically is sufficient to result in a stable control system for a motion system, which have a low-frequency 180° phase delay, since the controller is able to provide ample phase lead. With the four parameters, four independent features of the controller can be adapted: the gain of $C_y(\tilde{\theta}^l, q)$, the zero of $C_y(\tilde{\theta}^l, q)$, the shared pole of $C_y(\tilde{\theta}^l, q)$ and $C_r(\tilde{\theta}^l, q)$ and the gain of $C_r(\tilde{\theta}^l, q)$.

A schematic representation of (7.19) is shown in Fig. 7.5.

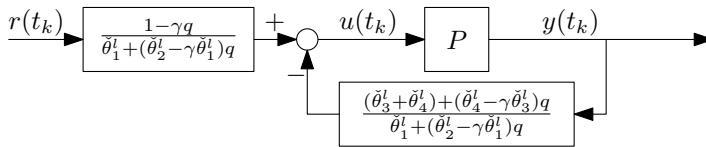


Figure 7.5: Schematic representation of the controlled system with controller structure (7.18).

7.4.4 Initialization

The initial data in the experiment is obtained with the controller $\tilde{\theta}^0 = [10 \ 0.14 \ 1 \ 0]$ and $\gamma = 1.0$. The data obtained with this controller is shown in Fig. 7.6.

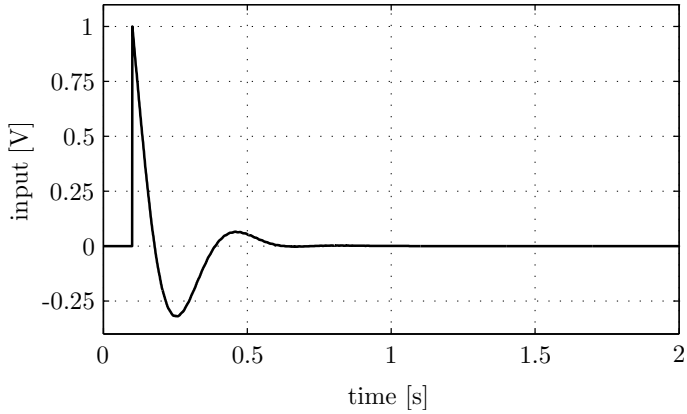
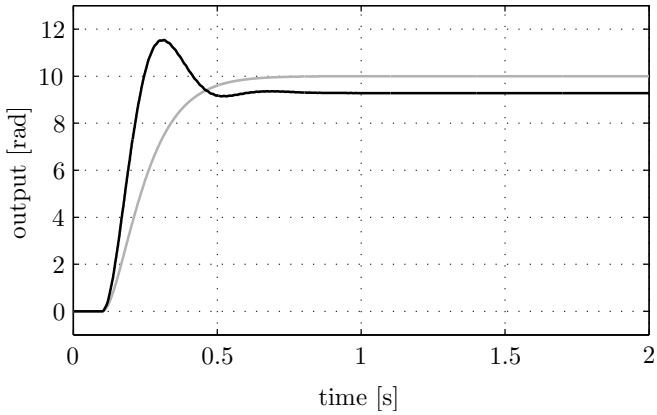
(a) Plant input signal $u(t_k^0)$ (b) Plant output signal $y(t_k^0)$ (black) and desired output $G_m(q)r(t_k)$ (grey)

Figure 7.6: Data obtained with initial controller.

For batch $l = 1$, $\check{\theta}^1$ is chosen as the result of optimization (7.13) with data $u(t_k^0)$ and $y(t_k^0)$. The maximum-volume-inscribed-ellipsoid matrix B^1 is used as a coordinate transformation in subsequent batches, as described in Section 7.3.3, to save computation time. So, for batches $l \in \{2, 3, 4, 5\}$, $\check{\theta}^l$ is chosen as the result of optimization (7.14) with data $u(t_k^{l-1})$ and $y(t_k^{l-1})$ and coordinate transformation $\check{\zeta} = B^{l-1}\check{\theta}$. The batch of data $u(t_k^l)$ and $y(t_k^l)$ is collected with controller $\check{\theta}^l$ implemented.

7.4.5 Time domain results

The resulting tracking errors $e(t_k^l)$ for batch 1, 3 and 5 are shown in Fig. 7.7. For all batches, the tracking error is smaller than the predefined $\alpha = 0.2$. The steady state error after 1 second results from physical phenomena of the system, such as friction and cogging. This effect was not encountered in a simulation of a similar (but linear) plant. Nevertheless, the results in Fig. 7.7 show that the controller of batch 5 is able to nearly eliminate this effect. The parameter values per batch for batches 1 through 5 are shown in Fig. 7.8, and the parameter values for batch 5 are given by

$$\check{\theta}^5 = \begin{bmatrix} 14.2882 \\ 0.5923 \\ 17.0880 \\ -0.8056 \end{bmatrix}$$

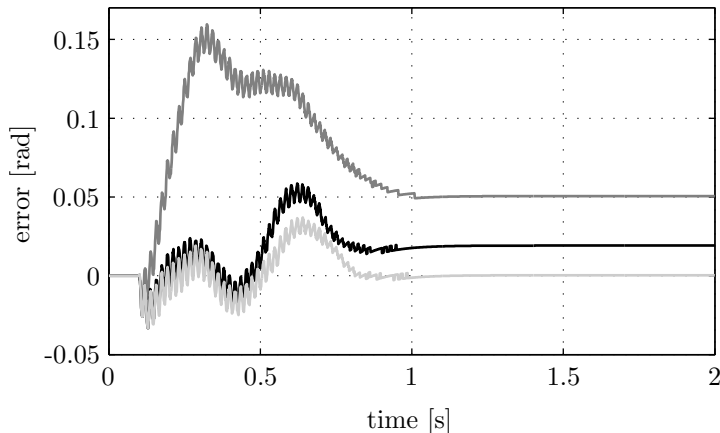


Figure 7.7: Plot of error $e(t_k^l) = G_m(q)r(t_k) - y(t_k^l)$, for batch $l = 1$ (dark grey), $l = 3$ (black) and $l = 5$ (light grey).

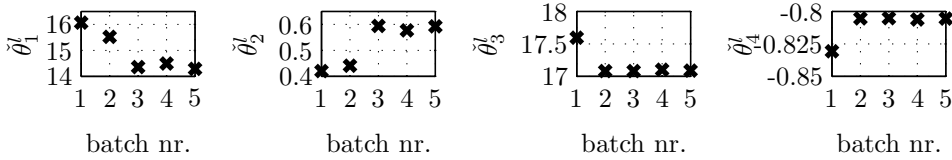


Figure 7.8: The controller parameter values for batch 1 through 5.

7.4.6 Frequency domain results

Figure 7.7 shows that the tracking errors exhibit a high frequency oscillation. This phenomenon is caused by the resonance of the plant, as can be seen from the Bode plot of the open loop transfer function $PC_y(\check{\theta}^5, q)$ with the feedback controller of batch 5, see Fig. 7.9. The Bode plot of $C_y(\check{\theta}^5, q)$ is shown in Fig. 7.11. From this figure, the bandwidth of the controlled system is determined at 4 Hz, however, the resonance peak at 52 Hz crosses the 0 dB amplification. This does not induce instability since there is ample phase margin at this frequency. However, it produces the high frequent oscillation that is observed.

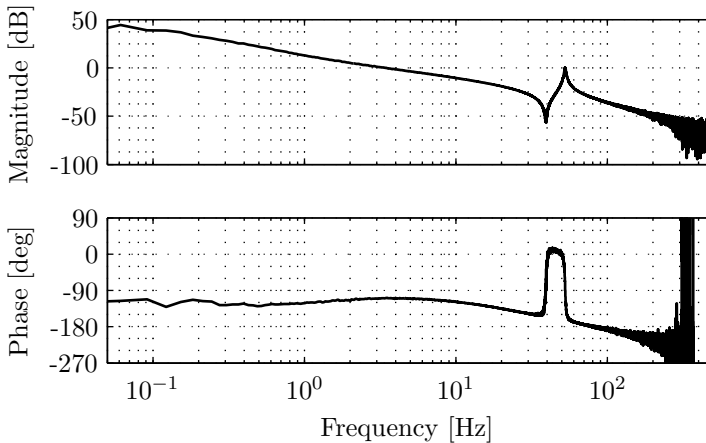


Figure 7.9: Bode plot (magnitude top, phase bottom) of the open loop frequency response $PC_y(\check{\theta}^5, q)$ constructed with the measured frequency response of the plant, as shown in Fig. 7.2.

Despite the inherent drawbacks of a high frequent oscillation such as increase wear, the high frequent oscillation is not directly the limiting factor for the performance requirement, so the feedback controller of only first order is not required to achieve more suppression at this frequency. A higher order controller might compensate the resonance dynamics, if it becomes the limiting factor for performance. Or the weighting filter $W(q)$ might be designed to emphasize the error near the resonant frequency. However, these extensions are not examined here.

Although in the open loop frequency response $PC_y(\check{\theta}^5, q)$ the resonance peak crosses the 0 dB amplification, in the closed loop frequency response $\frac{PC_r(\check{\theta}^5, q)}{1+PC_y(\check{\theta}^5, q)}$ the amplification of the peak is attenuated. The Bode plot of the closed loop frequency response is shown in Fig. 7.10 and the controller $C_r(\check{\theta}^5, q)$ is shown in Fig. 7.12. The attenuation of the resonance is achieved by the smaller magnitude at high frequencies of $C_r(\check{\theta}^5, q)$ compared to that of $C_y(\check{\theta}^5, q)$.

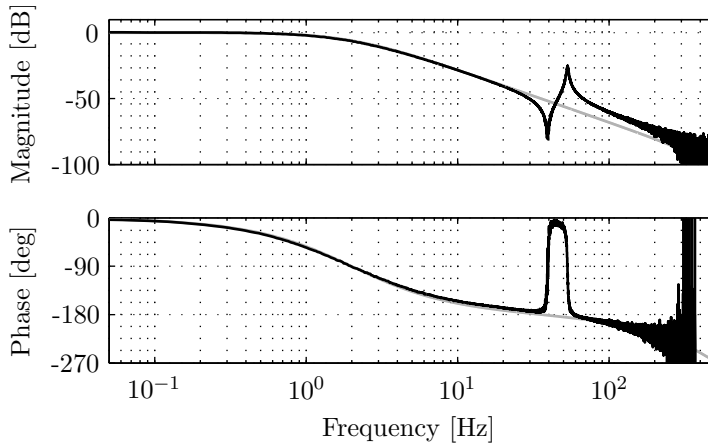


Figure 7.10: Bode plot (magnitude top, phase bottom) of the closed loop frequency response with $\check{\theta}^5$ (black) and desired closed loop behavior $G_m(q)$ (grey).

The bandwidth of the controlled system of 4 Hz is higher than is required by the desired closed loop behavior $G_m(q)$. A higher bandwidth, which with the first order controller corresponds to a larger low-frequent gain, is favorable for suppression of low frequent disturbances such as Coulomb friction, however, it results in a closed loop response that is too fast compared to the desired response. An investigation of the feedforward controller explains how this problem is handled by this data-driven control design method. The explanation is clearest if instead of the factorization in $C_r(\check{\theta}^l, q)$ and $C_y(\check{\theta}^l, q)$ as in (7.19), we consider a factorization of a feedback controller and a feedforward controller as in:

$$u(t_k) = C_{fb}(\check{\theta}^l, q)(r(t_k) - y(t_k)) + C_{ff}(\check{\theta}^l, q)r(t_k) \quad (7.20)$$

with

$$C_{fb}(\check{\theta}^l, q) = C_y(\check{\theta}^l, q) \quad (7.21)$$

$$C_{ff}(\check{\theta}^l, q) = C_r(\check{\theta}^l, q) - C_y(\check{\theta}^l, q) \quad (7.22)$$

The Bode plots of $C_y(\check{\theta}^5, q)$, $C_r(\check{\theta}^5, q)$ and $C_{ff}(\check{\theta}^5, q)$ are shown in Fig. 7.11 through 7.13. The Bode plot of $C_y(\check{\theta}^5, q)$, Fig. 7.11, shows a first order lead-lag that creates phase lead at the bandwidth of the controlled system and, accordingly, stabilizes the feedback system. The Bode plot of $C_r(\check{\theta}^5, q)$, Fig. 7.12, also shows a first order lead-lag, albeit with only a small change in phase and magnitude. Nevertheless, controller $C_{ff}(\check{\theta}^5, q) = C_r(\check{\theta}^5, q) - C_y(\check{\theta}^5, q)$, shown in Fig. 7.13, is a first order high-pass filter that has a negative high-frequency gain and a zero outside the unit circle. This behavior is also observed from the unit step response of $C_{ff}(\check{\theta}^5, q)$, as shown in Fig. 7.14.

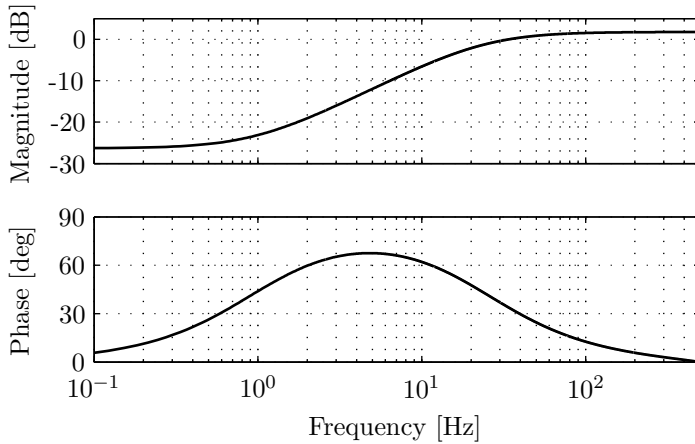


Figure 7.11: Bode plot (magnitude top, phase bottom) of the controller $C_y(\check{\theta}^5, q)$.

Apparently, the output of the closed loop controlled system is retarded by the negative high-frequency gain feedforward, resulting in a system that mimics the slower response as defined by $G_m(q)$, while still providing static disturbance suppression with a ‘high’ bandwidth.

7.4.7 Evaluation

The analysis above shows that the data-driven controller design accurately handles the experimental conditions, resulting in a controller that achieves good performance for the present trajectory and reference model. All predefined goals are

fulfilled. For different trajectories, different controllers will result, designed specifically for the trajectory at hand.

With the current controller structure, the performance requirement of $\alpha = 0.2$ is easily met. By decreasing the value α , an even better performance might be obtained. However, this is not the objective here. We explicitly refrain from optimization within the philosophy of unfalsification. If optimal performance really

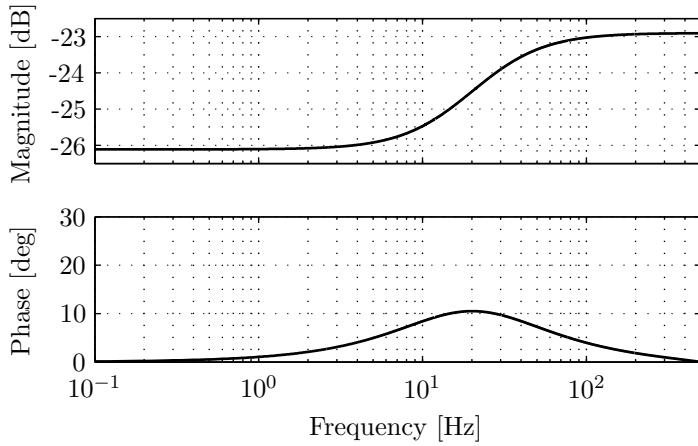


Figure 7.12: Bode plot (magnitude top, phase bottom) of the controller $C_r(\check{\theta}^5, q)$.

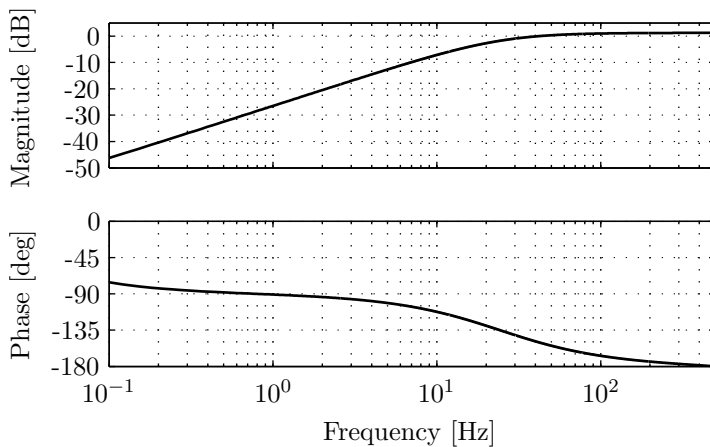


Figure 7.13: Bode plot (magnitude top, phase bottom) of the controller $C_{ff}(\check{\theta}^5, q) = C_r(\check{\theta}^5, q) - C_y(\check{\theta}^5, q)$.

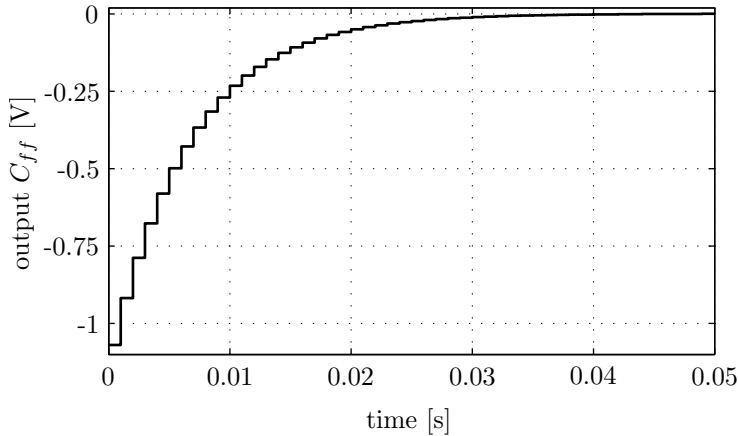


Figure 7.14: Plot of the unit step response of the controller $C_{ff}(\hat{\theta}^5, q)$. The first order controller has a negative high-frequency gain and a zero outside the unit circle.

were an issue, the controller structure also should be extended. A first order controller will not be able to improve the performance below a certain error level. The controller structure should therefore be extended with additional terms, which in the current framework is easily done. However, the terms of the controller structure determine the achievable performance, and the derivation of a substantiated choice for the additional terms might not be as easy.

In the experiment, the measurement data of batch 0 is acquired with a controller of different structure than the controllers afterwards. Since in Unfalsified Control the origin of the data is irrelevant, this poses no problem. As a consequence, it is also possible to change the controller structure between batches, for instance to be able to meet an increasing performance requirement or to cope with variations in the plant dynamics and disturbances.

7.5 Summary and remarks

In this chapter, a method for plant-model-free batch adaptive control via controller unfalsification is presented. The research modifies the method presented in (Woodley et al., 1999), which has the major drawback that the error signal has to be filtered with the numerator of the controller. This implies that the performance requirement used to evaluate the controller is not equal to the predefined

performance requirement.

A different controller structure is proposed to eliminate the need of filtering the error signal with the numerator of the controller. This controller structure is chosen such that the fictitious reference signal generator, which is used to evaluate the controllers without the need to implement them, is affine in the controller parameters. This choice enables the use of a freely chosen weighting filter. As controller selection, the center of the maximum volume inscribed ellipsoid in the set of unfalsified controllers is used.

The proposed algorithm has successfully been implemented in an experiment. No plant model is used in the selection of the controller parameters, since the proposed method is purely data-driven. For all batches did the resulting controller fulfill the performance requirement. The resulting controller features a relatively high bandwidth of the closed loop controlled system compared to the reference model to attenuate the steady state offset. The response of the system is restrained by a negative high-frequency gain feedforward such that the desired output is mimicked.

Chapter 8

Conclusions

DATA-DRIVEN control design is investigated in this thesis as an approach to improve the performance of motion systems. The contents focus on Unfalsified Control as a potential framework to derive adaptive control systems. In particular, an extension is proposed that enables fast and efficient evaluation of the update of the set of unfalsified controllers, with sufficient conditions to guarantee stability. A generalization of the method to multivariable controllers is proposed and a side-step to a batch adaptive algorithm is reported. In this chapter, conclusion are drawn regarding the proposed extension and its applicability to data-driven control design for performance improvement.

8.1 Ellipsoidal Unfalsified Control

The method of Ellipsoidal Unfalsified Control is developed as an extension to Unfalsified Control, for the efficient and fast evaluation of an infinite number of candidate controllers. It recursively approximates the set of unfalsified controllers with an ellipsoid, the Unfalsified Set. The update of the Unfalsified Set can be computed analytically due to the combination of a controller structure for which the fictitious reference generator is affine in the controller parameters together with an ℓ_∞ bound on the performance requirement. As a result, the computation of the update is fast, which enables online realtime implementation on a motion system at $\mathcal{O}(1 \text{ kHz})$.

The proposed update algorithm ensures that the volume of the Unfalsified Set

does not increase and that it includes only candidate controllers that are either in the previous Unfalsified Set or in the set unfalsified by current measurement data (and includes all candidates that are in both).

Although stability with a specific controller can not be guaranteed, nonetheless sufficient conditions are derived for the adaptive system of Ellipsoidal Unfalsified Control to be stable. These conditions are: 1) feasibility of the adaptive control problem, 2) Stably Causally-Left-Invertible candidate controllers, that, in combination with the performance requirement, discard demonstrable destabilizing controllers and 3) a limited number of controller switches. The latter is accomplished by imposing a minimum decrease on the volume of the Unfalsified Set between two consecutive distinctive ellipsoids and a minimum relative stepsize on the controller adjustments.

Since the computation of the update is fast, Ellipsoidal Unfalsified Control can be implemented with realtime adaptation at a fast sample rate as is demonstrated with an experiment on a motion systems. The method is applied to an industrial inkjet printer at a sample rate of 1 kHz. The results show that the algorithm updates the control parameter set when the performance requirement is not met with the currently implemented one. Meanwhile, the Unfalsified Set decreases almost continuously. The resulting closed loop behavior resembles the predefined reference model in the dominant frequency range.

An extension is proposed to cover a full-block multivariable controller, with an arbitrary number of inputs, outputs and performance channels. Inherent to the Ellipsoidal Unfalsified Control method, the controllers have a fixed, predefined structure. A reference model can be prescribed to enforce a desired closed loop behavior (e.g., decoupling). An l_∞ performance requirement is imposed on the tracking performance of the performance channel. The extension consists of a controller structure and an update procedure of the ellipsoidal Unfalsified Set that considers the intersection with the parallel half-spaces of $\mathcal{U}(t_k)$ sequentially. The effectiveness of the proposed method to find a decoupling controller is shown in a simulation example.

8.2 Batch Adaptive Unfalsified Control

The method of Batch Adaptive Unfalsified Control uses the same controller structure as Ellipsoidal Unfalsified Control, thereby eliminating the need of filtering the

error signal with the numerator of the controller as is encountered in other work. This choice enables the use of a freely chosen weighting filter. As controller selection, the center of the maximum volume inscribed ellipsoid in the set of unfalsified controllers is used.

The proposed algorithm has successfully been implemented in an experiment. No plant model is needed in the selection of the controller parameters, since the proposed method is purely data-driven.

Regrettably, at the moment, selection of an unfalsified controller does not guarantee that a stable closed loop will result in the next batch. More research is needed to investigate if guarantees can be provided by improving the performance inference for destabilizing controllers (Engell et al., 2007) or by application of a model-based measure for guaranteed stability, such as the ν -gap (Vinnicombe, 1993).

8.3 Applicability of Ellipsoidal Unfalsified Control

Ellipsoidal Unfalsified Control provides an extension to the framework of Unfalsified Control. It results in an adaptive system that adapts to the specific plant and disturbances under consideration, without a plant model, as is also shown in simulations and an experiment. The resulting controller is specifically configured for the actual reference.

The controller is adapted to the encountered circumstances and, consequently, for different trajectories and for different task, different controllers might result. Although for the adaptive system sufficient conditions are derived to guarantee stability, no guarantees are provided that the currently implemented controller is stabilizing. Therefore, the adaptive algorithm should not be terminated but should be active for the entire operation.

The achievable performance largely depends on the plant and controller structure, as does the performance improvement with regard to a model-based control design technique. A priori information is needed to assess the achievable performance and to select a controller structure, however, little is known on this subject. Especially with only partial or coarse information, this analysis is hard to perform. Extension of the controller structure, as proposed in Section 9.2, might be a method to enhance the suitability of a controller structure.

The influence of disturbances and noise is implicitly handled by the algorithm,

since a controller is selected that results in the required performance irrespective of the origin of the elements in the output signal. Of course, also here a priori information is needed to determine a realistic performance requirement and reference model.

In this thesis, performance improvement by Ellipsoidal Unfalsified Control is not conclusively established. As mentioned above, the results will largely depend on the application. Interesting examples for performance improvement arise from actual problems where model-based control designs have reached their limits. Especially applications that induce a lot of conservatism when modeling the plant and that require adaptation under normal operation conditions, as encountered for instance in mass production or operation in a large variety of conditions, might benefit from the proposed method.

Although performance improvement with Ellipsoidal Unfalsified Control is not established, it is shown that control design is facilitated. There is no need for plant modeling and identification, and the performance of the closed loop is directly addressed. Furthermore, the method allows for the design of controllers using an ℓ_∞ criterion, a feature that is encountered only rarely.

Chapter 9

Recommendations

SEVERAL observations are made during the development of *Ellipsoidal Unfalsified Control*. In this chapter, some fundamental open issues are stated. Besides, extensions to *Ellipsoidal Unfalsified Control* are proposed for which no direct obstacles are expected.

9.1 Open issues

Even though the results with *Ellipsoidal Unfalsified Control* are promising, still some issues need to be addressed. These issues concern the underlying working principles or desired extensions of the algorithm, for which no theory is available yet.

9.1.1 Influences on the obtained result

The result of the algorithm is influenced both by the choice of the controller structure and by the switching sequence of the controller parameters.

The controller structure directly influences feasibility of the adaptive control system. An, in retrospect, “unfortunate” choice of the filters easily results in infeasibility or, at best, induces a very elongated ellipsoid, which leads to an ill-conditioned Σ , hence, an ill-conditioned update. This latter scenario happens for

instance if the outputs of some filters are similar such that linear combinations of these filters result in the same time signal.

The initial controller conditions and measurement data, as well as the parameter values for the algorithm, determine the switching sequence of the controller parameters. The switching of the controller parameters induces transient behavior, which results in falsification of control parameter sets that would have been unfalsified with other switching sequences. Consequently, the resulting Unfalsified Set is influenced by the initial control parameter set $\check{\theta}(0)$ as well as by α , the specific shape of $\Delta(t_k)$ and $\kappa(t_k)$ and the initial Unfalsified Set $\mathcal{E}(0)$. The measurement data that is generated on the system also depends on the specific controller sequence, which thereby influences the result. Ideally, the result (at least, the achievable performance) should be insensitive to initial choices and the sequence of the implemented controller parameter sets.

Improvements might be achieved with the addition of supervisory loops that monitor the progression and accordingly adapt the controller structure or reinitialize the algorithm. However, the specifics of the adaptation and reinitialization procedures need to be addressed. Some ad hoc methods are proposed in Section 9.2. A validation of the proposed schemes would benefit from a comparison of the obtained Unfalsified Set with an analytically derived set of unfalsified controllers.

9.1.2 Feasibility

Feasibility is the one assumption that is still needed to assure stability of the adaptive control system. However, methods are lacking that could pass judgement on the chances of feasibility, if only some (limited) plant information is available. Nevertheless, the desire exists to be able to establish *a priori* if the adaptive control problem is feasible. As a next step, a method could be derived that maximizes the chances of feasibility during the design of the controller structure. However, to retain a data-driven control design method, the design of the controller structure should be performed prior to the implementation of the adaptive control scheme.

9.1.3 Performance inference

As observed in Section 3.3.1 on page 23, the performance inference with the fictitious reference is imperfect. In (Engell et al., 2007), an alternative is presented that uses Hankel matrices of the fictitious reference and the actual reference to improve the detection of a destabilizing candidate controller. Further investigation

is needed for applicability of the proposed solution in the framework presented in this thesis.

9.1.4 Time-varying systems

The current implementation of Ellipsoidal Unfalsified Control can only handle time-varying systems, if there exist a region in the candidate controller set that is unfalsified at all times for the encountered variations of the system. A relaxation might be proposed to handle disjunct sets for variations of the system, however, this requires that controllers that were once falsified are re-enable as candidate controllers. Possibilities are to gradually increase \mathcal{E} as a kind of ‘forgetting factor,’ or to reset \mathcal{E} to its initial volume and shape if the volume of the Unfalsified Set is below a certain threshold. However, this requires a new stability analysis, because no longer a finite number of switches will be guaranteed.

Hespana et al. (2003) and Stefanovic (2005) provide stability results with a limited number of switches on any time interval, rather than an overall limited number of switches. Since in Ellipsoidal Unfalsified Control an average volume decrease per controller switch is guaranteed, it would be interesting to investigate the application of these results combined with a re-enabling strategy in Ellipsoidal Unfalsified Control to control plants that are “slowly time-varying or subject to infrequent large jumps” (Stefanovic, 2005).

9.1.5 Convex Unfalsified Set

Current algorithms, both for Ellipsoidal Unfalsified Control and for Batch Adaptive Unfalsified Control, always result in a convex Unfalsified Set by construction. The derivation of the performance with the fictitious reference results in parallel half-spaces of unfalsified controllers, however, it is not clear how restrictive the derivation is. A comparison of the True Unfalsified Set with an analytically derived set of unfalsified controllers might provide useful insights.

9.1.6 Unfalsified Diagnosis

Instead of only deriving a controller with Ellipsoidal Unfalsified Control, the Unfalsified Set might also be used as a diagnosis tool. For instance, a sudden decrease in performance or falsification of a part of the Unfalsified Set might indicate wear or even a failure in the system. Nonetheless, for correct interpretation of the observed phenomena, e.g., identification or location of a failure, more information of

the system is required.

9.1.7 Stability for Batch Adaptive Unfalsified Control

As already discussed in Section 7.3.4, the guarantee of the stability of this data-driven controller design method has to be addressed. However, at the moment, we can only hint at such a proof. Not only should the adaptive system be stable, but the batch implementation also requires that the stability of the individual controllers is guaranteed. An approach to accomplish this might be the application of the ν -gap metric, which can be used to determine an upperbound on the change of the controller such that stability is guaranteed. However, the application of such a method would imply a departure from the purely data-driven approach.

9.2 Extensions

Several extension for Ellipsoidal Unfalsified Control are proposed, for which no major obstacles are expected.

- Based on the shape of the ellipsoidal Unfalsified Set, the controller structure can be adapted. Non-essential filters can be discarded, linear combinations of filters can be merged and the structure can be extended with filters based on, e.g., the error signal. A supervisory loop can monitor the signals in the system, and decide on these modifications. Attention should be payed to non-smooth transitions and initial conditions of the controller states. This extension, however, conflicts with the benefit of data-driven control design that the controller complexity is defined a priori.
- Although currently only one controller structure is regarded, evaluation of several controller structures simultaneously is possible. Each controller structure has its corresponding controller parameter set with accompanying Unfalsified Set. An extension of the controller selection algorithm is to be designed to select which controller structure is actually implemented.
- For faster convergence to the desired performance level, or for the determination of the achievable performance level all together, the decrease of the bound Δ can be made dependent on the error e . If the performance requirement is easily met, a faster decrease in the threshold can be realized.

-
- In the selection of the control parameters that are to be implemented additional constraints can be considered, such as, for instance, non-negativity constraints or the maximization/minimization of certain parameters. As examples, consider the selection of the maximal $\check{\theta}_1$ to minimize control effort, or the selection of the minimal $|\check{\theta}_9|$ in the experimental application example, to minimize the nonlinear contribution. Main point here is that the choice of parameters basically can be arbitrary, as long as it is from $\mathcal{E}(t_{k-1}) \cap \mathcal{U}(t_k)$.
 - Besides from the application to Multiple-Input Multiple-Output plants, the theory for multivariable controller design as presented in Chapter 6 can also be applied to bound the rate of variation of the inputs and outputs of the plant. By augmenting the plant with $du(t_k)/dt_k$ and/or $dy(t_k)/dt_k$, requirements can be imposed on the maximum rate of change of these signals.
 - In Batch Adaptive Unfalsified Control, currently only the measurement data of the last batch is used for unfalsification information. More consistent results might be obtained by retaining the data from previous batches. To avoid that the number of constraints grows linearly with the available data, an approximation should be made of the region of unfalsified controllers, for instance by approximation by a polytope of lower (fixed) complexity or by another geometric figure such as an ellipsoid.

Bibliography

- Aangenent, W. (2003). Data-based LQG control. Master's thesis, Technische Universiteit Eindhoven. DCT 2003.113.
- Aangenent, W., Kostić, D., De Jager, B., and Steinbuch, M. (2005). Data-based optimal control. In *Proc. Amer. Contr. Conf.*, pages 1460–1465, Portland, Oregon, USA.
- Ando, Y. (2004). Data-based control of integrated circuits. U.S. Patent 6792379.
- Åström, K. (1985). A commentary on the C.E. Rohrs et al. paper “robustness of continuous-time adaptive control algorithms in the presence of unmodeled dynamics”. *IEEE Trans. Automatic Control*, 30(9):889.
- Åström, K. and Wittenmark, B. (1972). On the control of constant but unknown systems. In *Proc. IFAC World Congress*, Paris, France.
- Åström, K. and Wittenmark, B. (1973). On self tuning regulators. *Automatica J. IFAC*, 9(2):185–199.
- Åström, K. and Wittenmark, B. (1995). *Adaptive Control*. Addison Wesley, Reading, Massachusetts, USA, second edition.
- Athans, M., Fekri, S., and Pascoal, A. (2005). Issues on robust adaptive feedback control. In *IFAC World Congress*, Prague, Czech Republic.
- Boyd, S., El Ghaoui, L., Feron, E., and Balakrishnan, V. (1994). *Linear Matrix Inequalities in System and Control Theory*, volume 15. SIAM Studies in Applied Mathematics, Philadelphia, Pennsylvania, USA.
- Boyd, S. and Vandenberghe, L. (2004). *Convex Optimization*. Cambridge University Press, Cambridge, England, UK.

- Brozenec, T., Tsao, T.-C., and Safonov, M. (2001). Controller validation. *Internat. J. Adapt. Control Signal Process.*, 15(5):431–444.
- De Bruyne, F. and Kammer, L. (1999). Iterative feedback tuning with guaranteed stability. In *Proc. Amer. Contr. Conf.*, pages 3317–3321, San Diego, California, USA.
- Cabral, F. and Safonov, M. (2004). Unfalsified model reference adaptive control using the ellipsoid algorithm. *Internat. J. Adapt. Control Signal Process.*, 18(8):683–696.
- Campi, M., Lecchini, A., and Savaresi, S. (2002). Virtual reference feedback tuning: a direct method for the design of feedback controllers. *Automatica J. IFAC*, 38(8):1337–1346.
- Collins, E. and Fan, C. (1999). Automated PI tuning for a weigh belt feeder via unfalsified control. In *Proc. Conf. Dec. & Contr.*, pages 785–790, Phoenix, Arizona, USA.
- Egardt, B. (1979). *Stability of Adaptive Controllers*, volume 20 of *Lecture Notes in Control and Information Sciences*. Springer-Verlag, Berlin, Germany.
- Engell, S., Tometzki, T., and Wonghong, T. (2007). A new approach to adaptive unfalsified control. In *Proc. Eur. Contr. Conf.*, pages 1328–1333, Kos, Greece.
- Fu, M. and Barmish, B. (1986). Adaptive stabilization of linear systems via switching control. *IEEE Trans. Automatic Control*, 31(12):1097–1103.
- Van Helvoort, J., De Jager, B., and Steinbuch, M. (2005). Unfalsified control using an ellipsoidal unfalsified region applied to a motion system. In *Proc. IFAC World Congress*, Prague, Czech Republic.
- Van Helvoort, J., De Jager, B., and Steinbuch, M. (2006a). Ellipsoidal Unfalsified Control: Stability. In *Proc. Amer. Contr. Conf.*, pages 4094–4099, Minneapolis, Minnesota, USA.
- Van Helvoort, J., De Jager, B., and Steinbuch, M. (2006b). Sufficient conditions for data-driven stability of ellipsoidal unfalsified control. In *Proc. Conf. Dec. & Contr.*, pages 453–458, San Diego, California, USA.
- Van Helvoort, J., De Jager, B., and Steinbuch, M. (2007a). Data-driven controller unfalsification with analytic update applied to a motion system. *IEEE Trans. Contr. Syst. Tech.*, submitted.
- Van Helvoort, J., De Jager, B., and Steinbuch, M. (2007b). Data-driven multi-variable controller design using ellipsoidal unfalsified control. In *Proc. Amer. Contr. Conf.*, pages 510–515, New York, New York, USA.

-
- Van Helvoort, J., De Jager, B., and Steinbuch, M. (2007c). Data-driven multi-variable controller design using ellipsoidal unfalsified control. *Systems Control Lett.*, submitted.
- Van Helvoort, J., Verkooijen, R., De Jager, B., and Steinbuch, M. (2007d). Plant-model-free batch adaptive control via controller unfalsification. *Internat. J. Adapt. Control Signal Process.*, submitted.
- Van Helvoort, J., De Jager, B., and Steinbuch, M. (2008). Direct data-driven recursive controller unfalsification with analytic update. *Automatica J. IFAC*, 44(1).
- Henrion, D., Tarbouriech, S., and Arzelier, D. (1998). LMI approximations for the radius of the intersection of ellipsoids. In *Proc. Conf. Dec. & Contr.*, pages 1759–1764, Tampa, Florida, USA.
- Hespana, J., Liberzon, D., and Morse, A. (2003). Hysteresis-based switching algorithms for supervisory control of uncertain systems. *Automatica J. IFAC*, 39(2):263–272.
- Hiraoka, T., Takegawa, H., Asada, K., and Ikeda, T. (2003). Database control system. Eur. Patent EP1318454.
- Hjalmarsson, H. (2002). Iterative feedback tuning - an overview. *Internat. J. Adapt. Control Signal Process.*, 16(5):373–395.
- Hjalmarsson, H. (2005). From experiment design to closed-loop control. *Automatica J. IFAC*, 41(3):393–438.
- Jun, M. and Safonov, M. (1999). Automatic PID tuning: An application of unfalsified control. In *Proc. Int. Symp. Comp. Aided Contr. Syst. Design*, pages 328–333, Kohala Coast-Island of Hawaii, Hawaii, USA.
- Kammer, L., Bitmead, R., and Bartlett, P. (2000). Direct iterative tuning via spectral analysis. *Automatica J. IFAC*, 36(9):1301–1307.
- Katsaggelos, A., Biemond, J., Schafer, R., and Mersereau, R. (1991). A regularized iterative image restoration algorithm. *IEEE Trans. Signal Process.*, 39(4):914–929.
- Kostić, D. (2004). *Data-driven Robot Motion Control Design*. PhD thesis, Technische Universiteit Eindhoven.
- Kostić, D., De Jager, B., and Steinbuch, M. (2004). Data-based design of high-performance motion controllers. In *Proc. Amer. Contr. Conf.*, pages 722–727, Boston, Massachusetts, USA.

- Krstić, M. (2000). Performance improvement and limitations in extremum seeking control. *Systems Control Lett.*, 39(5):313–326.
- Krstić, M. and Wang, H.-H. (2000). Stability of extremum seeking feedback for general nonlinear dynamic systems. *Automatica J. IFAC*, 36(4):595–601.
- Lecchini, A., Campi, M., and Savaresi, S. (2002). Virtual reference feedback tuning for two degree of freedom controllers. *Internat. J. Adapt. Control Signal Process.*, 16(5):355–371.
- Maksarov, D. and Norton, J. (1996). State bounding with ellipsoidal set description of the uncertainty. *Internat. J. Control*, 65(5):847–866.
- Manuelli, C., Cheong, S., Mosca, E., and Safonov, M. (2007). Stability of unfalsified adaptive control with non SCLI controllers and related performance under different prior knowledge. In *Proc. Eur. Contr. Conf.*, pages 702–708, Kos, Greece.
- Mårtensson, B. (1985). The order of any stabilizing regulator is sufficient a priori information for adaptive stabilization. *Systems Control Lett.*, 6(2):87–91.
- Van der Meulen, S. (2005). Machine-in-the-loop control optimization: Application to high-precision motion systems. Master’s thesis, Technische Universiteit Eindhoven, Eindhoven, The Netherlands.
- Van der Meulen, S., Tousain, R., and Bosgra, O. (2007). Fixed structure feed-forward controller tuning exploiting iterative trials, applied to a high-precision electromechanical servo system. In *Proc. Amer. Contr. Conf.*, pages 4033–4039, New York, New York, USA.
- Narendra, K. and Balahrishnan, J. (1994). Improving transient response of adaptive control systems using multiple models and switching. *IEEE Trans. Automatic Control*, 39(9):1861–1866.
- Pan, Y. and Lee, J. (2003). Recursive data-based prediction and control of product quality for a PMMA batch process. *Chem. Eng. Science*, 58:3215–3221.
- Paul, A. (2005). *Multi-Controller Adaptive Control (MCAC): Cost Detectability, Stability and some Applications*. PhD thesis, University of Southern California, Los Angeles, California, USA.
- Paul, A., Stefanovic, M., Safonov, M., and Akar, M. (2005). Multi-controller adaptive control (MCAC) for a tracking problem using an unfalsification approach. In *Proc. Conf. Dec. & Contr. and Eur. Contr. Conf.*, pages 4815–4820, Seville, Spain.

- Popper, K. R. (2002). *The Logic of Scientific Discovery (transl. of 'Logik der Forschung' (1935))*. Routledge Classics, London, England, UK.
- Pronzato, L. and Walter, E. (1994). Minimal volume ellipsoids. *Internat. J. Adapt. Control Signal Process.*, 8(1):15–30.
- Rohrs, C., Valavani, L., Athans, M., and Stein, G. (1985). Robustness of continuous-time adaptive control algorithms in the presence of unmodeled dynamics. *IEEE Trans. Automatic Control*, 30(9):881–889.
- Ros, L., Sabater, A., and Thomas, F. (2002). An ellipsoidal calculus based on propagation and fusion. *IEEE Trans. Systems Man Cybernet.*, 32(4):430–442.
- Rugh, W. (1996). *Linear System Theory*. Prentice Hall, Upper Saddle River, New Jersey, USA, second edition.
- Safonov, M. and Tsao, T.-C. (1994). The unfalsified control concept and learning. In *Proc. Conf. Dec. & Contr.*, pages 2819–2824, Lake Buena Vista, Florida, USA.
- Safonov, M. and Tsao, T.-C. (1997). The unfalsified control concept and learning. *IEEE Trans. Automatic Control*, 42(6):843–847.
- Shi, G. and Skelton, R. (2000). Markov data-based LQG control. *J. of Dyn. Syst., Meas., and Control*, 122(3):551–559.
- Skelton, R. (1989). Model error concepts in control design. *Internat. J. Control*, 49(5):1725–1753.
- Skogestad, S. and Postlethwaite, I. (2005). *Multivariable Feedback Control*. Wiley, Chichester, England, UK, second edition.
- Stefanovic, M. (2005). *Safe Switching Adaptive Control: Stability and Convergence*. PhD thesis, University of Southern California, Los Angeles, California, USA.
- Stefanovic, M., Paul, A., and Safonov, M. (2005). Safe adaptive switching through infinite controller set: Stability and convergence. In *Proc. IFAC World Congress*, Prague, Czech Republic.
- Steinbuch, M. and Norg, M. (1998). Advanced motion control: An industrial perspective. *Eur. J. Control*, 4(4):278–293.
- Tsao, T.-C., Brozenec, T., and Safonov, M. (2003). Unfalsified adaptive spacecraft attitude control. In *Proc. AIAA Guid. Nav. Contr. Conf.*, Austin, Texas, USA.
- Tsao, T.-C. and Safonov, M. (2001). Unfalsified direct adaptive control of a two-link robot arm. *Internat. J. Adapt. Control Signal Process.*, 15(3):319–334.

- Verkooijen, R. (2007). Plant-model-free batch adaptive control via controller unfalsification. Master's thesis, Technische Universiteit Eindhoven. DCT 2007.003.
- Vinnicombe, G. (1993). Frequency domain uncertainty and the graph topology. *IEEE Trans. Automatic Control*, 38(9):1371–1383.
- Wang, R., Paul, A., Stefanovic, M., and Safonov, M. (2005). Cost-detectability and stability of adaptive control systems. In *Proc. Conf. Dec. & Contr. and Eur. Contr. Conf.*, pages 3584–3589, Seville, Spain.
- Wang, R., Paul, A., Stefanovic, M., and Safonov, M. (2007). Cost detectability and stability of adaptive control systems. *Internat. J. Robust Nonlinear Control*, 17(5–6):549–561.
- Woodley, B., How, J., and Kosut, R. (1999). Direct unfalsified controller design - Solution via convex optimization. In *Proc. Amer. Contr. Conf.*, pages 3302–3306, San Diego, California, USA.
- Zhang, J. and Ioannou, P. (2006). Non-identifier based adaptive control scheme with guaranteed stability. In *Proc. Amer. Contr. Conf.*, pages 5456–5461, Minneapolis, Minnesota, USA.

Summary

Unfalsified Control: Data-Driven Control Design for Performance Improvement

To improve the performance of motion systems over model-based control design, data-driven control design is adopted in this thesis. With a system-in-the-loop approach, measurement data of the actual system to be controlled is used in the adaptation of the controller parameters. Main conditions on the method are that 1) assumptions and approximations introduced by modeling are avoided by refraining from the use of a plant model and 2) the algorithm is computationally cheap such that realtime adaptation is feasible.

Unfalsified Control is a data-driven control design framework that recursively discards controllers that demonstrably fail, i.e., whose ability is falsified, to meet the predefined performance requirement. No plant model is required for the inference of the performance of candidate controllers and, moreover, the controllers need not be implemented for their evaluation. Existing realtime approaches that consider an infinite set of candidate controllers only update the set of candidate controllers with new falsification information if the currently implemented controller is falsified. If this specific condition is not fulfilled, the new falsification information is discarded and the old set of candidate controllers is maintained.

In this thesis, Ellipsoidal Unfalsified Control is introduced as a realtime adaptive Unfalsified Control approach that considers an infinite number of candidate controllers and that is computationally cheap nonetheless. The candidate controllers are defined by an ellipsoidal region in the controller parameter space, whereas the controllers that are unfalsified by the current measurement data define two parallel half-spaces. This latter quality is realized by specific design choices for

the controller structure and the performance requirement. The optimal ellipsoidal approximation of the intersection of the two regions can be computed analytically. The resulting algorithm is computationally cheap and can be applied to motion systems on commodity hardware. Furthermore, the stability of the proposed method can be guaranteed, provided that stabilization of the adaptive system is feasible.

An extension has been proposed for the derived method to cover full-block multi-variable controllers. Furthermore, the application in a batch-wise adaptation is considered with the same controller structure and performance requirement as in realtime adaptation. Since the computational load is of less importance in batch adaptation, the exact region of unfalsified controllers can be exploited.

The results of the application in simulations and experiments are shown. Although performance improvement is not conclusively established, the applicability of the proposed method to motion systems and its capability to derive a controller without a plant model are demonstrated.

With Ellipsoidal Unfalsified Control a data-driven control design method is constructed that derives controllers using only measured data on the systems to be controlled, without any plant models. Although the method considers infinitely many candidate controllers, it is computationally cheap and can be implemented at the fast sample rate that is encountered in motion systems.

Samenvatting

Dit proefschrift beschouwt data-gebaseerd regelaarontwerp om de prestaties van bewegende systemen te verbeteren ten opzichte van model-gebaseerd regelaarontwerp. Met een systeem-in-de-lus aanpak wordt meetdata van het te regelen systeem gebruikt om de regelaarparameters aan te passen. De belangrijkste voorwaarden voor de te ontwikkelen methode zijn dat 1) modelleer-aannames en -benaderingen worden vermeden door geen gebruik te maken van een systeemmodel en 2) het algoritme snel te evalueren is zodat de regelaarparameters op iedere tijdstap kunnen worden aangepast (realtime adaptatie).

“Unfalsified Control” is een concept voor data-gebaseerd regelaarontwerp. Deze methode verwerpt recursief regelaars waarvan kan worden aangetoond dat ze niet voldoen aan de vooraf gestelde eisen. Er is geen model nodig voor het afleiden van de prestatie van de kandidaat-regelaars, en bovendien vereist deze evaluatie geen implementatie van de regelaars. Bij de bestaande methodes die een onbeperkt aantal regelaars beschouwen wordt de set van kandidaat-regelaars alleen maar aangepast indien de huidige regelaar is gefalsificeerd. Wanneer niet aan deze specifieke voorwaarde wordt voldaan, wordt de nieuwe informatie over falsificatie verworpen en wordt de oude set van kandidaat-regelaars gehandhaafd.

In dit proefschrift wordt “Ellipsoidal Unfalsified Control” geïntroduceerd. Deze methode gaat uit van de theorie van Unfalsified Control, maar door enkele specifieke ontwerpkeuzes kunnen hiermee een oneindig aantal regelaars snel worden geëvalueerd, zonder de restricties van de bestaande methodes. Ten eerste worden de kandidaat-regelaars beschreven door een ellips in de ruimte die wordt beschreven door de regelaarparameters. Ten tweede vormen de regelaars, die worden gefalsificeerd door de huidige meetdata, twee parallelle halfvlakken. Deze speciale vorm wordt verkregen door specifieke ontwerpkeuzes voor de regelaar-structuur en

de prestatie-eis. De set van ongefalsificeerde regelaars kan efficiënt worden geactualiseerd door de intersectie van de twee hierboven genoemde gebieden te benaderen met een nieuwe ellips, aangezien deze nieuwe ellips analytisch kan worden beschreven. De evaluatie van het resulterende algoritme is zo snel dat het kan worden toegepast op bewegende systemen met standaard hardware. Bovendien kan de stabiliteit van het voorgestelde data-gebaseerd regelaarontwerp worden gegarandeerd, indien stabiliteit überhaupt haalbaar is.

Met een uitbreiding van de ontwikkelde methode kunnen ook multivariabele regelaars worden beschouwd. Daarnaast is een batch-gewijze aanpak bekeken met dezelfde regelaarstructuur en prestatie-eis als bij realtime adaptatie. Aangezien de evaluatiekosten bij een batch-gewijze aanpak van minder belang zijn, kan de exacte beschrijving van het gebied met ongefalsificeerde regelaars worden gebruikt in plaats van de ellipsvormige benadering.

De ontwikkelde methodes zijn toegepast in simulaties en in experimenten. Ofschoon de prestatie-verbetering niet onomstotelijk wordt aangetoond, is wel gedemonstreerd dat de voorgestelde methode kan worden toegepast op bewegende systemen en dat de methode in staat is om regelaars af te leiden zonder een model.

Met Ellipsoidal Unfalsified Control is een methode voor data-gebaseerd regelaarontwerp ontwikkeld die regelaars instelt met uitsluitend meetdata van het te regelen systeem, zonder enig model daarvan. De methode beschouwt oneindig veel regelaars, maar is desondanks snel te evalueren en kan zodoende worden toegepast met korte tijdstappen, zoals nodig is bij bewegende systemen.

Dankwoord

Yes! Mijn “boekje” is af! Althans, bijna, wanneer ik dit schrijf. Hoewel mijn onderzoek heel individueel is geweest, had ik het toch niet kunnen volbrengen zonder de mensen om mij heen. Daarom wil ik op de daarvoor aangewezen plaats iedereen bedanken die me de afgelopen vier jaar heeft geholpen bij de verwezenlijking van dit proefschrift, zowel met de afleidingen als met afleiding.

Allereerst wil ik mijn professor Maarten Steinbuch bedanken voor de kans die hij mij heeft gegeven om dit project te mogen doen. Zeer dankbaar ben ik ook voor de vrijheid die ik kreeg om mijn eigen richting te bepalen, voor de altijd motiverende besprekingen en voor de haast vanzelfsprekende mogelijkheden voor het bijwonen van conferenties en cursussen. Ook wil ik mijn copromotor Bram de Jager bedanken voor zijn begeleiding en ondersteuning. De onderlinge discussies hebben veel bijgedragen aan het verfijnen van de inhoud van dit proefschrift.

Ook de studenten die hebben meegewerkt aan mijn onderzoeksonderwerp ben ik zeer erkentelijk. Robert, Michael en Rob, bedankt voor jullie inzet en resultaten. Niet alleen voor jullie zullen de discussies leerzaam en inspirerend zijn geweest, ook zelf werd ik daardoor weer aan het denken gezet. En ook Roel en Bjorn bedankt voor de vernieuwende blik, en succes met het afronden van jullie afstudeertraject.

Mijn collega's wil ik bedanken voor de hulp en steun, maar vooral ook voor de afleidende discussies tijdens de vele koffiepauzes en lunches. Ondanks dat, of wellicht juist doordat, deze meestal over een compleet ander onderwerp gingen, waren ze vaak zeer inspirerend. En natuurlijk wil ik jullie ook bedanken voor het gezelschap, als we van ‘de baas’ weer eens ergens ver van huis moesten acclimatiseren voor een conferentie...

Een speciaal woord van dank is er ook voor mijn team, TechUnited, ook al vormt dat een grote overlap met de hierboven genoemde groep collega's. Het samen in

een informele setting werken aan een uitdagend probleem is altijd zeer motiverend geweest. RoboCup heeft voor mij tijdens mijn promotie een grote toegevoegde waarde gehad en veel plezier gebracht. Bedankt daarvoor!

Buiten de universiteit wil ik ook mijn vrienden van Isis bedanken voor de nodige afleiding en uitglijders. “Geestelijke ontspanning door lichamelijke inspanning” heeft voor mij altijd zeer goed gewerkt. Met veel plezier kijk ik terug op de trainingen, het naborrelen in ’t Schaetshuys en de diverse activiteiten, van step-estafette tot een weekje Weißensee.

Dan ben ik tenslotte aangekomen bij mijn (schoon-)familie, die ik wil bedanken voor alle getoonde interesse, steun en de nodige relativering. Ik wil specifiek mijn ouders bedanken, die mij altijd de kans hebben gegeven om mijn eigen keuzes te maken, en die altijd voor me klaar hebben gestaan. Mede daardoor heb ik toch maar mooi goed gebruik kunnen maken van mijn eigenwijsheid en mijn grenzeloos verlangen om dingen open te maken om te kijken hoe het werkt! Ik kan alleen maar een heel goed voorbeeld aan jullie nemen. Papa en mama, bedankt voor alle mogelijkheden die jullie me hebben gegeven.

Dit dankwoord ga ik afsluiten met een speciaal bedankje voor een speciale vrouw. Linda, met jouw luisterend oor en jouw goede raad & daad heb je me door de dieptepunten geholpen en hebben we samen kunnen genieten van de hoogtepunten. De gesprekken samen en de onvoorwaardelijke steun die ik van je kreeg hebben zeker bijgedragen aan het succes van mijn promotietraject. Lin, bedankt voor alles.

Curriculum Vitae

Jeroen van Helvoort was born on January 15th, 1980 in Vlijmen, the Netherlands. After finishing his secondary education at the Stedelijk Gymnasium in 's-Hertogenbosch, he started his study Mechanical Engineering at the Technische Universiteit Eindhoven (TU/e), where he received the “TUE motivatiebeurs” scholarship. He received his M.Sc. Degree (Cum Laude) in January 2004. For his traineeships, he went to the University of California, San Diego (UCSD), San Diego, USA, and to Philips Research, Eindhoven, the Netherlands. His master’s thesis was entitled “Analytical and experimental LFT modeling of a double scara robot” and was performed at the TU/e. Since January 2004, Jeroen has been a Ph.D. student in the Control Systems Technology group at the department of Mechanical Engineering of the TU/e on the topic “Data- and disturbance-driven control,” resulting in this thesis.

